N° d'ordre Année 2016

Université Djillali Liabès de Sidi- Bel-Abbes

Faculté de Génie Electrique
Département D'électronique
Laboratoire de Télécommunications et de Traitement Numérique du Signal

THESE DE DOCTORAT

Pour l'obtention du Diplôme de Doctorat en Sciences

Spécialité: Electronique
Option: Signal et Télécommunications

Présentée par

M. ZOUGGARET Abdelhak

Effects of Codes and Subcarrier Interleaving on Multi-code Multicarrier CDMA System

---

Soutenue le : 08 Novembre 2016

Devant le jury composé de :

Président	**Pr. ELAHMAR Sid Ahmed**	**Univ. Djillali Liabès-Sidi Bel-Abbès**
Examinateur	**Dr.MAACHOU Abdelkader**	**Univ. de Mascara**
Examinateur	**Dr. BOUASRIA Fatima**	**Univ. de Saida**
Rapporteur	**Pr. DJEBBARI Ali**	**Univ. Djillali Liabès-Sidi Bel-Abbès**

Année Universitaire 2016-2017

ملخص

ثمة حاجة لأنظمة الاتصالات اللاسلكية في المستقبل لنقل البيانات بمعدلات بث عالي، وهذا ما يحفز الباحث للعمل على التكنولوجيات الجديدة للجيل القادم من أنظمة الاتصالات اللاسلكية المتنقلة.

يعتبر نمتعدد الرمز متعدد الناقل CDMA (MC-MC-CDMA) كمرشح قوي نظرا لقدراتها لتقليل تلاشي تردد والتداخل الوصول المتعدد (MAI). هذه طريقة تجمع بين تقنيات الوصول متعددة CDMA،(MC-CDMA) و متعدد الرمز CDMA (Multi-Code CDMA).حيث تركز هذه الأطروحة البحثية حول تأثير التداخل في تنوع الوقت وتنوع التردد في نظام MC-MC-CDMA

هذه الرسالة اولا تحلل النظام MC-MC-CDMA وتدرس نسبة خطأ البت (BER) على أساس عدة عوامل مثل: عدد المستخدمين، وعدد الرمز، ونوع الموحد.

بعد ذلك، تقدم هذه الأطروحة نوع جديد من التداخل في الوقت و التردد في نظام MC-MC-CDMA الذي يسمح بتنوع ثنائي الأبعاد في كل من الوقت والتردد. مما يمكننا من تنفيذ تداخل ثنائي الأبعاد داخل تنوع الوقت وتنوع التردد. نتائج المحاكاة تبرهن أن الطريقة المقترحة تعطي أداء أفضل في (BER). أيضا، نلاحظ أن (BER) كل من التداخل D2-رئيس والتداخلD2-عشوائي متشابهة.اضافة على ذلك، فإن المكسب من التداخل أكبر في تنوع التردد من تنوع الوقت. وأخيرا، نصل إلى أفضل ذروة نسبة إشارة الضوضاء (PSNR) عندما نقوم بنقل الصور (الملونة، أبيض وأسود) من خلال تقنية المقترحة.

Abstract

Future wireless communication systems are required to transport data at much higher bit rates and this motivates a researcher to work on the new technologies for the next generation of wireless mobile communication systems.

Multi-code Multi-carrier CDMA (MC-MC-CDMA) has emerged as a powerful candidate due to its capabilities of minimizing frequency selective fading and Multiple Access Interference (MAI).This transmission method combining the multiple access technologies (CDMA), to those multiple codes and multiple carriers. This research thesis focuses on the effect of interleaving in time and frequency diversity in MC-MC-CDMA system.

This thesis first analyses the MC-MC-CDMA system and investigates the Bit Error Ratio (BER) performance on the basis of several factors such as: users number, *M-ary* symbol number, code sequence and combiner type.

Next, this thesis presents a new time-frequency interleaving in a MC-MC-CDMA system, which allows two-dimensional spreading in both time and frequency domains. Our contribution consists in implementing a two-dimensional interleaving inside the time and frequency diversity. We demonstrate via simulation results that the proposed method yields better performances in BER. Also, we observe that BER of both the 2D-prime interleaving and the 2D-random interleaving are similar. Furthermore, the interleaving gain is larger in a frequency-diversity than time-diversity. Finally, we reach better Peak Signal to Noise Ratio (PSNR) when we transmit images (color, black and white) through the proposed technique.

Acknowledgements

Firstly I would like to express my deepest appreciation and gratitude to my supervisor, Pr. DJEBBARI Ali, for his availability, his advice, constructive feedback and support throughout my years at Laboratory of Telecommunications and Digital Signal Processing (LTTNS) Djilali Liabes University in Sidi Bel Abbes.

I warmly thank Pr. ELAHMAR Sid Ahmed for agreeing to preside my jury also, I thank all the examiners: Dr. BOUASRIA Fatima from Saida University and Dr. MAACHOU Abdelkader from Mascara University who have done me the honor of accepting to report this work.

I would like to express a special gratitude to Pr. DJEMAL Khalifa from IBISC Laboratory, Evry University in France. DJEMAL has been very professional in his approach and has taught me a great deal. He has been very supportive throughout my candidature.

I also thank my colleagues and friends from the electrical department in Mascara University, with particular thanks to: Dr. MOUFFAK Adnane, Dr. CHAOUCH Djamal Eddine and Mr AZZEDDINE Hocine.

Last but not least, I dedicate this thesis to my parents, my wife, and my son.

Table of Contents

Abstract..... I
Acknowledgments..... II
Table of Contents..... III
List of Figures..... VII
List of Tables..... IX
Abbreviations..... X

Introduction..... 1

Chapter1. Generalities

Introduction 4
1.1 Digital transmission link 5
1.1.1 Source coding..... 5
1.1.2 Channel coding..... 5
1.1.3 Digital modulation..... 6
1.1.4 The propagation channel..... 6
1.2 Fading in a mobile radio environment 7
1.2.1 Physical propagation mechanisms..... 7
1.2.1.1 Reflection /refraction..... 7
1.2.1.2 Diffraction..... 7
1.2.1.3 Scattering..... 7
1.2.2 Large-scale fading (*slow fading*)..... 8
1.2.2.1 Path loss..... 8
1.2.2.2 Shadowing..... 8
1.2.3 Small-scale fading..... 8
1.2.3.1 Multi-path fading..... 8

1.3 Characterization in Time and Frequency ……..…….. 8
1.3.1 Delay spread…… 8
1.3.2 Doppler spread…… 9
1.3.3 The coherence time……. 9
1.3.4 The coherence bandwidth……... 9
1.3.5 Channel not frequency selective……. 9
1.3.6 Channel frequency selective……... 10
1.3.7 Channel not time selective…….. 10
1.3.8 Channel time selective…… 10
1.3.9 The interferences types……... 10
1.4 OFDM modulation ……..…. 11
1.5 Multiple access techniques ……..… 13
1.5.1Duplexing…… 13
1.5.1.1 Frequency Division Duplex (FDD)…… 13
1.5.1.2Time Division Duplex (TDD)……. 14
1.5.2 Multiple access schemes…… 15
1.5.2.1 FDMA technical…….. 15
1.5.2.2 TDMA technical……. 15
1.5.2.3 CDMA technical……. 16
1.6 Spreading ……..……... 16
1.6.1 Spreading in time…… 18
1.6.2 Spreading in frequency……... 18
1.6.3 Two dimensional spreading in time-frequency……... 18
1.6.4 Orthogonal multiple access……. 20
1.6.4.1 Walsh code……. 20
1.6.5 Quasi-Orthogonal CDMA……... 22
1.7 Interleaving……..…. 22
1.7.1 Block Interleaving……. 23
1.7.1.1 Random Interleaving……... 24
1.7.1.2 Prime Interleaving…….. 24
1.7.1.3 Chaotic interleaving……... 25
1.7.2 Convolutional interleaving…….. 26
Conclusion……..……...…….. 27

Chapter2. MC-MC-CDMA system presentation

Introduction 29
2.1 Multi-code and M-ary CDMA techniques..... 29
2.1.1 Orthogonal code system..... 29
2.1.2 Parallel combinatorial system..... 31
2.1.3 BPSK M-ary CDMA system..... 33
2.1.4 Multi-Code CDMA system..... 34
2.2 Multi-Carrier CDMA system..... 36
2.3 Multi-Code Multi-Carrier CDMA system..... 37
2.3.1 Transmitter model..... 37
2.3.2 Channel model..... 39
2.3.3 Receiver model..... 39
2.3.4 Performance Comparison for MC-MC-CDMA..... 41
Conclusion..... 45

Chapter3. Interleaving in Time-frequency Diversity on MC-MC-CDMA System

Introduction 47
3.1 System Model..... 47
3.1.1 Transmitter model 47
3.1.2 Receiver model 48
3.2 New Time Frequency Interleaving 49
3.2.1 Two dimensional Prime interleaving..... 49
3.2.2 Two dimensional random interleaving 50
3.3 Results and discussions 51
3.3.1 Performance evaluation of MC-MC-CDMA with 2D-interleaving 51
3.3.2 Images transmission over MC-MC-CDMA with 2D-interleaving. 54
3.3.2.1 Color images..... 55
3.3.2.2 Black and white images..... 59
Conclusion..... 63

Conclusions and prospects…… 64

Appendix A. BPSK M-ary CDMA System analysis……..…… 66

Appendix B. Pseudo Noise Sequences…… 69

Introduction…… 69
b.1 m-Sequence……... 69
b.2 Gold Sequences…… 74
b.3. Kasami Sequence…… 76

List of References……... 77

List of Figures

1.1	Digital transmission link…..……..	**5**
1.2	Interference presentation in the time-frequency-code……...	**10**
1.3	Guard interval……	**12**
1.4	Block diagram of OFDM modulator……..	**12**
1.5	Frequency Division Duplex FDD……..	**14**
1.6	Time Division Duplex TDD……..	**14**
1.7	FDMA scheme……...	**15**
1.8	TDMA scheme……...	**16**
1.9	CDMA scheme……...	**16**
1.10	Different scheme of spreading……...	**17**
1.11	Three different time-frequency spreading dimensions…….	**19**
1.12	Different strategies for (4x4) block interleaving……..	**23**
1.13	Random interleaving of length 16……..	**24**
1.14	Prime interleaving of length 16……..	**25**
1.15	Chaotic interleaving of an 4×4 matrix……...	**26**
1.16	Convolutional interleaving ……	**27**
2.1	Orthogonal code system transmitter……..	**30**
2.2	Orthogonal code system receiver……...	**31**
2.3	Parallel combinatorial system transmitter……..	**31**
2.4	Parallel combinatorial system receiver……..	**32**
2.5	Multi-code CDMA system transmitter……..	**35**
2.6	Multi-code CDMA system receiver……...	**35**
2.7	Multi-carrier CDMA system receiver……	**36**
2.8	Multi-carrier CDMA system receiver……	**37**
2.9	Transmitter model of MC-MC-CDMA system…….	**38**
2.10	Power delay profile……	**39**
2.11	Receiver model of MC-MC-CDMA system……..	**40**
2.12	Simulation results for BER vs SNR for Multi-code CDMA, MC-CDMA, MC-MC-CDMA……...	**42**

2.13	BER versus SNR for MTC CDMA system using Walsh, Gold, and Kasami codes.....	**43**
2.14	Simulation results for BER versus SNR for MC-MC-CDMA with various *M*...	**43**
2.15	The effect of the user's number on BER performance……	**45**
2.16	BER comparison of MC-MC-CDMA system with using EGC and MRC……..	**45**
3.1	Transmitter model of MC-MC-CDMA system with 2D-interleaving…….	**47**
3.2	Receiver model of MC-MC-CDMA system with 2D De-interleaving……	**48**
3.3	2D-prime interleaving of 8 subcarriers and code sequence length $N = 8$……	**50**
3.4	BER comparison of MC-MC-CDMA system with/without 2D-interleaving…..	**52**
3.5	Comparison of code sequence and subcarrier interleaving for MC-MC-CDMA	**52**
3.6	Average BERvs SNR for MC-MC-CDMA with different number of subcarrier	**53**
3.7	Average BERvsSNR for MC-MC-CDMAwith different length of code sequence……...	**54**
3.8	The original medical images……	**56**
3.9	Received medical images over MC-MC-CDMA system without 2D-Prime interleaving at SNR= 20dB …….	**57**
3.10	Received medical images over MC-MC-CDMA system with 2D-Prime interleaving at SNR= 20dB……...	**57**
3.11	Average PSNR versus SNR for the received images over MC-MC-CDMA system……...	**58**
3.12	The original images……..	**60**
3.13	Received images over MC-MC-CDMA system without interleaving.....	**61**
3.14	Received images over MC-MC-CDMA system with 2D-prime interleaving….	**61**
3.15	Average PSNR versus SNR for the received images over MC-MC-CDMA….	**62**
3.16	PSNR comparison between the received cameraman image over MC-MC-CDMA system with 2D-prime interleaving and MC-CDMA with chaotic…….	**63** **94**
a.1	*K*-user signal formulation process for a BPSK *M-ary* CDMA system.....	**66**
a.2	Receiver of a BPSK *M-ary* CDMA system.....	**67**
b.1	Binary Linear Feedback Shift Register Sequence Generator.....	**70**
b.2	LFSR [5, 3] with image generated.....	**72**
b.3	Example of Generating a Set of Gold Sequences……..	**74**

List of Tables

2.1 Mapping table for orthogonal code system with $M = 8$…… **30**

2.2 Mapping table for a parallel combinatorial system with $M = 3$ and $u = 2$…… **32**

2.3 Mapping table for a BPSK M-ary CDMA system with $M = 3$…… **34**

2.4 Simulation parameters…… **41**

3.1 Simulation parameters…… **51**

3.2 Simulation parameters…… **55**

3.3 PSNR values for the received images in dB without interleaving…… **58**

3.4 PSNR values for the received images in dB with 2D-Prime interleaving…… **58**

3.5 Simulation parameters…… **59**

3.6 PSNR values for the received images in dB without interleaving using MRC combiner…… **62**

3.7 PSNR values for the received images in dB without interleaving using MRC combiner…… **62**

b.1 Circuit with Shift Registers for Generating 15 m-Sequence Initial sequence 0001…… **71**

b.2 Feedback connections for linear m-sequences…… **73**

Abbreviations

AWGN	Additive White Gaussian Noise
BER	Bit Error Rate : Taux d'erreur binaire
BT	Bottom to top
BPSK	Binary Phase Shift Keying
CDMA	Code Division Multiple Access
DFT	Discret Fourier Transform: transformée de Fourier discrète
DL	Down-links
EGC	Equal Gain Combining
ERFC	Fonction d'erreur complémentaire
FDD	Frequency Division Duplex
FDMA	Frequency Division Multiple Access
FFT	Fast Fourier Transform
ICI	Inter Channel Interference
IFFT	Inverse Fast Fourier Transform
IDFT	Inverse Discret Fourier Transform
ISI	Inter Symbol Interference
LFSR	Linear Feedback Shift Register Sequence
LR	left to right
MAI	Multiple Access Interference
MC-CDMA	Multi Carrier Code Division Multiple Access
MC-MC-CDMA	Multi Code Multi Carrier Code Division Multiple Access
MIMO	Multiple Input Multiple Output
MRC	Maximum-Ratio Combining
MSE	Mean squared error

OFDM	Orthogonal Frequency-Division Multiplexing
PN	Pseudo-noise
P/S	Conversion Parallèle/ Série
PSNR	Peak Signal to Noise Ratio
RF	Radio-frequency
RL	Right to left
SNR	Signal to Noise Ratio
S/P	Conversion série/parallèle
TB	Top to bottom
TDD	Time Division Duplex
TDMA	Time Division Multiple Access
UL	Up-links
1D	One-dimension
2D	Two-dimensional

Introduction

Future cellular radio networks will offer services that require the transfer data at high rate, while maintaining high mobility users. One approach currently being an important focus of research in this area is Multi-carrier CDMA technology [1]. It combines the multi-carrier OFDM transmission with the multiple access technique to division by CDMA codes. OFDM is commonly used in newer wireless communication systems. It has many advantages such as the ability to provide a high data rate while remaining robust to the multipath propagation, simplified implementation with IDFT operations and DFT and low receiver complexity with equalizing in the frequency domain [2]. CDMA meanwhile is a very flexible multiple access which allows multiple users to access the channel at the same time and on the same frequency, by allocating a distinct spreading code to each of them. It ensures that the complete time-frequency space is always used for signal transmission. Hence, the power of an active user is spread over the whole time frequency space, and the interference created in a multi cellular context is averaged in the same way. This interference can be further reduced by using different scrambling codes in the cells, which considerably facilitates the cell planning task [3] [4].

Another approach to increase the data rate found in the Multi-code CDMA association [5]. The main idea is to assign an additional spreading code for the user who wants to transmit at a higher rate; the user data sequence is divided into a plurality of digital symbols, each symbol is multiplied by an orthogonal code that allows discrimination and reducing inter symbol interference[6]. In a variant of multi code scheme where a user needs M times the basic data rate, the user converts his signal stream using a serial to parallel converter into M basic rate streams, encodes each with a different code, modulates them with a different modulator and super imposes them before transmission [7] [8], Thereby, with M codes, a user can transmit $log_2 M$ bits per sequence period. The data rate is increased by increasing the number of codes used for the transmission. [9].

All of these techniques form the system Multi-code Multi-carrier CDMA or MC-MC-CDMA that combines the benefits of each of the techniques mentioned above, namely CDMA, OFDM, Multi-code CDMA.

In Multi-carrier CDMA system, modulated signals of each user are spread by user-specific spreading code. Spreading is done only in the frequency domain and the spread data symbols are assigned to allocated subcarriers and transmitted. For obtaining the diversity gain, MC-CDMA may use subcarrier interleaving technique. Subcarrier interleaving in MC-CDMA system can achieve the frequency diversity gain by making the randomization effect of burst error in frequency domain [10].

The MC-MC-CDMA system offers two-dimensional gains in both the time and frequency domains by using a multi-code signal and multicarrier modulation, respectively [11]. Two-dimensional spreading exploits time-diversity and frequency-diversity. As a consequence, time and frequency diversity can be achieved by transmitting redundant information over positions that cannot be covered by coherence time-bandwidth. Redundancy is added to the data symbols by creating different versions of the same symbol, i.e. spreading [4]. To ensure that redundant versions of the same information are transmitted over uncorrelated positions a two-dimensional interleaving both code sequence and subcarriers is generally performed, thus can minimizes a frequency selective fading and Multiple Access Interference (MAI).

The object of our thesis is the study of MC-MC-CDMA system; we are primarily interested in the effect of interleaving in time and frequency diversity.

The manuscript is divided into three chapters which detail the progress of our work.

In the first chapter, we present the basic tools for understanding our work. Initially, the main concepts relating to digital communication are briefly discussed. Next, we provide an overview on different fading types in a mobile radio environment which are: the large-scale fading due to the path loss and shadowing, and the small-scale fading caused by multi-path propagation. It then presents the multi carrier OFDM and multiple access technique; we are interested in two-dimensional spreading. We conclude this chapter by introducing some fundamental principles of interleaving technique which presents the context of our study.

The second chapter presents the conventional system MC-MC-CDMA combines the advantages of Multi-code CDMA and Multi-carrier CDMA systems; we describe and analyze this system, then we examine its performance on the basis of several factors such as: users number, *M-ary* symbol number, code sequence and combiner type. To make a comparative study; the BER's of MC-MC-CDMA, Multi-carrier CDMA and Multi-code CDMA systems were presented.

In the last chapter, we present the study of interleaving effect in time-frequency diversity on MC-MC-CDMA system. A new time-frequency interleaving is then proposed. The results of simulations are evaluated on the basis of several factors such as number of subcarrier and code sequence length. An application of images (color, black and white) transmission is presented with the proposed mecanisme.

Finally the general conclusion brings together different conclusions on the studies conducted and indicates some prospects for further work.

The main contribution of this thesis is:

- We have presented a new time-frequency interleaving method based on MC-MC-CDMA systems allowing two-dimensional spreading in both time and frequency domains. The originality of proposed technique lies in fact that we have implemented a two-dimensional interleaving inside the time and frequency diversity which was the subject of international publication in [12].

Chapter 1

Generalities

Contents

Introduction 4
1.1 Digital transmission link 5
1.2 Fading in a mobile radio environment 7
1.3 Characterization in Time and Frequency 8
1.4 OFDM modulation 11
1.5 Multiple access techniques 13
1.6 Spreading 16
1.7 Interleaving 22
Conclusion 27

Introduction

This chapter aim to present the main concepts relating to digital communication systems. First, the digital communication description will be done. Next, we provide an overview on different effects that influence the signal received after propagation through the radio channel. It also briefly discusses the general concepts of OFDM and multiple access technique. Some fundamental principles of interleaving technique will be introduced.

1.1 Digital transmission link

Digital transmission systems carry information in digital forms between a source and one or more destinations using a physical support such as cable, fiber optics or propagation on a radio channel[13][14]. The signals can be transported directly digital, as in data networks or analog source (speech, image ...) but converted to digital form. The task of the transmission system is to move information from the source to the destination with the highest possible reliability. Figure 1.1 describes an overview of a digital communication channel. The various blocks are as detailed:

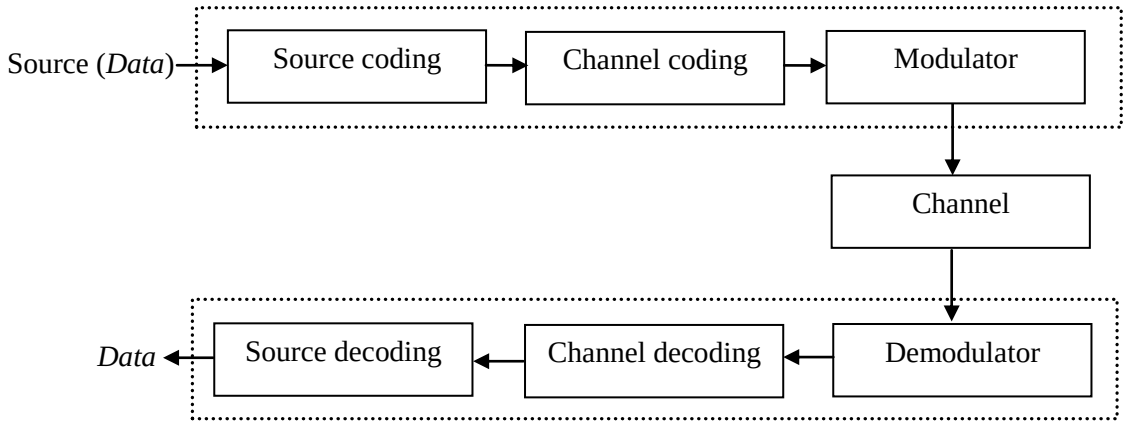

Figure 1.1. Digital transmission link[14]

1.1.1 Source coding

The sequence transmitted by the source must be the shortest be necessary to increase the transmission rate and optimize the use of systems resources. The source coder aims to compress data by eliminating non-significant bits [14]. The principle of source code was published by Shannon [15].

1.1.2 Channel coding

When passing through the transmission channel, the signal is subjected to various interferences, introducing errors in reception. In order to increase the reliability of the transmission, a channel coding introduces redundancy into the information sequence. The receiver knows the coding law used and is therefore capable of detecting and correcting erroneous binary data [14].

1.1.3 Digital modulation

The binary information sequence through a digital modulator as an interface with the communication channel giving the signal a physical envelope. Each element or group of binary elements is associated with a waveform according to a modulation law. Each waveform associated with a group of bits is called a "symbol", all while forming a signal that can be sent in the channel.

1.1.4 The propagation channel

Is the physical support used to transmit information. The support differs between applications. In our study, we will consider instead the mobile radio transmissions, which use the propagation of electromagnetic waves in free space [14].

The evaluation of transmission systems is dictated by two features: the quality of transmission and the complexity of calculating the modulation / demodulation operations.
The factors to quantify the quality of the transmission are [14]:

- *The bit error rate (BER):* it corresponds to the ratio between the number of erroneous bits and the total number of bits transmitted.

- *Mean squared error (MSE):* determines the average difference between the issued and received symbols.

- *The spectral efficiency:* is a measure the bit rate of unit time of frequency. For transmission of d bits for a duration T_s and a bandwidth B allocated to the transmission, the bit rate is given by the ratio d/T_s and spectral efficiency by the ratio d/BT_s.

- *The signal to noise ratio (SNR):* is generally adopted in digital transmission as receiver input parameter for which we will evaluate the quality of the recovered digital message.

1.2 Fading in a mobile radio environment

The mobile radio channel is decomposed into two fading components: the large-scale fading which regroups the path loss and shadowing, and the small-scale fading which reflects the most rapid distortions caused by multi-path propagation [2].

1.2.1 Physical propagation mechanisms

A radio signal transmitted through a mobile radio channel undergoes all the mechanisms that control the propagation of electromagnetic waves. Three basic mechanisms influence the propagation of electromagnetic waves, namely, reflection, diffraction, and scattering [2].

1.2.1.1 Reflection /refraction

The phenomena of reflection and refraction occur when the wave interacts with an obstacle whose dimensions are very large compared to the wavelength. [6], [16], [17].

1.2.1.2 Diffraction

Diffraction occurs when the signal encounters an obstacle whose dimensions are very large compared to the wavelength that obstructs the direct radio visibility between the transmitter and receiver. Secondary waves are generated, propagated behind the obstacle, this is called mask effect (shadowing) [6], [16].

1.2.1.3 Scattering

The scattering occurs when the obstacle has many irregularities whose dimensions are of the same order of magnitude or smaller than the wavelength. The reflected energy is scattered in all directions [6], [16].

The propagation mechanisms described above lead to three different effects (*path Loss, shadowing, multi-path fading*) that influence the signal received after propagation through the

radio channel. In the following, we distinguish two groups of fading. The first group is called the *large-scale fading* and regroups the attenuations due to *path loss* and *shadowing*.
The second group is called the *small-scale fading* and reflects the rapid fluctuations caused by *multi-path propagation* [2].

1.2.2 Large-scale fading (*slow fading*)

1.2.2.1 Path loss

The path loss expresses the loss in power that a transmitted signal experiences due to the distance separation between the transmitter and receiver [2].

1.2.2.2 Shadowing

Shadowing is a phenomenon of attenuation in radio telecommunications. It caused by the refraction or reflection on obstacles. The signal power will vary as a function of the propagation medium. The attenuation of the signal power is due to the properties of the media traversed by the wave [18].

1.2.3 Small-scale fading

1.2.3.1 Multi-path fading

For transmission by radio the transmitted signal undergoes reflections on the obstacles in this case, the receiver receives both the direct path, on the other hand with a propagation delay time (called propagation delay), the same signal by the reflected path. The powers received by the direct and reflected paths may be different [18].

1.3 Characterization in Time and Frequency

1.3.1 Delay spread

The delay spread describes the time spread of the signal caused by multi-path propagation with several paths of different lengths and, thus, of different delays [2].

1.3.2 Doppler spread

The Doppler effect is a phenomenon due to the displacement of the mobile station relative to the base station. They involve changes in the frequency of the received signal called Doppler shift. This frequency shift depends on two factors: the direction of travel and speed of the receiver relative to the transmitter [14].

Each path has a Doppler shift frequency of the form:

$$f_d = f_m cos\theta \tag{1.1}$$

where θ is the angle between the direction of mobile and direction of the path considered

$$f_m = \frac{\nu}{\lambda} \tag{1.2}$$

where ν represents the speed of the moving and λ represents the wavelength of the carrier.

1.3.3 The coherence time T_c

This is the time over which the characteristics of the transmission channel remains quasi-constant. This grandeur is approximately the inverse of the frequency spreading of the channel [14].

1.3.4 The coherence bandwidth B_c

This is the minimum frequency difference on which the channel characteristics are correlated. This quantity is approximately the inverse of the temporal spreading of the channel.

1.3.5 Channel not frequency selective

If $B << B_c$, all the frequency components of the signal undergo the same attenuation, the channel is said not frequency selective.

1.3.6 Channel frequency selective

If $B>>B_c$, all the frequency components of the signal undergo the different attenuation, the channel is said frequency selective.

1.3.7 Channel not time selective

If $T_s<< T_c$, the channel characteristics do not change during the transmission duration for the symbol and the channel is said not time selective.

1.3.8 Channel time selective

If $T_s>>T_c$, the channel characteristics change during the transmission duration for the symbol and the channel is said time selective.

We note B the band occupied by the signal to be transmitted and T_s the duration of a symbol.

1.3.9 The interferences types:

The different types of interference on time-frequency-code are shown in Figure 1.2.

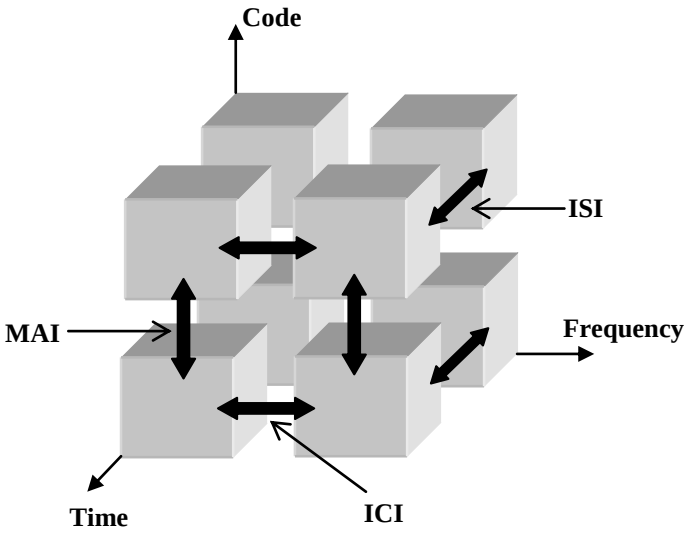

Figure 1.2. Interference presentation in the time-frequency-code [14]

We distinguish three types of interference in the communications systems (Figure 1.2) [14]:

- *Inter Symbol Interference (ISI):* when the propagation channel causes a significant delay spread before the time symbol.
- *Inter Carrier Interference (ICI):* when the propagation channel causes a significant frequency spreading before the spacing of the carrier frequencies of the waveforms.
- *Multiple Access Interference (MAI):* it refers to the interference due to other active signals (other codes).

1.4 OFDM modulation

The radio interfaces must meet several criteria. First be adapted to the propagation channel which is more or less sensitive to multipath and interference [14]. Then offer the best spectral efficiency in *bit / s / Hz* [14]. When the debit and band increase, it is necessary to use the conventional techniques of modulation to combat against the selective fading because this time the coherence bandwidth is too low. A solution is based on OFDM techniques that are best able to correct distortions of frequency selective channel [14], [19]. The idea is to distribute information on multiple subcarriers much lower band, and especially lower than the coherence bandwidth of the propagation channel, which are then affected by a flat fading. Each subcarrier may be assigned attenuation and a phase different that should be estimated. Non-selective fading remaining will be corrected by the usual interleaving techniques [14].
The analysis shows that the modulator and demodulator can be realized from inverse Fourier transformers and direct Fourier transformers [14], [20]. To combat against the interference inter symbols a guard interval is introduced between the symbols is larger than the propagation delay between the path guarantees and other paths (Figure 1.3).

$$T_g \geq \tau_{max} \tag{1.3}$$

where T_g is guard interval duration and τ_{max} is a channel delay.

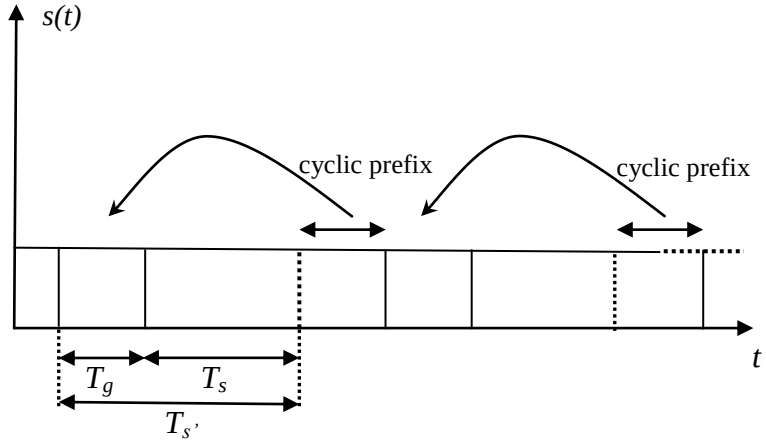

Figure 1.3. Guard interval [4]

Figure 1.4 shows an OFDM modulator. Consider a sequence of L symbols $d_0,d_1,\ldots..d_{L-1}$ the modulated OFDM signal is given by the following expression [4]:

$$s(t) = \sum_{l=0}^{L-1} d_l e^{j2\pi f_l t} \quad \text{with } f_l = f_0 + \frac{l}{T_s} \tag{1.4}$$

where f_l is the frequency of the carrier index l and f_0 is the frequency of the original carrier.

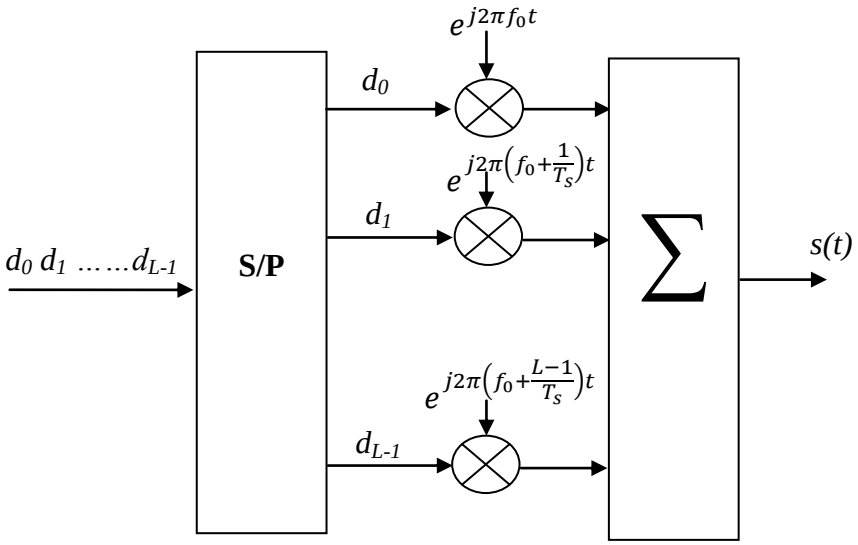

Figure 1.4. Block diagram of OFDM modulator

The choice of the parameters of an OFDM system is a trade-off between various conflicting requirements. A typical design is based on a given system bandwidth B_{OFDM} and a given maximum channel delay τ_{max} [4], [21]. To ensure an *ISI* free system, the guard interval is chosen according to Eq 1.3. Recalling that the carrier spacing for OFDM is $\Delta f = 1/T_S$, the limit is given by the minimum carrier spacing that is tolerable by the system requirements[4], [21]. Indeed, the Doppler spread broadens the spectrum of the received signal and the spectra of closely spaced subcarriers may overlap for high velocities [4], [21]. This gives rise to *Inter Carrier Interference (ICI)*. To avoid this effect, the subcarrier spacing has to be chosen much larger than the range of the Doppler power spectrum, i.e. $\Delta f >> 2f_m$ (cf. Eq 1.2). A low carrier spacing also makes the system more sensitive to frequency offsets and phase noise [4], [21].

1.5 Multiple access techniques

Modern cellular systems are intended to enable simultaneous communications of multiple users. These users have to share the bandwidth available for a wireless communication system. The aim of multiple access techniques is to efficiently use the bandwidth, while ensuring good transmission quality for all active users [4].

1.5.1 Duplexing

Duplexing is a property known from the conventional telephone system, where the user can speak and listen simultaneously, and is provided by most wireless systems. The duplex mode in wireless communications defines the way the bandwidth is shared between the downlink and the uplink [4].
Two basic duplex modes are depicted briefly in the following subsections [4].

1.5.1.1 Frequency Division Duplex (FDD)

In FDD (Figure 1.5) the up- and down-links are allocated in different frequency bands. These frequency bands are separated by a guard band [4]. FDD requires a special device in the transceiver called duplexer that separates the RF chains of the receiver and the transmitter so that they can operate simultaneously [4], [22]. Other drawbacks of FDD are the loss in bandwidth due to the guard band and a lack of flexibility due to the fact that a constant bandwidth is always allocated to the UL and the DL regardless of the traffic conditions. On

the other hand, the independent simplex links of FDD facilitate synchronisation and may have some advantages in multi-cellular contexts [4].

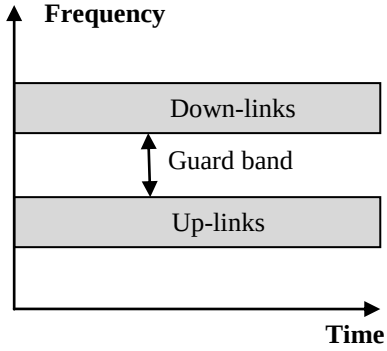

Figure 1.5. Frequency Division Duplex [4]

1.5.1.2Time Division Duplex (TDD)

TDD uses the same frequency band for UL and DL and allocates them in different time slots. Thus, this system is not real duplex, but the UL and DL transmissions alternate so quickly that the user is not aware of the difference [4], [22]. TDD requires a precise time synchronisation of the mobile and the terminal to ensure that the UL and DL transmission slots are well respected [4], [22].

Additionally, a guard time is generally left between the slots as shown in Figure 1.6. The advantages of TDD are the simplified transceiver, which does not require the duplexer, and an increased flexibility to cope with variable traffic, since the length of UL and DL slots can be varied [4], [22]. However, because of its high demands in terms of synchronisation TDD is generally limited to indoor transmissions within a short range [4], [22].

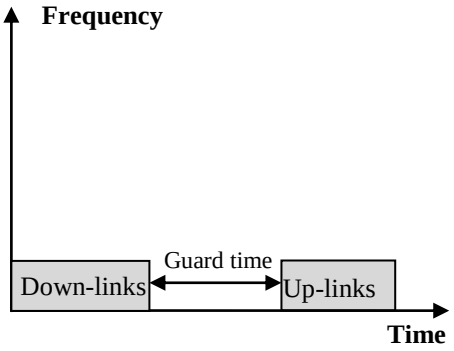

Figure 1.6. Time Division Duplex TDD [4]

1.5.2 Multiple access schemes

The duplex modes are used to allocate the UL and DL of a single user within the considered frequency band. Similar principles can also be used to allocate the signals of different users sharing the same system resources. The three dimensions representing the system resources are frequency, time and the spreading code [4], [22].

1.5.2.1 FDMA technical

FDMA technology was the first method developed and used in analog telephony systems. It divides the spectrum into frequency bands associated with each user (Figure 1.7). In reception, a selective filter tuned to the frequency band of desired user allows to recover data [4].

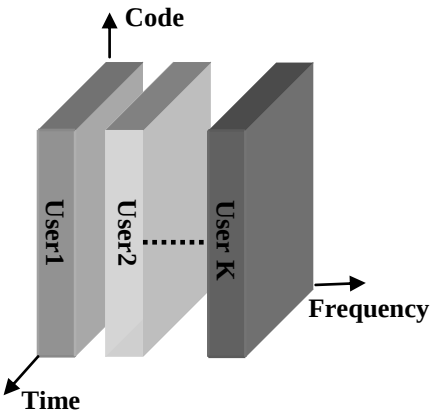

Figure 1.7. FDMA scheme [4]

1.5.2.2 TDMA technical

The TDMA technology is based on the distribution of resources in time. The users share the same bandwidth and data to be transmitted in different time intervals (Figure 1.8). The receiver executes the demultiplexing operation to retrieve data [4].

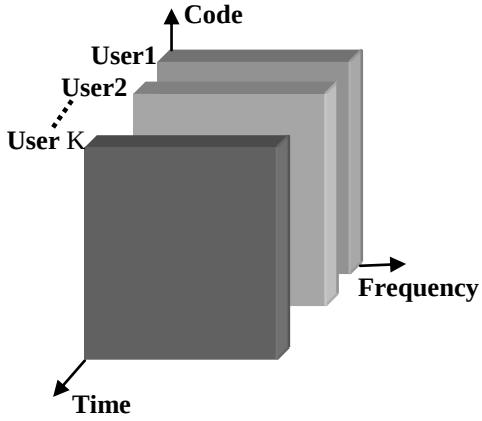

Figure 1.8. TDMA scheme [4]

1.5.2.3 CDMA technical

It is a technical used for several radio communications technologies. The basic idea is several users send information simultaneously through a single channel and occupy the same frequency band (Figure 1.9).

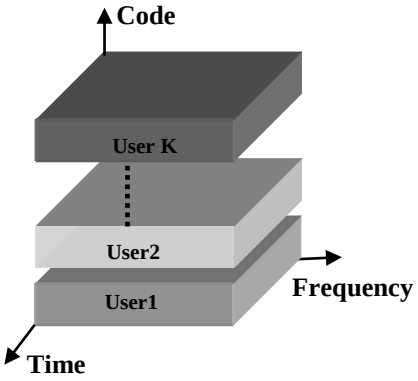

Figure 1.9. CDMA scheme [4]

1.6 Spreading

The spreading code is given by a normalised code vector of length L composed of elements $c_{k,l}$ and defined as follows [4]:

$$c_{k,l} = \left[c_{k,1} c_{k,2} \dots \dots \dots \dots . c_{k,L}\right]^T \text{ with } \quad \left|c_{k,l}\right|^2 = 1 \tag{1.5}$$

where $[\,.\,]^T$ denotes the vector transposition.

Several choices for the spreading codes are presented in section 1.6.4 and 1.6.5. The role of this code is to separate the signals of the different users so that each of them can be extracted from the received signal by despreading with the user-specific code [4].

The choice of the spreading code depends on several factors such as the orthogonality and correlation properties of the codes, the synchronism of users, the implementation complexity. In the downlink, where the signals of the different users are synchronously transmitted, orthogonal code sets are generally used. Examples of such orthogonal codes are Walsh-Hadamard codes, Golay codes, and orthogonal Gold codes [4], [23], [24]. In the uplink, code orthogonality is less important since the users' signals propagate through different transmission channels, which irreparably breaks their orthogonality. Here, simple *Pseudo Noise (PN)* sequences [25] can be chosen. For asynchronous uplink systems, codes with a good cross-correlation property, e.g. Gold, Kasami code [4], [25], are required. Different scheme of spreading are shown in Figure 1.10.

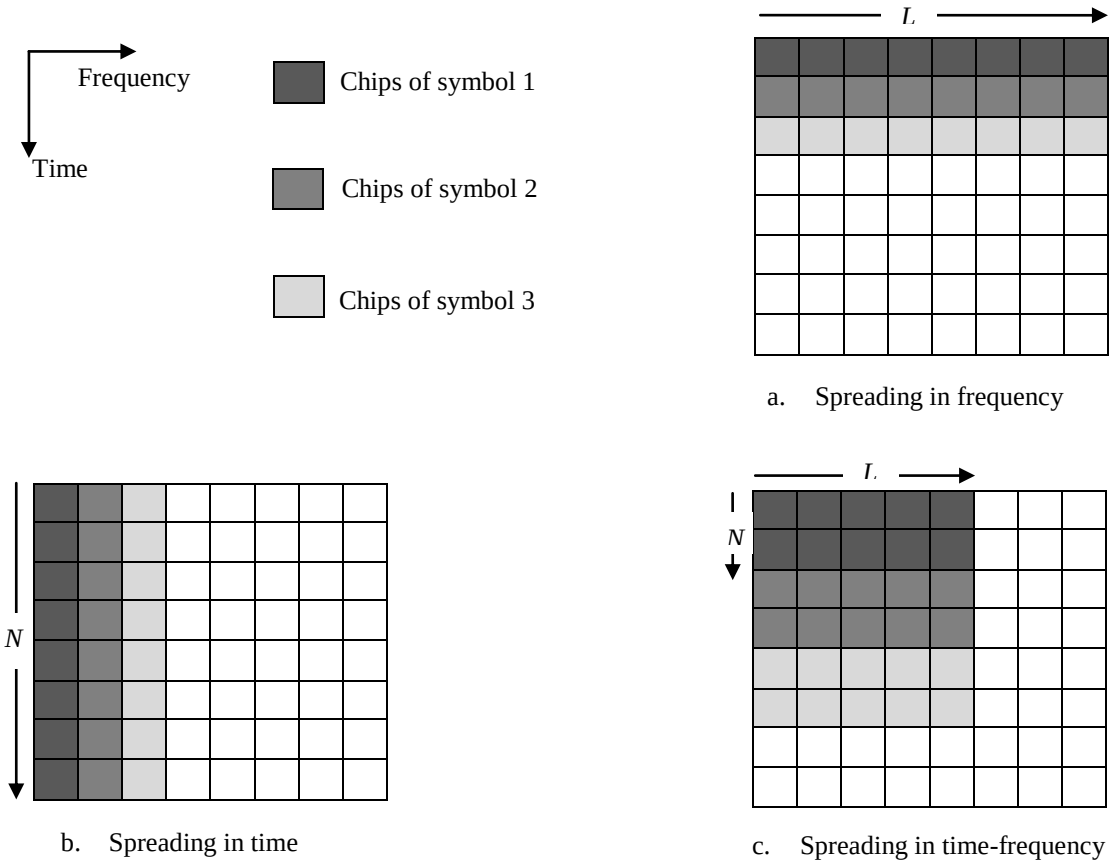

a. Spreading in frequency

b. Spreading in time

c. Spreading in time-frequency

Figure 1.10. Different scheme of spreading [4]

1.6.1 Spreading in time

The first mapping (1.10.a) corresponds to a symbol spreading in the time dimension only [4]. In practice, spreading in the time dimension yields a high correlation of the channel coefficients affecting the different chips since the coherence time of the channel generally spans a large number of OFDM symbols [4]. A strong correlation of the fading coefficients affecting the chips has the advantage that the orthogonality of the users' signals is almost conserved, which leads to a low MAI at the receiver [4]. The disadvantage of correlated fading on the chips is that only a low diversity gain is obtained from spreading. In this case, an efficient bit interleaving is required to benefit from the diversity offered by the channel [4].

1.6.2 Spreading in frequency

Spreading in frequency according to the scheme (1.10.b). Depending on the relation of the spreading factor and the coherence bandwidth of the channel, this scheme can benefit from a high frequency diversity by spreading over subcarriers spanning several times the coherence bandwidth. However, the diversity is obtained at the price of a high MAI level [4].

1.6.3 Two dimensional spreading in time-frequency

Scheme (1.10.c) represents two dimensional spreading in time-frequency. For two dimensional spreading, the code vectors can be built from different spreading codes in frequency-time of lengths L and N, respectively [26]. Alternatively, the chips of a single spreading code of length L can be consecutively mapped to the frame positions. There is again the trade-off between diversity and MAI [4]. A large spreading factor together with two dimensional spreading in the OFDM frame can collect the maximum diversity offered by the channel [4], [26]. In contrast, two dimensional spreading within the rectangle given by the coherence time and bandwidth yields a high correlation of the fading affecting different chips and consequently a low MAI level [4], [27].

We can change the values for N and L to form different spreading dimensions in both time and frequency domains, as shown in Figure 1.11, where three different time-frequency domains spreading dimensions are shown [4].

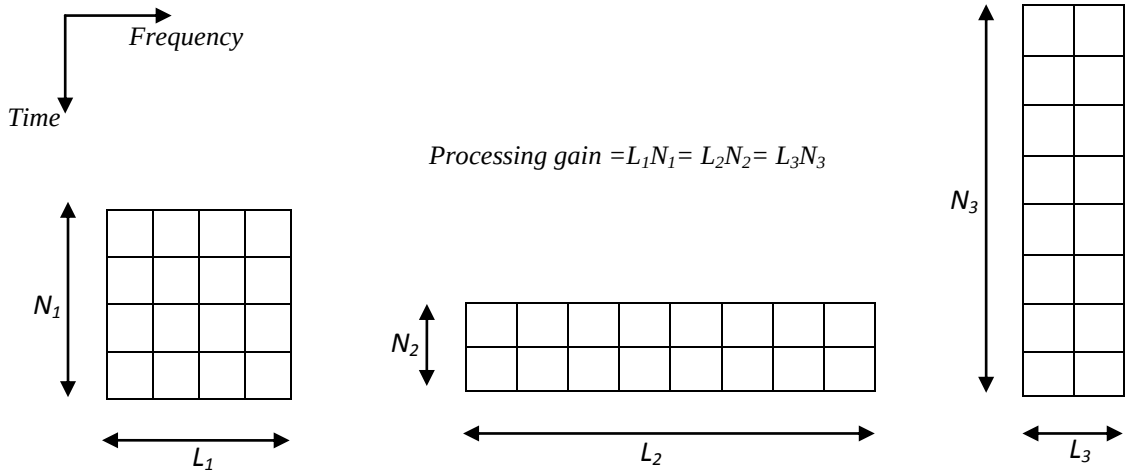

Figure 1.11. Three different time-frequency spreading dimensions [4].

The capability to allow dynamic change in time-frequency domain spreading factors can help to exploit different characteristic features in the time-requency domain spreading [4]. For instance, if we use a relatively large time domain spreading factor N and relatively small frequency domain spreading factor L, the orthogonality of the spreading codes will relay mainly on the time domain orthogonality of the spreading codes [4]. Therefore, in this case the orthogonality of the codes is relatively sensitive to the time-variant properties of the channel, but less susceptible to the frequency-selective fading effect in the channel. On the other hand, if we choose to use two-dimensional spreading codes with a relatively small time domain spreading factor but relatively large frequency domain spreading factor, the orthogonality of the two-dimensional spreading codes will be more sensitive to the frequency-selectivity of the channel than to the time-selective fading caused by the Doppler effect. Therefore, dynamically choosing the right N and L will give us another degree-of-freedom in designing a wireless communication system for many future applications [4].

The two dimensional spreading in the time-frequency domain allows us to implement some new two dimensional interleaving schemes for a wireless communication system. In the chapter 3, we will give some more detailed discussions.

1.6.4 Orthogonal multiple access

The CDMA system requires orthogonal codes for channel selection. Since CDMA systems use the same frequency bands for all transmissions, only a different code can be used to select a channel.
Orthogonal codes have the following characteristics:

$$\sum_{k=1}^{K} c_i(kT_s)c_j(kT_s - lT_s) = 0, i \neq j\,, l = 0,1, \ldots\ldots\ldots L \quad (1.6)$$

Where c_i and c_j is the i^{th} and j^{th} orthogonal members of an orthogonal set, L is length of set, T_s is the symbol duration.

Equation 1.6 implies that the cross-correlation of two different symbol shapes is zero for all time offsets and each spreading code is orthogonal to itself. The orthogonality conditions in this equation mean that different user signals can be separated at the receiver, even though they use the same frequency channel and the same period.

1.6.4.1 Walsh code

An important set of orthogonal codes is the Walsh set [28]. Walsh functions are generated using an iterative process of constructing a Hadamard matrix, starting with H_1 = [0].
The Hadamard matrix is built by:

$$H_{2n}=\begin{bmatrix} H_n & H_n \\ H_n & \bar{H}_n \end{bmatrix} \quad (1.7)$$

For example, the Hadamard matrix of order 2 and 4 will be:

$$H_2 =\begin{bmatrix} 0 & 0 \\ 0 & 1 \end{bmatrix} \quad (1.8)$$

and

$$H_4 = \begin{bmatrix} 0 & 0 & 0 & 0 \\ 0 & 1 & 0 & 1 \\ 0 & 0 & 1 & 1 \\ 0 & 1 & 1 & 0 \end{bmatrix} \tag{1.9}$$

From the corresponding Hadamard matrix, the Walsh codes are given by the rows. We usually map the binary data to polar form so we can use real number arithmetic when computing correlations. So, 0^s are mapped to 1^s and 1^s are mapped to -1^s [28].
This means the k^{th} row of the $H(n)$ Hadamard matrix is [28]:

$$H(0)=1 \tag{1.10}$$

where $C(0, 0) = 1$

$$H_2 = \begin{bmatrix} 1 & 1 \\ 1 & -1 \end{bmatrix} \tag{1.11}$$

where: $C(0, 2) = 1, 1$; $C(1, 2) = 1, -1$

$$H_4 = \begin{bmatrix} 1 & 1 & 1 & 1 \\ 1 & -1 & 1 & -1 \\ 1 & 1 & -1 & -1 \\ 1 & -1 & -1 & 1 \end{bmatrix} \tag{1.12}$$

where: $C(0, 4) = 1, 1, 1, 1$; $C(1, 4) = 1, -1, 1, -1$; $C(2, 4) = 1, 1, -1, -1$; $C(3, 4) = 1, -1, -1, 1$

To illustrate the orthogonality between two Walsh-Hadamard codewords, we can test them as follows. For example, let us see if the second and the third codeword of H_4 are orthogonal. Hence we get the following two codewords, in vector form, as [28]:

$$C(1, 4) \otimes C(2, 4) = (1 \times 1) + ((-1) \times 1) + (1 \times (-1)) + ((-1) \times (-1)) = 1 - 1 - 1 + 1 = 0 \tag{1.13}$$

where the operator $\otimes$ denotes the element-by-element multiplication operation between two vectors or sequences.

1.6.5 Quasi-Orthogonal CDMA

As mentioned in Section 1.6.4.1, the Walsh codes provide good orthogonality properties when they are aligned in time. Their orthogonality may suffer when they are not aligned in time [28]. Ideally, we would like to have sequences that are orthogonal for all time shifts. However, in practice the sequences that are approximately orthogonal are achievable. One class of sequences that satisfies this condition is the class of quasi-orthogonal codes [28]. The name quasi-orthogonal codes indicates that all of these spreading codes or sequences are not exactly orthogonal even if they are used in a synchronous transmission CDMA system. However, their cross-correlation functions are somehow still quite acceptable in the sense that at different chip offsets they are under control, usually being below a certain level to limit multiple access interference (MAI) [28].
As a matter of fact, the quasi-orthogonal CDMA codes comprise a fairly large number of codes, and thus the majority of the work on the subject of CDMA coding in the literature was dedicated to them. The most widely used quasi-orthogonal CDMA codes include Gold codes, Kasami codes, m-sequences [28]. In the appendix B, we will give some more detailed discussions.

1.7 Interleaving

Interleaving is a technique commonly used to disperse the sequences of bits in a bit-stream so as to minimize the effect of correlated channel noise such as burst error or fading [29]. In interleaving mechanism, the input data rearranges itself such that consecutive data are split among different blocks. At the receiver end, the interleaved data is arranged back into the original sequence by the de-interleaving. As a result of interleaving, correlated noise introduced in the transmission channel appears to be statistically independent at the receiver and thus allows better error correction.

Based on different implementation aspects, the interleaving are divided in two main categories named as block interleaving and convolutional interleaving [29].

1.7.1 Block Interleaving

The block interleaving [30], [31] is one of the most basic and commonly used types of interleaving in communication systems. It scrambles the information sequence by writing it row wise and reading it column wise. In general a block interleaving can be described in terms of a (*N* x *M*) matrix. There exist four variations for this scheme [31].

The schemes vary according to the order in which columns are read (LR: left to right or RL: right to left) and the order in which rows are read (TB: top to bottom or BT: bottom to top). A (4x4) block interleaving is shown in Figure 1.12, where the matrix elements represent the index of the information sequence. All of the four possible schemes of a block interleaving are shown in this Figure.

There are some other classifications based on their properties, which will also be discussed briefly in the following subsections.

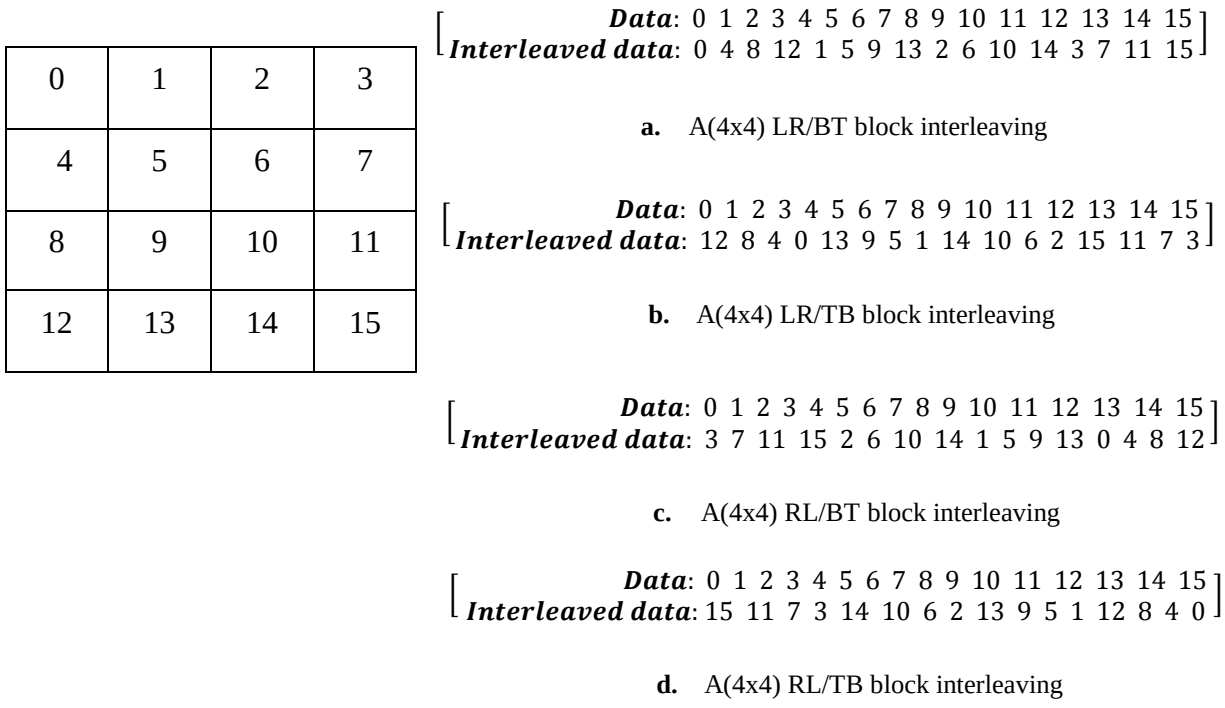

Figure 1.12. Different strategies for (4x4) block interleaving [31]

1.7.1.1 Random Interleaving

This interleaving is a special kind of the block interleaving that input the symbols in block and arranged by a random permutation [32]. The main disadvantage is that once generated through some random function, they cannot be reproduced as such. However, they tend to perform very well against any form of the burst errors.

All types of theoretical work regarding interleaving design is usually compared with a random interleaving, therefore it serves as a bench marking tool towards performance for newly evolved interleaving types.

A random interleaving scheme is shown below in Figure 1.13.

0	1	2	3
4	5	6	7
8	9	10	11
12	13	14	15

$$\begin{bmatrix} \boldsymbol{Data}: & 0 & 1 & 2 & 3 & 4 & 5 & 6 & 7 & 8 & 9 & 10 & 11 & 12 & 13 & 14 & 15 \\ \boldsymbol{Interleaved\ data}: & 5 & 9 & 8 & 15 & 4 & 14 & 7 & 1 & 6 & 2 & 11 & 3 & 13 & 0 & 12 & 10 \end{bmatrix}$$

Figure 1.13. Random interleaving of length 16.

1.7.1.2 Prime Interleaving

Prime interleaving rotates about a prime number *P* as seed of interleaving. Given a block size *K*, a simple prime interleaving can be constructed by defining just one prime number *P*, as follows:

$$Position_{new} = (1 + (position - 1)P) mod\ K \qquad (1.14)$$

where *position* = 1, 2, 3,……..*K* .

They are considered to be easier to implement as compared to random interleaving.

As shown in Figure 1.14, if we have input sequence as: 1, 2, 3, 4, 5, 6, 7, 8, 9, 10, 11, 12, 13, 14, 15,16 the prime interleaving output with *P*=3 is: 1, 4, 7, 10, 13, 16, 3, 6, 9, 12, 15, 2, 5, 8, 11, 14.

1	2	3	4
5	6	7	8
9	10	11	12
13	14	15	16

$$\begin{bmatrix} \boldsymbol{Data}: & 1 & 2 & 3 & 4 & 5 & 6 & 7 & 8 & 9 & 10 & 11 & 12 & 13 & 14 & 15 & 16 \\ \boldsymbol{Interleaved\ data}: & 1 & 4 & 7 & 10 & 13 & 16 & 3 & 6 & 9 & 12 & 15 & 2 & 5 & 8 & 11 & 14 \end{bmatrix}$$

Figure 1.14. Prime interleaving of length 16.

1.7.1.3 Chaotic interleaving

The chaotic interleaving generates permuted sequences with lower correlation between their samples and adds a degree of encryption to the transmitted signal. Let $B(n_1, \ldots, n_c)$, denote the discretized map, where the vector $[n_1, \ldots, n_c]$ represents the secret key S_{key}. Defining K as the number of data items in one row, the secret key is chosen such that each integer n_i divides K, and $n_1 + \cdots + n_c = K$. Let $k_i = n_1 + \cdots + n_i$. The data item at the indices (r, s) is moved to the indices [33], [34], [35]:

$$B(r,s) = \left[\frac{K}{k_i}(r - K_{\mathrm{i}}) + s \bmod \left(\frac{K}{k_i}\right), \frac{k_i}{K}\left(s - s \bmod \left(\frac{K}{k_i}\right)\right) + K_i\right] \tag{1.15}$$

where $K_i \leq r < K_i + n_i$, and $0 \leq s < K$.

In steps, the chaotic interleaving is performed as follows [33], [36], [37]:

1. An $K \times K$ square matrix is divided into K rectangles of width n_i and number of elements K.
2. The elements in each rectangle are rearranged to a row in the permuted rectangle. Rectangles are taken from left to right beginning with upper rectangles then lower ones.

3. Inside each rectangle, the scan begins from the bottom left corner towards upper elements.

Figure 1.15, shows an example for the chaotic interleaving of an (4×4) square matrix (i.e. K=4). The secret key $S_{key} = [n_1, n_2, n_3] = [1, 2, 1]$.

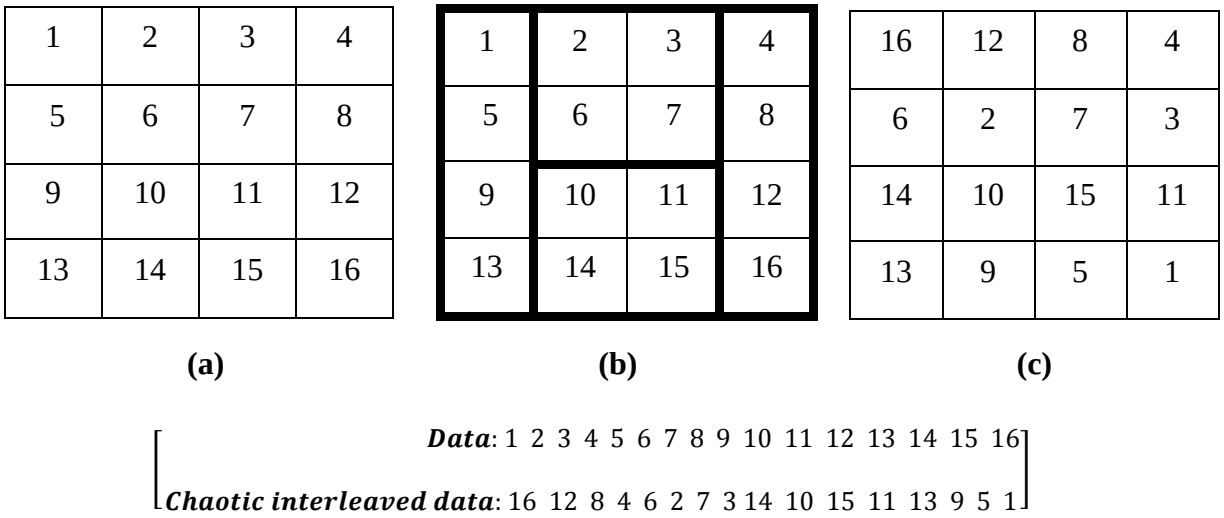

Figure 1.15. Chaotic interleaving of an 4×4 matrix [33]

(a) : the 4×4 matrix
(b) : the 4×4 matrix divided into rectangles
(c) : block interleaving of the matrix

1.7.2 Convolutional interleaving

The structure of a convolutional interleaving is shown in Figure 1.16.
where M is the register number and J is the amount of storage. d indicate one symbol delay. The first branch does not provide any storage, and it acts as a direct connection. The input and output of the all the branches are connected to commutator switches [29]. The commutator switch at the input is connected to the output of encoder. The code symbols from encoder are sequentially shifted in different registers through the input commutator switch, which connects to all the branches in a cyclic way [29].

With each new code symbol the commutator returns to the first branch and restarts again. The output commutator switch works in synchronization to the input commutator switch, and takes the data from different branches sequentially [29].

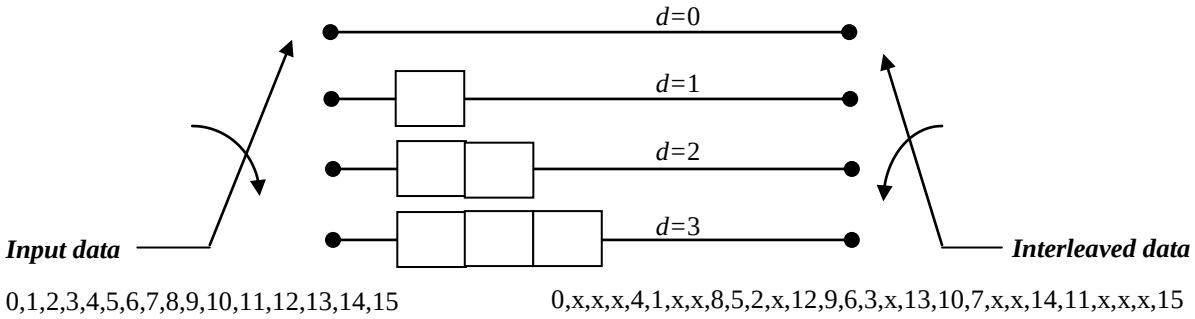

Figure 1.16. Convolutional interleaving with register number M=4 and symbol storage J=1, [32].

For example if we have input sequence as 0, 1, 2, 3, 4, 5, 6, 7, 8, 9, 10, 11, 12, 13, 14, 15 the convolutional interleaving output is 0, x, x, x, 4, 1, x, x, 8, 5, 2, x, 12, 9, 6, 3, x, 13, 10, 7, x, x, 14, 11, x, x, x, 15.
where ‘x’ indicate the empty element at the time instant.

Conclusion

We introduced in this chapter the basics to understand digital transmissions systems. The general scheme and different effects that influence the signal received after propagation through the radio channel were presented. This chapter also introduced the general concepts of OFDM and Multiple access technique. We then focused on the different scheme of spreading; the two dimensional spreading in the time-frequency domain allows us to implement some new two dimensional interleaving scheme, which will be the subject of study in Chapter 3.

Chapter 2

MC-MC-CDMA
system presentation

Contents

Introduction 29

2.1 Multi-code and *M-ary* CDMA techniques..... 29

2.1.1 Orthogonal code system..... 29

2.1.2 Parallel combinatorial system..... 31

2.1.3 BPSK M-ary CDMA system..... 33

2.1.4 Multi-Code CDMA system..... 34

2.2 Multi-Carrier CDMA system..... 36

2.3 Multi-Code Multi-Carrier CDMA system..... 37

2.3.1 Transmitter model..... 37

2.3.2 Channel model..... 39

2.3.3 Receiver model..... 39

2.3.4 Performance Comparison for MC-MC-CDMA..... 41

Conclusion..... 45

Introduction

The ambition of the next generation of transmission is to achieve higher rates. That said, more spectral efficiency increases, the transmission constraints of mobility and diversity of services are increasing. The solution is given by the MC-MC-CDMA (Multi-code Multi-carrier CDMA) which is combinations of the multi-code CDMA and multi-carrier CDMA.
In this chapter, we describe and analyze this system and then we look at its performance. A new expression of MRC is established. Then we present the numerical results of the BER's. To make a comparative study; the BER's of MC-MC-CDMA, Multi-carrier CDMA and Multi-code CDMA systems were determined.

2.1 Multi-code and *M-ary* CDMA techniques

There are a lot of varieties of multi-code CDMA schemes. So, we present the major systems, such [28]:

- Orthogonal code system
- parallel combinatorial system
- BPSK *M*-ary CDMA system
- multi-code system

2.1.1 Orthogonal code system

The first multi-code CDMA scheme was named the orthogonal code system and was proposed in 1987 by *Enge* and *Sarwate* [38]. The basic idea for an orthogonal code system is described as follows [28].
Assume that there are *M* different spreading codes available to a particular user in the system. Each transmitter will first group the original information data stream into symbols, each of which will consist of m bits such that $m = log2M$ [28]. The transmission from the transmitter will choose one from *M* different codes, depending on the bit patterns of a symbol (which contains *m* bits). The mapping strategy of the orthogonal code system is shown in Table 2.1, where there are eight spreading codes (g_1, g_2, g_3, g_4, g_5, g_6, g_7, g_8) and each code will be selected to denote a particular data bit pattern of (d_0, d_1, d_2). More spreading codes could be used to encode more bits in each symbol [28]. Obviously, in this scheme a transmitter will

only send one particular spreading code each time to denote a particular data bit pattern in a symbol [28].

Data			Spreading code							
d_0	d_1	d_2	g_1	g_2	g_3	g_4	g_5	g_6	g_7	g_8
0	0	0	+1	0	0	0	0	0	0	0
0	0	1	0	+1	0	0	0	0	0	0
0	1	0	0	0	+1	0	0	0	0	0
0	1	1	0	0	0	+1	0	0	0	0
1	0	0	0	0	0	0	+1	0	0	0
1	0	1	0	0	0	0	0	+1	0	0
1	1	0	0	0	0	0	0	0	+1	0
1	1	1	0	0	0	0	0	0	0	+1

Table 2.1. Mapping table for orthogonal code system with M = 8, [28].

The block diagrams for the transmitter and receiver in a orthogonal code system are shown in Figures 2.1 and 2.2, respectively. In the transmitter diagram, there are in total M spreading codes, which are denoted ($g_1, g_2, \ldots, g_M$) [28]. The transmitter should select one of the M spreading codes for a particular input data bit pattern in each symbol. In the receiver block diagram, the received signal $r(t)$ should be despread by all M spreading codes, as the receiver has no way of knowing in advance which spreading code will appear at a given time [28]. The output from the M despreading units will be fed into a processor to select the largest value among the M inputs. This largest value will be considered as the code the transmitter sent and will then be sent into a de-mapping unit to decode the sent information using the mapping relation shown in Table 2.1[28].

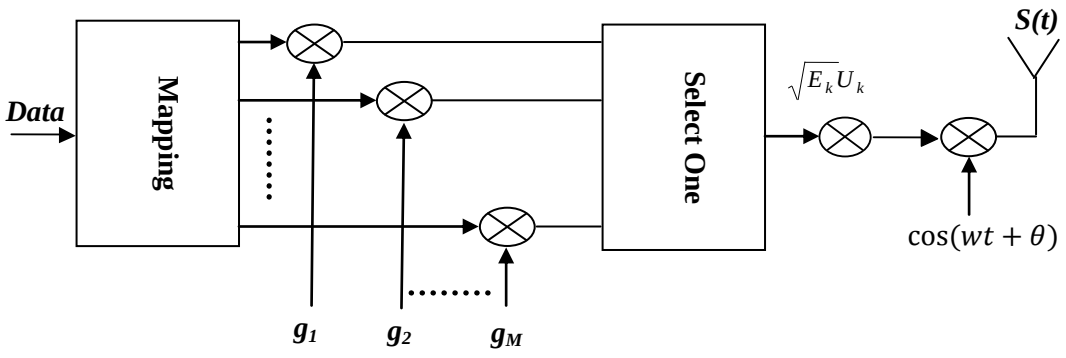

Figure 2.1. Orthogonal code system transmitter [28]

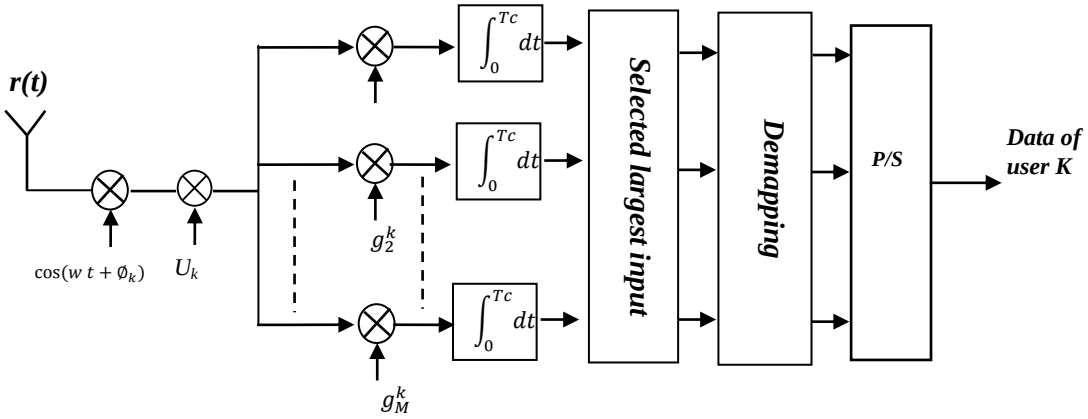

Figure 2.2. Orthogonal code system receiver [28]

2.1.2 Parallel combinatorial system:

Another multi-code CDMA scheme is the parallel combinatorial system, which was proposed in 1999 by *Guo* and *Milstein* [39]. In the parallel combinatorial system, each user will also be allocated *M* different spreading codes [28]. However, the user can encode its data bit symbol by using different possible combinations of the number of sent spreading codes and their signs. In this way, the parallel combinatorial system will have a greater degree of freedom in controlling the data transmission rate, compared with the multi-code system discussed above. The block diagrams for a transmitter and a receiver for the parallel combinatorial system are shown in Figures 2.3 and 2.4, respectively [28]. In the parallel combinatorial system transmitter, there are three important parameters, which are the number of spreading codes assigned to a transmitter *M*, the number of actual codes sent each time u, and the number of bits in each symbol $m = log_2 2^u C_u^M$, where C_u^M stands for calculation of combinations to select *u* samples from *M* elements [28].

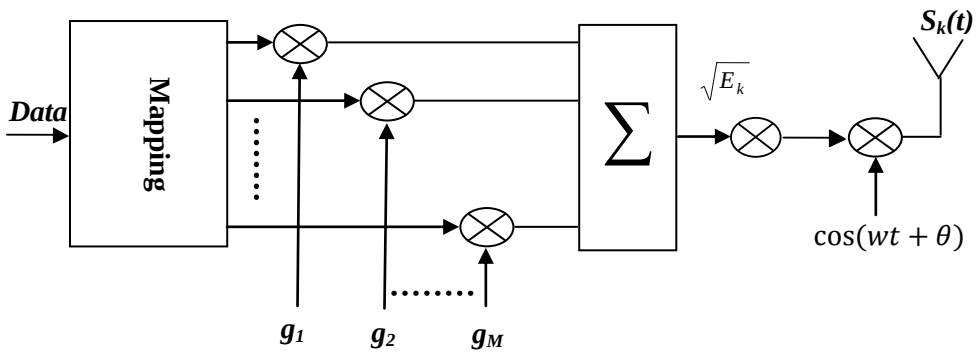

Figure 2.3. Parallel combinatorial system transmitter [28]

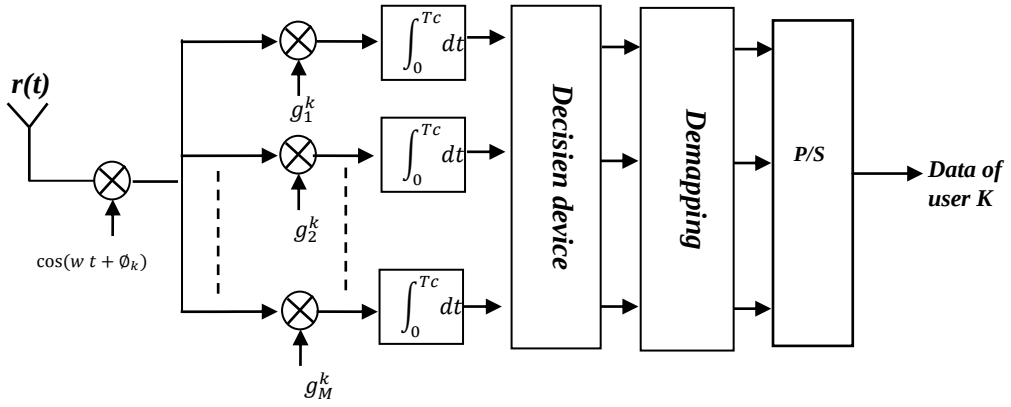

Figure 2.4. Parallel combinatorial system receiver [28]

Table 2.2 illustrates the mapping algorithm to encode the original data bit patterns in each symbol to the spreading codes which are to be sent into the channel [28].

Data			Spreading code		
d_0	d_1	d_2	g_1	g_2	g_3
0	0	0	+1	+1	0
0	0	1	+1	−1	0
0	1	0	−1	−1	0
0	1	1	−1	+1	0
1	0	0	+1	0	+1
1	0	1	+1	0	−1
1	1	0	−1	0	−1
1	1	1	−1	0	+1
\	\	\	0	+1	+1
\	\	\	0	+1	−1
\	\	\	0	−1	−1
\	\	\	0	−1	+1

Table 2.2. Mapping table for a parallel combinatorial system with M = 3 and u = 2, [28].

2.1.3 BPSK *M-ary* CDMA system

As the most general multi-code CDMA system, the BPSK *M-ary* CDMA system (see appendix A) is capable of offering the highest data transmission rate among all multi-code CDMA schemes. In addition, it is the most flexible multi-code CDMA scheme in terms of its suitability for multimedia transmissions, where the data rate from a user may change from time to time according to its real-time data rate requirements [28].

In the BPSK *M-ary* CDMA system, each user is given M (>1) spreading codes, each of which can be encoded by three different values, +1, −1, and 0. It is noted that when a code is encoded by 0, it simply means the transmitter will send nothing. Let us use an example to illustrate how it works [28].

Letting $M = 3$ (there are three codes g_1, g_2, and g_3), we can have the following possible states for a transmitter to send different spreading codes. It can send one code (which has six possibilities: $+g_1$, $-g_1$, $+g_2$, $-g_2$, $+g_3$, $-g_3$); it can send two codes (which has 12 possibilities[28]: $+g_1\ +g_2$, $+g_1\ +g_3$, $+g_2\ +g_3$, $-g_1\ +g_2$, $-g_1\ +g_3$, $-g_2\ +g_3$, $+g_1\ -g_2$, $+g_1\ -g_3$, $+g_2\ -g_3$, $-g_1\ -g_2$, $-g_1\ -g_3$, $-g_2\ -g_3$); and it can also send three codes (which has eight possibilities: $+g_1\ +g_2\ +g_3$, $-g_1\ +g_2\ +g_3$, $+g_1\ -g_2\ +g_3$, $+g_1\ +g_2\ -g_3$, $-g_1\ -g_2\ +g_3$, $-g_1\ +g_2\ -g_3$, $+g_1\ -g_2\ -g_3$, $-g_1\ -g_2\ -g_3$). Therefore, altogether we have 6 + 12 + 8 = 26 different states, which is just equal to $3^M - 1 = 3^3 - 1 = 26$. In this way, we conclude that such a BPSK *M-ary* CDMA system can have $3^M - 1$ different code states which can be used to encode information data. Table 2.3 shows the mapping between the data symbol and sent codes for a BPSK *M-ary* CDMA system with $M = 3$ [28].

However, we usually may not be able to make full use of all $3^M - 1$ states. Take again $M = 3$ as an example. In this case we have altogether 26 code transmission states but we can only use any 16 of the 26 states, as we can only choose a symbol block size of 4 bits, in this case due to the fact that $2^4 = 16$ and $2^5 = 32 > 26$. In general, we have $m = log_2(3^M - 1)$ [28].

Data				Spreading code		
d_0	d_1	d_2	d_3	g_1	g_2	g_3
0	0	0	0	+1	0	0
0	0	0	1	−1	0	0
0	0	1	0	0	+1	0
0	0	1	1	0	−1	0
0	1	0	0	0	0	+1
0	1	0	1	0	0	−1
0	1	1	0	+1	+1	0
0	1	1	1	+1	−1	0
1	0	0	0	−1	−1	0
1	0	0	1	−1	+1	0
1	0	1	0	+1	0	+1
1	0	1	1	+1	0	−1
1	1	0	0	−1	0	−1
1	1	0	1	−1	0	+1
1	1	1	0	0	+1	+1
1	1	1	1	0	+1	−1
\	\	\	\	0	−1	−1
\	\	\	\	0	−1	+1
\	\	\	\	+1	+1	+1
\	\	\	\	−1	+1	+1
\	\	\	\	+1	−1	+1
\	\	\	\	+1	+1	−1
\	\	\	\	−1	−1	+1
\	\	\	\	−1	+1	−1
\	\	\	\	+1	−1	−1
\	\	\	\	−1	−1	−1

Table 2.3. Mapping table for a BPSK M-ary CDMA system with $M = 3$ [28].

2.1.4 Multi-Code CDMA system

A novel multi-code system has been proposed in [40] to support variable data rates. The block diagrams for a transmitter and a receiver for the Multi-Code CDMA system is shown in Figures 2.5 and 2.6, each user has a set of M code sequences, where M is the ratio of the base data rate and required data rate. The base rate is achieved with set of just two sequences. The *M-ary* symbol to be transmitted selects one of the code sequences of length N, which is then multiplied chip-wise with the user specific sequence. The user-specific sequence is a U_k sequence of the same length N as the code sequences [9].

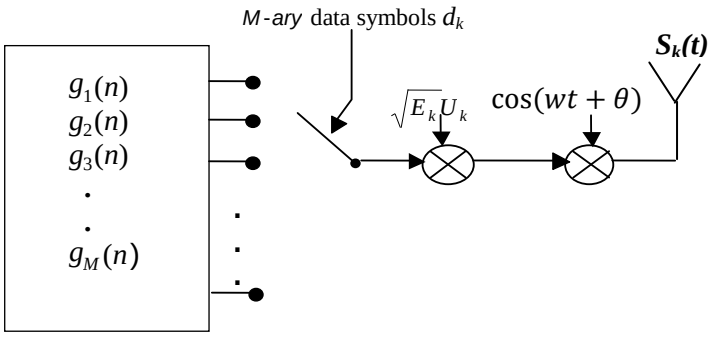

Figure 2.5. Multi-code CDMA system transmitter [9]

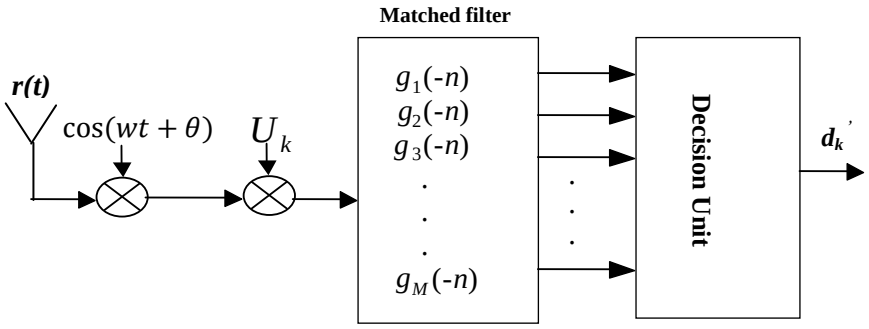

Figure 2.6. Multi-code CDMA system receiver [9]

With these, *M-ary* data symbols d_k are transmitted at rate $1/T_s$,where T_s is symbol duration. The sequence set of each user is implemented as a chip wise product of a user specific sequence $U_k(n)$.

The symbols d_k is mapped onto [9]:

$$G_m(n) = \{g_m(n), 1 \le m \le M\} \tag{2.1}$$

The transmitted signal for user *k* is described as [9]:

$$s_k(t) = \sqrt{E_k} \sum_{n=0}^{N-1} g_{d_k}(n) f(t - nT_c) U_k(n) \cos(wt + \theta_k) \tag{2.2}$$

Where E_k represents the symbol energy for the k^{th} user, $g_{d_k}(n)$ is the selected code sequence, f is a rectangular pulse of duration T_c and *w* is the angular frequency. θ_k is random phase.

The received code sequence is first multiplied chip-wise with user sequence and the resultant is correlated with each of the possible *M* code sequences. The sequence that gives maximum correlation is then mapped back into an *M-ary* symbol.

2.2 Multi-Carrier CDMA system

The principle of MC-CDMA was to perform spreading in the frequency domain. In Figure 2.7, the transmitter of a MC-CDMA system is depicted. Each chip is copied onto *L* branches and multiplied by the corresponding chip of the user specific spreading code. Each branch then modulates a subcarrier and the modulated subcarriers are summed together and transmitted [9], [11].

Consider a MC-CDMA system with *k* users $(0 \le k < K)$. The transmitted signal for user *k* is described by the following equation [41]:

$$s_k(t) = \sqrt{E_k} \sum_{n=-\infty}^{\infty} \sum_{l=1}^{L} d_k(n) f(t - nT_s) c_{kl}(n) \cos(w_l t + \theta_{K,l}) \tag{2.3}$$

where E_k represents the symbol energy for the k^{th} user, $d_k(n)$ is the data bit of user *k* at time *n*, c_{kl} is the spreading sequence chip for user *k* on subcarrier *l*, and ω_l is the angular frequency of subcarrier *l*. $\theta_{k,l}$ is random phase of the l^{th} subcarrier of user *k* and uniformly distributed over $[0,2\pi]$. *Ts* is the symbol interval and *f* is a rectangular pulse of duration *Ts* used to isolate successive symbols.

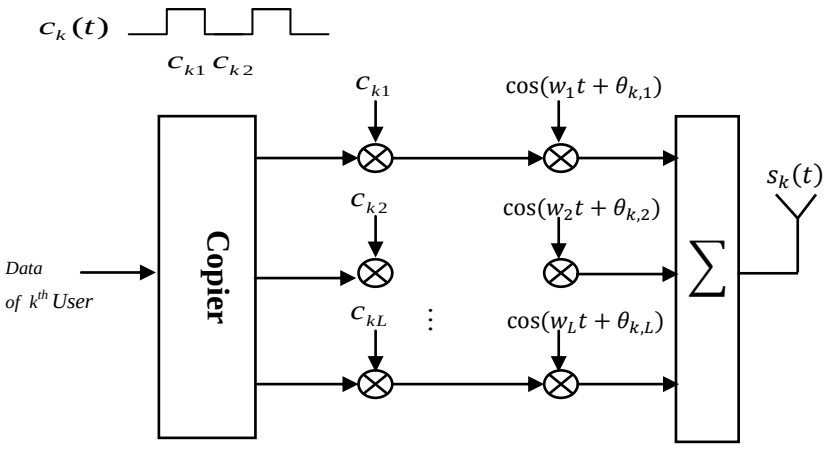

Figure 2.7. Multi-carrier CDMA system receiver [41].

The block diagrams receiver in a Multi-carrier CDMA system is shown in Figures 2.8.

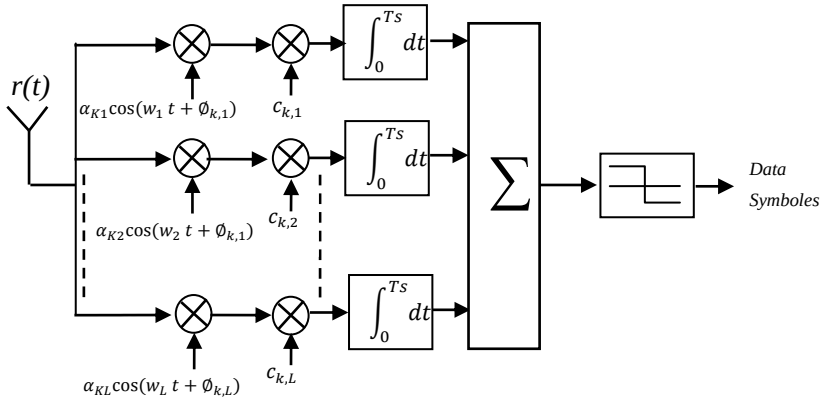

Figure 2.8. Multi-carrier CDMA system receiver [41].

There are several advantages of using MC-CDMA. One of them is multipath mitigation [9]. There is constructive and destructive interference at the receiver due to multipath. Destructive interference causes deep nulls in the received signal power [9]. For a narrowband transmission, if the frequency response null occurs at the signal frequency then the entire signal can be lost [9]. However in wideband signals, dips in the spectrum result in a small loss of signal power. Also, if the transmission bandwidth is divided into many subcarriers, then spectral nulls are unlikely to occur at all of the subcarrier frequencies. Another advantage of MC-CDMA is simplified equalization in the frequency domain [9].

2.3 Multi-Code Multi-Carrier CDMA system

We consider a MC-MC-CDMA model given by [11].

2.3.1 Transmitter model

As shown in Figure 2.9, each user has the same code sequence $g_m(n)$ [11].

$$G_m(n) = \{g_m(n) / \ 1 \leq m \leq M\} \tag{2.4}$$

where $G_m(n)$ is the total matrix of code sequences.

An *M-ary* symbol $d_{k,i}$ of *log2M* bits selects one of *M* Code sequences in $G_m(n)$ for transmission. The i^{th} code sequence of length *N* of user *K* is [11]:

$$S_{k,i}(t) = \sum_{n=0}^{N-1} g_{d_{k,i}}(n) f(t - nT_c - iT_s) \tag{2.5}$$

where T_s is symbol duration and *f* is a rectangular pulse of duration T_c.

Each chip of the selected code sequence is copied onto *L* subcarrier branches and multiplied with the user-specific scrambling code of the corresponding branch $c_{k,l}$. Each of these branches then modulates one of the *L* orthogonal subcarriers and the results are summed [10] [11].

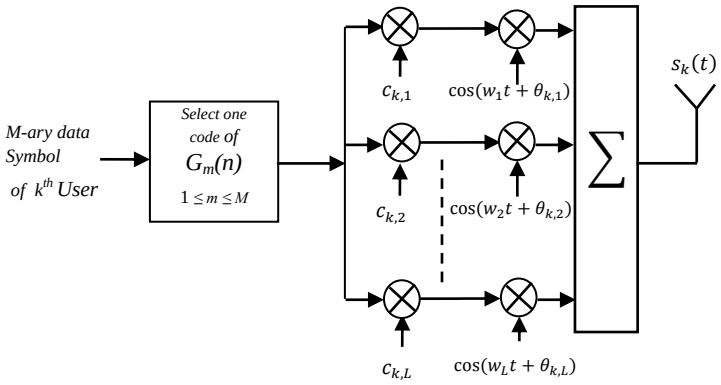

Figure 2.9. Transmitter model of MC-MC-CDMA system [11]

Therefore the transmitted Binary Phase Shift Keying (BPSK) signal of user *K* similar to [11], can be written as:

$$s_k(t) = \sum_{i=-\infty}^{+\infty} \sum_{l=1}^{L} \sum_{n=0}^{N-1} g_{d_{k,i}}(n) f(t - nT_c - iT_s) c_{k,l}(Ni + n) \cos\left(w_l t + \theta_{k,l}\right) \tag{2.6}$$

where w_l is l^{th} carrier frequency, $\theta_{k,l}$ is random phase of the l^{th} subcarrier of user *K* and uniformly distributed over [*0,2π*], and $(Ni + n)$ *i*s the location of l^{th} chip which is multiplied by the n^{th} bit in the i^{th} code sequence of length *N*.

2.3.2 Channel model

Without lose of generality, we consider a frequency-selective Rayleigh fading as a channel model. This choice allows that the MC-MC-CDMA system transmits waveform consisting of a large number of narrowband subcarriers.

Each subcarrier can be writing as a function of a complex flat-fading channel; so, we have [41], [42], [43]:

$$h_{k,l}(t) = h_{k,l}^{I}(t) + jh_{k,l}^{Q}(t)$$
$$= \beta_{k,l}(t)e^{j\varphi_{k,l}(t)} \qquad (2.7)$$

Which is a complex Gaussian random variable with zero mean and variance σ^2. The path gains $h_{k,l}(t)$ is assumed uncorrelated and identically distributed for different *k* and *l*. $\beta_{k,l}(t)$ is a Rayleigh distributed amplitude attenuation and phase shift $\varphi_{k,l}(t)$ are considered to be constant over the time interval $[0,\ T_c]$, [41].

A *Clarke* and *Gans* fading model [9], [11], [22] is considered to produce frequency-selective Rayleigh fading channel with variable gains and three time delays with respect to direct wave by two, three and four chips.

The power delay profile of initial multipath fading channels is depicted in Figure 2.10.

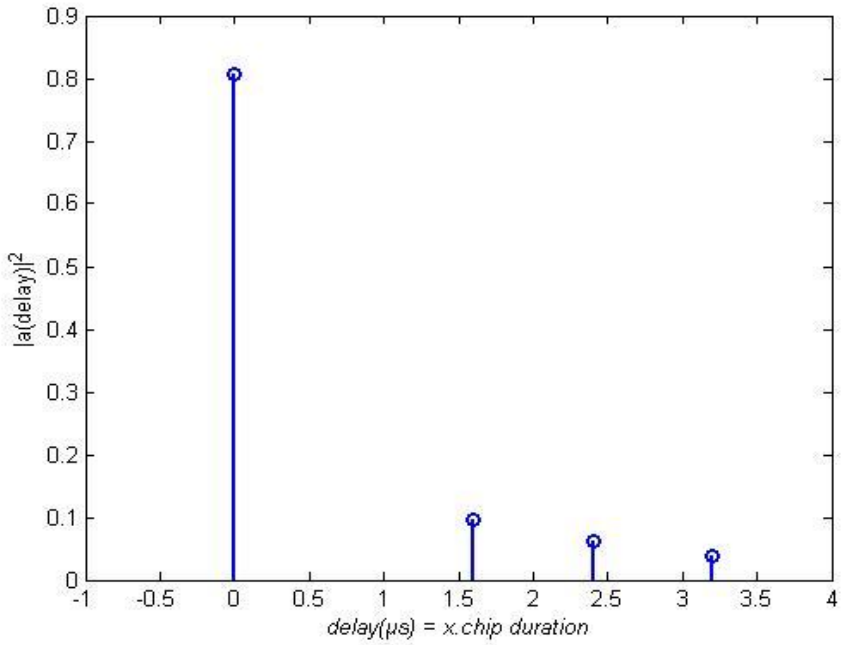

Figure 2.10. Power delay profile.

2.3.3 Receiver model

At the receiver as shown in Figure 2.11, the incoming BPSK signal is [11]:

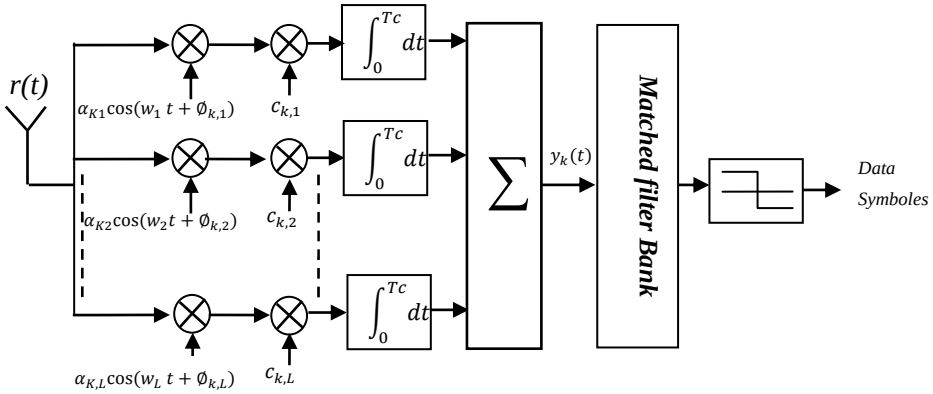

Figure 2.11. Receiver model of MC-MC-CDMA system [11]

$$r(t) = \sum_{i=-\infty}^{+\infty} \sum_{k=1}^{K} \sum_{l=0}^{L} \sum_{n=0}^{N-1} \beta_{k,l}(t) g_{d_{k,i}}(n) f(t - nT_c - iT_s) c_{k,l}(Ni + n) \cos\left(w_l t + \emptyset_{k,l}\right) + \eta(t) \quad (2.8)$$

where $\emptyset_{k,l} = \theta_{k,l} + \varphi_{k,l}$ is the received phase and $\eta(t)$ is the additive white Gaussian noise with zero mean and variance σ^2.

The demodulated code sequence of user 1 after dispreading is [11]:

$$y_1(t) = \sum_{j=0}^{N-1} y_{1,j} f(t - jT_c) \quad (2.9)$$

$$y_{1,j} = \frac{1}{T_c} \int_{jT_c}^{(j+1)T_c} r(t) \sum_{l=1}^{L} c_{1,l}(j) \cos\left(w_l t + \emptyset_{1,l}(j)\right) \alpha_{1,l} dt \quad (2.10)$$

The demodulated code sequence after the matched filter bank of user 1 is [11]:

$$U_{1,m} = \int_0^{T_s} y_1(t) \sum_{n=0}^{N-1} g_m(n) f(t - nT_c) dt \quad (2.11)$$

Several combining systems can implemented according of choice of $\alpha_{1,l}$. Without lose of generality, we consider in our study the case of EGC ($\alpha_{1,l} = 1$) and MRC ($\alpha_{1,l} = \beta_{1,l}$) [11], [41], [43].

2.3.4 Performance Comparison for MC-MC-CDMA

In this section, the BER performance of MC-MC-CDMA system is compared to the performance of Multi-carrier CDMA and Multi-code CDMA. Also, the BER performance for MC-MC-CDMA system is presented and discussed. Some parameters effects on the system performance such as the number of users *K*, the number of *M-ary* symbol *M*, the code sequence and combiner type were investigated. The parameters listed in Table 2.4 are used for the simulation in this section.

Parameters description	**Value / type**
Code Sequence	Walsh-Hadamard, Gold, Kasami
Spreading Code	Walsh-Hadamard
M-ary symbol (*M*)	2 – 4 – 8 – 16
Number of User(*K*)	2 – 4 – 6 – 8 – 10
Number of subcarrier(*L*)	16
Code Sequence length(*N*)	64
Combining	EGC, MRC

Table 2.4. Simulation parameters

Figure 2.12 shows the comparison of BER performance of the MC-MC-CDMA system with those of the Multi-carrier CDMA and Multi-code CDMA systems; Due to the gain which comes from time and frequency diversity, the MC-MC-CDMA system shows better performance than Multi-carrier CDMA and Multi-code CDMA systems.

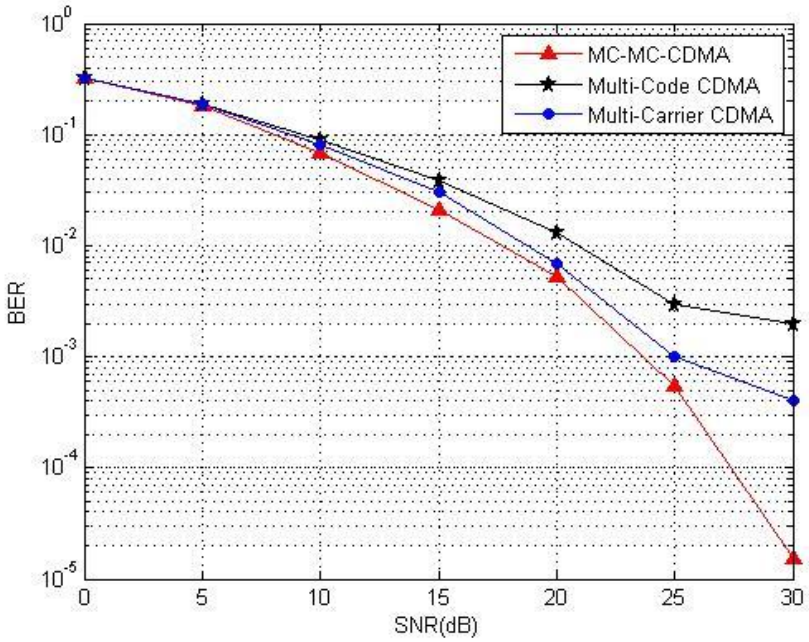

Figure 2.12. Simulation results for BER versus SNR for Multi-code CDMA systems, Multi-carrier CDMA and MC-MC-CDMA

In Figure 2.13, it can be seen that the MC-MC-DMA system using *Walsh* codes for the multi-code sequence sets outperforms the system using *Gold* and *Kasami* codes in a frequency-selective Rayleigh fading channel. The analysis in [11] shows that the decoding decision variable at the receiver of user 1 is related to the correlation properties of the code, which is used for the multi-code sequence sets. Since *Walsh* code has the best orthogonality among the three codes used, the system using Walsh code performs the best.

In Figure 2.14, the simulation results in a frequency-selective Rayleigh fading channel for the MC-MC-CDMA using different *M-ary* are compared. Here, M = 2, 4, 8, 16. The performance is better for M = 2, because with 16-ary the MC-MC-CDMA system uses more code sequences, therefore the data rate is increased by increasing the number of codes and more spectral efficiency increases, the transmission constraints are increasing.

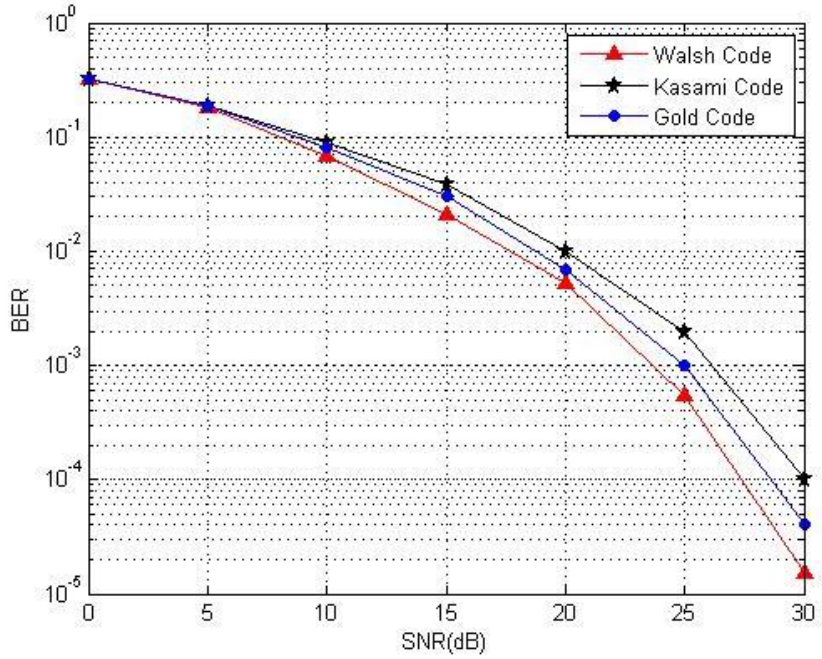

Figure 2.13. BER versus SNR for MC-MC-DMA system using Walsh, Gold, and Kasami codes

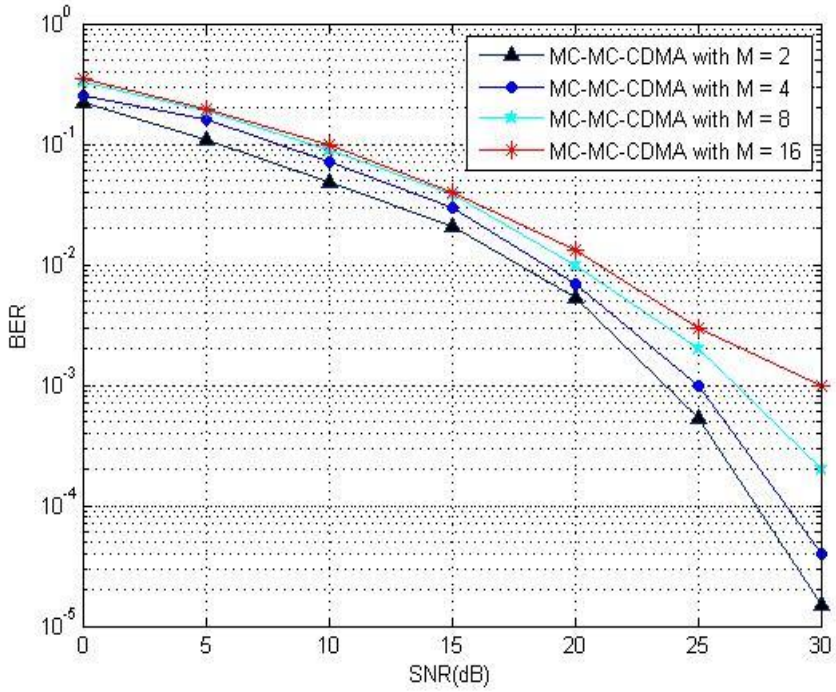

Figure 2.14. Simulation results for BER versus SNR for MC-MC-CDMA with various *M*

Figure 2.15 shown BER performances versus SNR using different values of *K*. In this simulation, the same parameters that listed in Table 2.4 are used except *K* is taken to be 2, 4, 6, 8 and 10 users. From this figure, it can be noted that as many user are transmitting signal simultaneously the BER increases. This is because increasing the number of users increases the superimposed interference caused by the *K*-1 users. That is, increasing the number of users decreases the performance of the system.

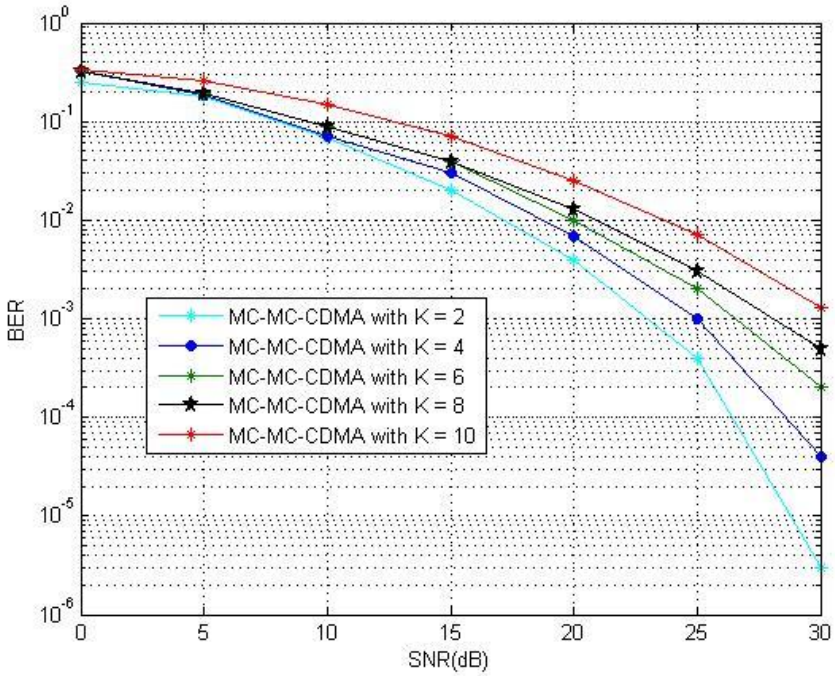

Figures 2.15. The effect of the user's number on BER performance.

In Figure 2.16, the BER's of MC-MC-CDMA system with using EGC and MRC are plotted when SNRs are varied from 0 to 30 dB in 5dB steps. It is clear from the figure that MRC performs better than EGC.

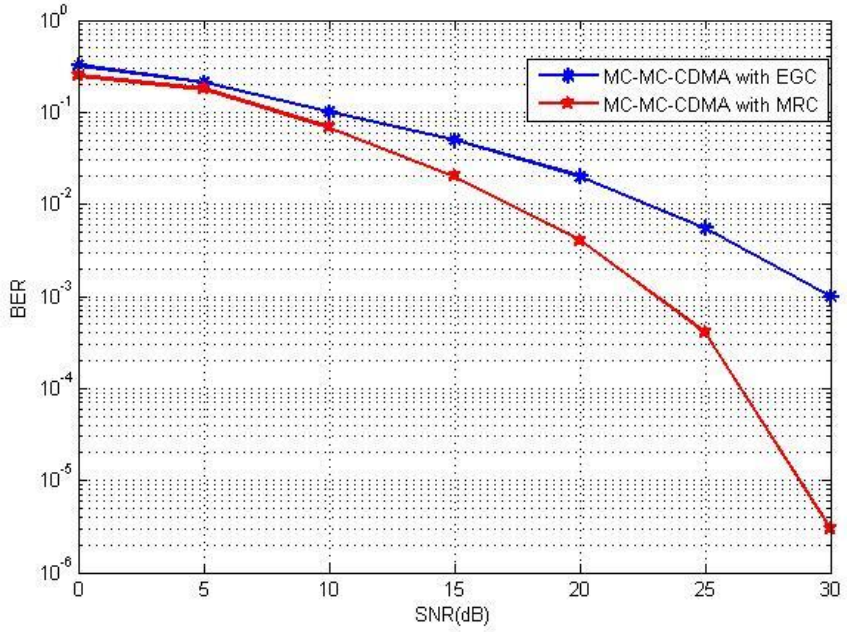

Figure 2.16. BER comparison of MC-MC-CDMA system with using EGC and MRC

Conclusion

In the second chapter, the MC-MC-CDMA, Multi-carrier CDMA and Multi-code CDMA were studied; we followed the path of the signal from the transmitter to the receiver via the channel. The study of MC-MC-CDMA systems, allowed us to determine the different signals (transmitter and receiver). Then we presented the results of simulation, to make a comparative study, the BER's of MC-MC-CDMA, Multi-carrier CDMA and Multi-code CDMA systems were determined, which shows that the MC-MC-CDMA system has better performance and could be useful in future transmission systems. Also, the BER performance for MC-MC-CDMA system is evaluated and discussed on the basis of several factors.

Chapter 3

Interleaving in Time-frequency Diversity on MC-MC-CDMA System

Contents

Introduction 47

3.1 System Model..... 47

3.1.1 Transmitter model 47

3.1.2 Receiver model 48

3.2 New Time Frequency Interleaving 49

3.2.1 Two dimensional Prime interleaving..... 49

3.2.2 Two dimensional random interleaving 50

3.3 Results and discussions 51

3.3.1 Performance evaluation of MC-MC-CDMA with 2D-interleaving 51

3.3.2 Images transmission over MC-MC-CDMA with 2D-interleaving. 54

3.3.2.1 Color images..... 55

3.3.2.2 Black and white images..... 59

Conclusion..... 63

Introduction

The MC-MC-CDMA system offers two-dimensional gains in both the time and frequency domains by using a multi-code signal and multicarrier modulation, respectively [11]. Two-dimensional spreading exploits time-diversity and frequency-diversity. This advantage can allow us implement two-dimensional interleaving both code sequence and subcarriers, thus can minimizes a frequency selective fading and Multiple Access Interference (MAI). In this chapter, we will present 2D-interleaving on MC-MC-CDMA system. The results of simulations will be presented on the basis of several factors such as number of subcarrier and code sequence length. An application of images (color, black and white) transmission will be presented with the proposed system.

3.1 System Model

We used the same model of MC-MC-CDMA given by [11] presented in chapter two, with adding 2D block interleaving.

3.1.1 Transmitter model

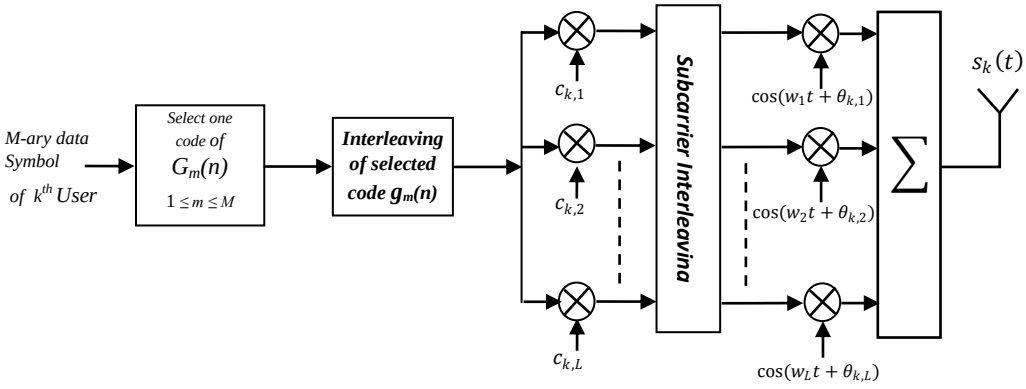

Figure 3. 1. Transmitter model of MC-MC-CDMA system with 2D-interleaving

As shown in Figure 3.1, each chip of the selected code sequence is interleaved (interleaving in time) and copied into *L* subcarrier branches and multiplied with the user-specific scrambling code of the corresponding branch, $c_{k,l}$. After, the *L* chips are interleaved (subcarrier interleaving) which can achieve to MC-MC-CDMA system the frequency diversity gain by making the randomization effect of burst error in frequency domain. Each of these branches then modulates one of the *L* orthogonal subcarriers and the results are summed [10] [11].

3.1.2 Receiver model

At the receiver as shown in Figure 3.2, a demodulated code sequence of user 1 is applied to the input of subcarrier de-interleaving and the output is then despread to generate each chip of the received code sequence.
Detection then continues using the filter bank after de-interleaved demodulated code sequence.

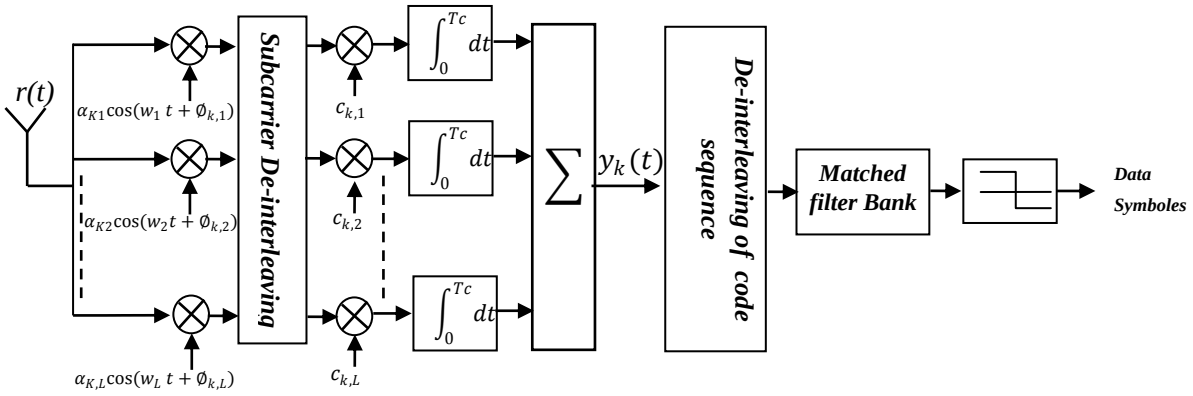

Figure 3.2. Receiver model of MC-MC-CDMA system with 2D De-interleaving

Depending on the choice of $\alpha_{1,l}$ there is a number of combining which can be implemented; in our chapter we consider MRC because the best BER performance of such a system is achieved by the use of this combining [42], [44].

3.2 New Time Frequency Interleaving

There are a lot of varieties of interleaving modules, which can be implemented. So, we present two major 2D-interleavers, such, the 2D-prime and 2D-random interleaving.

3.2.1 Two dimensional Prime interleaving

This type of interleaver is given in [45], [46] and [47], the idea of extending from 1D prime interleaved into 2D is used in image matrix. For understanding the mechanism of 2D-prime interleavers in time-frequency, let us consider a case of 2D interleaving of matrix size (N x L), such as N is a code sequence length and L is a number of subcarriers. Firstly, we distributed the interleaving scheme into code sequence interleaving in row-wise and subcarriers interleaving in column-wise. Secondly, we affect the value of seed as P_{row} (row-wise seed) and P_{col} (column-wise seed) to code sequence and subcarriers interleaving respectively then the new positions of bits after 2D-interleaving will be as follows:

$$n_{new} = (1 + (n-1)P_{row}) mod\ N \tag{3.1}$$

$$l_{new} = (1 + (l-1)P_{col}) mod\ L \tag{3.2}$$

where n = 1, 2, 3,……..N and l = 1, 2, 3,……L.

For example if we have a code sequence of length $N=8$ modulates of L=8 orthogonal subcarriers and we wish to 2D-interleavers these 8 x 8 matrix with P_{row}=5 and P_{col}=3. The new positions of bits are illustrated in Figure 3.3.

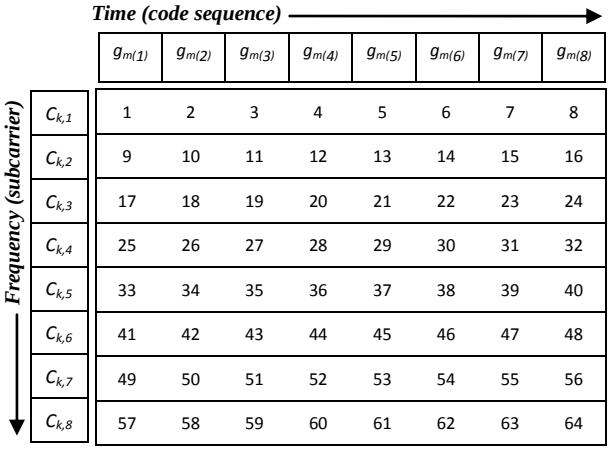

	$g_{m(1)}$	$g_{m(2)}$	$g_{m(3)}$	$g_{m(4)}$	$g_{m(5)}$	$g_{m(6)}$	$g_{m(7)}$	$g_{m(8)}$
$C_{k,1}$	1	2	3	4	5	6	7	8
$C_{k,2}$	9	10	11	12	13	14	15	16
$C_{k,3}$	17	18	19	20	21	22	23	24
$C_{k,4}$	25	26	27	28	29	30	31	32
$C_{k,5}$	33	34	35	36	37	38	39	40
$C_{k,6}$	41	42	43	44	45	46	47	48
$C_{k,7}$	49	50	51	52	53	54	55	56
$C_{k,8}$	57	58	59	60	61	62	63	64

(a)

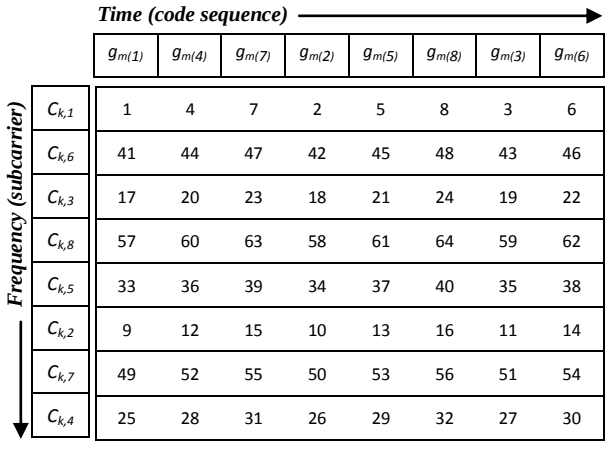

	$g_{m(1)}$	$g_{m(4)}$	$g_{m(7)}$	$g_{m(2)}$	$g_{m(5)}$	$g_{m(8)}$	$g_{m(3)}$	$g_{m(6)}$
$C_{k,1}$	1	4	7	2	5	8	3	6
$C_{k,6}$	41	44	47	42	45	48	43	46
$C_{k,3}$	17	20	23	18	21	24	19	22
$C_{k,8}$	57	60	63	58	61	64	59	62
$C_{k,5}$	33	36	39	34	37	40	35	38
$C_{k,2}$	9	12	15	10	13	16	11	14
$C_{k,7}$	49	52	55	50	53	56	51	54
$C_{k,4}$	25	28	31	26	29	32	27	30

(b)

Figure 3.3. 2D-prime interleaving of 8 subcarriers and code sequence length $N = 8$

(a) Befor 2D-prime interleaving

(b) After 2D-prime interleaving

3.2.2 Two dimensional random interleaving

1D-random interleaving rearranges the elements of its input vector using a random permutation, our 2D-random interleaving is the same of 2D-prime interleaving [47]. It is also distributed into 1D row-wise and 1D column-wise interleaving. But, it uses random permutation for interleaving instead of using an exchange follows the value of seed [46].

In [45], the Prime interleaver is quite easy to generate and is outperforming of random interleaver in terms of bandwidth consumption problems and computational complexity. The 2D-prime and 2D-random interleaving would be taken into BER comparison in section 3.3.1.

3.3 Results and discussions

In section 3.3.1, the BER performance of MC-MC-CDMA system with/without using 2D-interleaving is analyzed and evaluated considering the some parameters such as number of subcarrier *L* and code sequence length *N*. Also, PSNR performance of received images over MC-MC-CDDA with and without 2D-iterleaving is presented in section 3.3.2. A frequency-selective Rayleigh fading channel is considered.

3.3.1 Performance evaluation of MC-MC-CDMA with 2D-interleaving

The parameters listed in Table 3.1 are used for the simulation in this section.

Parameters description	**Value / type**
Code Sequence	Walsh-Hadamard
Spreading Code	Walsh-Hadamard
M-ary symbol (*M*)	8
Number of User(*K*)	4
Number of subcarrier(*L*)	4 – 16 – 32
Code Sequence length(*N*)	16 – 64
Interleaving	Random – Prime
Combining	MRC

Table 3.1. Simulation parameters

Figure 3.4 shows the BER performance of MC-MC-CDMA scheme with both 2D-random interleaving and 2D-prime interleaving with MRC detection. From this figure we can see that the performance with 2D-interleaving is far better than that without interleaving. Also the BER performance of 2D-prime interleaving comes out similar to that of BER performance of 2D-random interleaving with MRC detection. Figure 3.5 compares the interleaved BER performances of code sequence and subcarrier. It is seen that the interleaving gain is larger in a frequency-diversity than time-diversity.

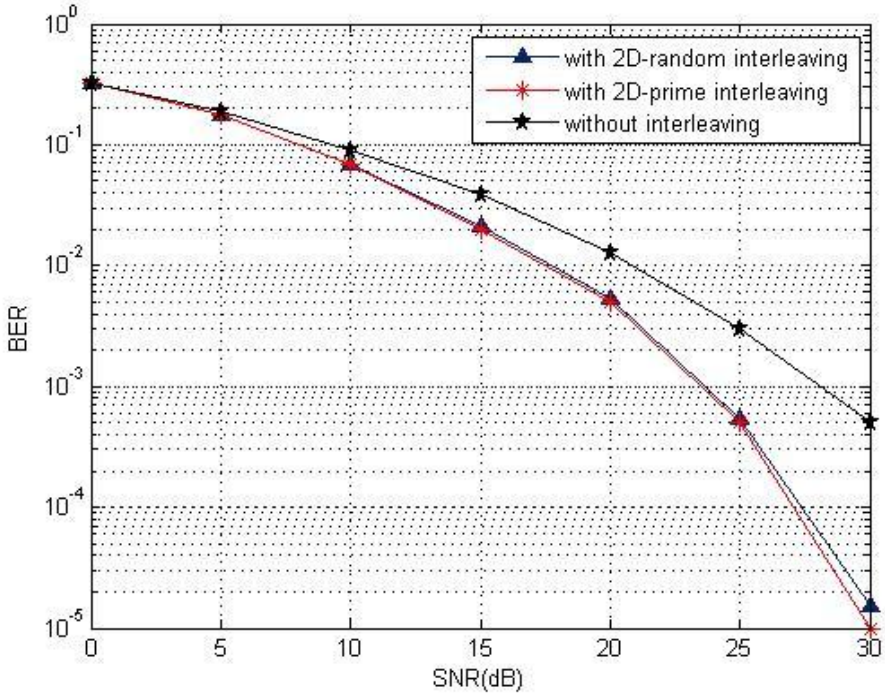

Figure 3.4. BER comparison of MC-MC-CDMA system with/without 2D-interleaving. L=16, N=16, K=4.

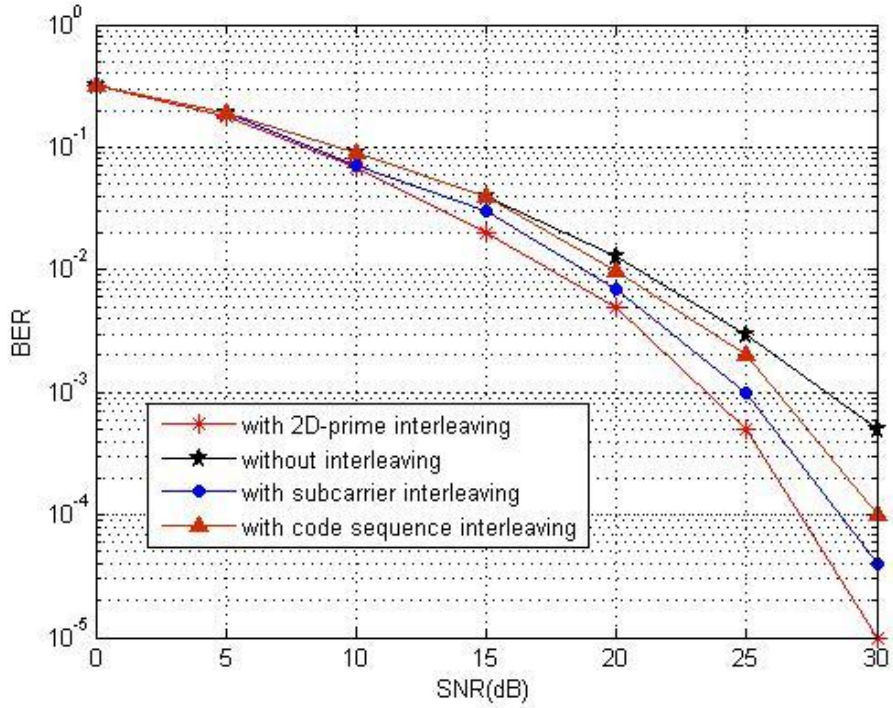

Figure 3.5. Comparison of code sequence and subcarrier interleaving for MC-MC-CDMA with L=16, N=16, K=4.

From Figure 3.6 and Figure 3.7, we see the BER performance of the MC-MC-CDMA system with different values of *L* and *N*. Both code sequence and subcarrier interleaved by prime interleaving. It can be noticed that as *L* and *N* increases, the BER performance improves, because of the increase in the diversity effect. Even for all values of *L* and *N*, the interleaved BER performance is seen to be better than that without interleaving. This leads us to say that the higher time-frequency diversity, more interleaving gain is larger.

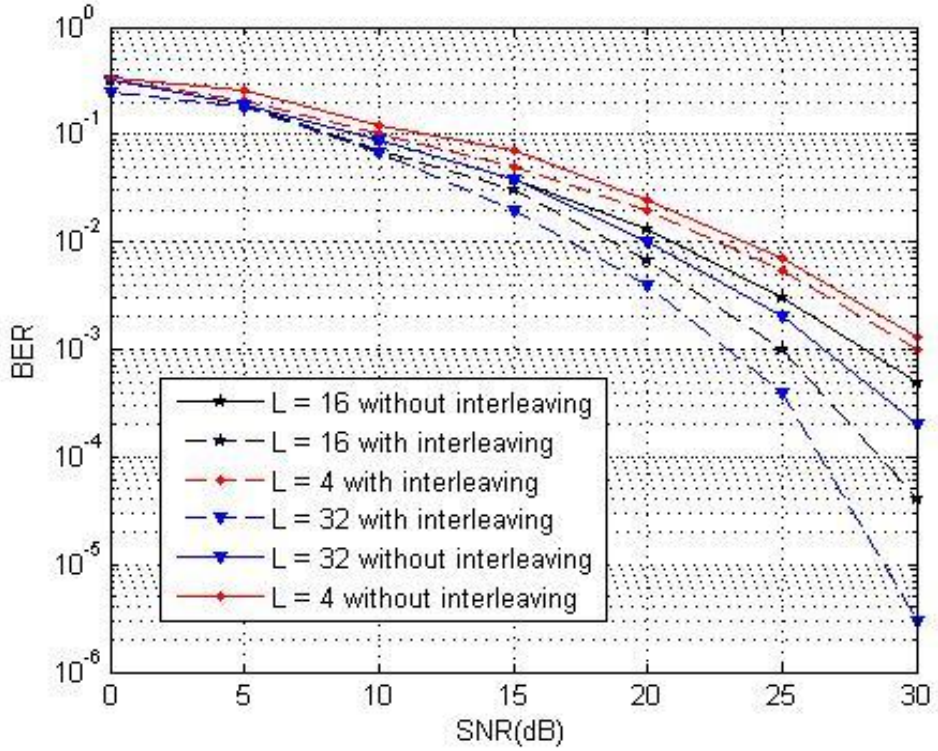

Figure 3.6. Average BER versus SNR for MC-MC-CDMA with different number of subcarrier, *K*=4, *N*=16.

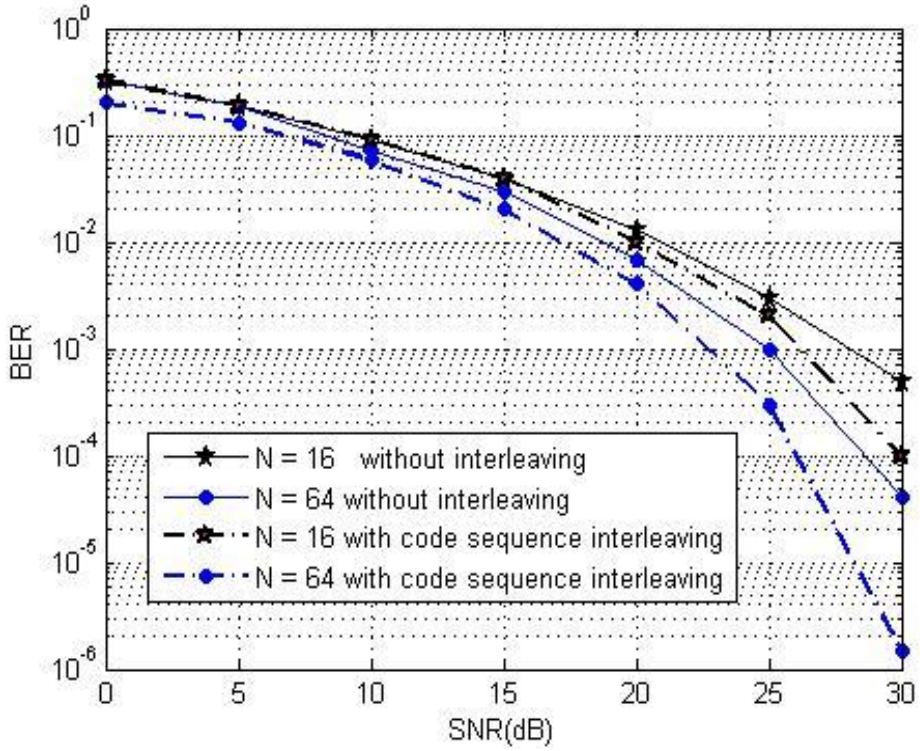

Figure 3.7. Average BER versus SNR for MC-MC-CDMAwith different length of code sequence, *K*=4, *L*=16.

3.3.2 Images transmission over MC-MC-CDMA with 2D-interleaving

To confirm the results found previously of BER performance, we transmit images shown in Figure 3.8 Figure 3.12 and over MC-MC-CDMA system with and without 2D-prime interleaving.

The PSNR metric, is used to measure the quality of the reconstructed images at the receiver, which is defined as [33]:

$$PSNR = 10.Log_{10}\left(\frac{MAX^2}{MSE}\right) \tag{3.3}$$

where *MAX is* the maximum possible pixel value of the image. The Mean Squared Error *MSE* is defined as [33]:

$$MSE = \frac{1}{e.f}\sum_{i=0}^{e-1}\sum_{j=0}^{f-1}[A(i,j) - B(i,j)]^2 \quad (3.4)$$

where *(e . f)* is the image size. *A* and *B* are the original and the recovered images, respective.

3.3.2.1 Color images

The simulation parameters are provided in Table 3.2.

Parameters description	**Value / type**
Code Sequence	Walsh-Hadamard
Spreading Code	Walsh-Hadamard
M-ary symbol (*M*)	8
Number of User(*K*)	4
Number of subcarrier(*L*)	16
Code Sequence length(*N*)	16
Interleaving	Prime
Combining	MRC
Images dimensions	200x150x3

Table 3.2. Simulation parameters

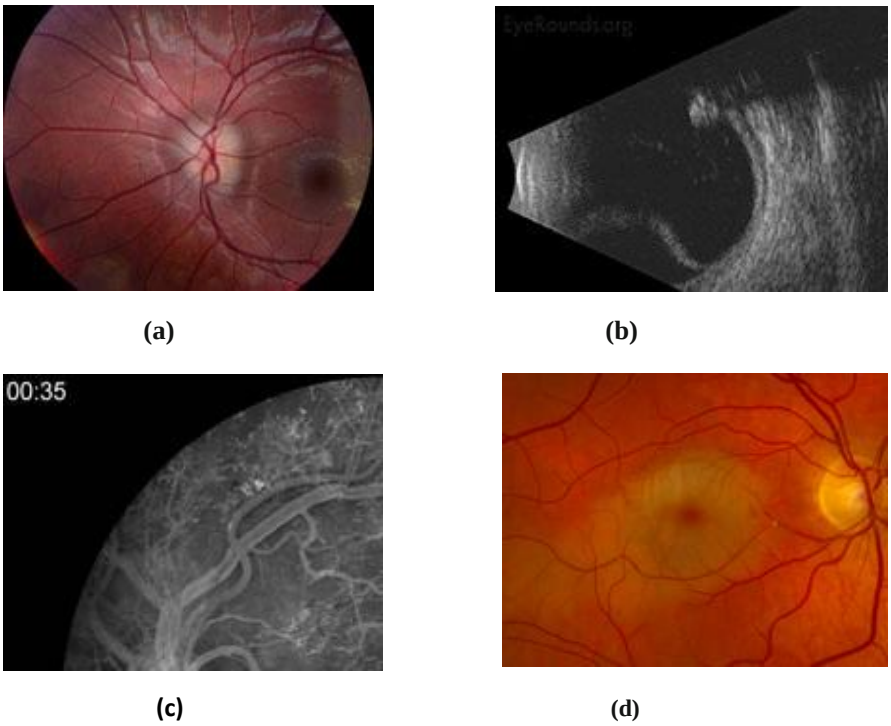

Figure 3.8. The original medical images [48].

(a) is the transmitted image of user 1

(b) is the transmitted image of user 2

(c) is the transmitted image of user 3

(d) is the transmitted image of user 4

Figure 3.9 and Figure 3.10 show the received images with and without 2D-prime interleaving at SNR=20 dB. Figure 3.11 shows the variation of the PSNR summarized in Table 3.3 and Table 3.4, at SNRs from 0 to 30 dB in 5dB steps. From these figures, it is clear that the best results are obtained when we use 2D-prime interleaving.

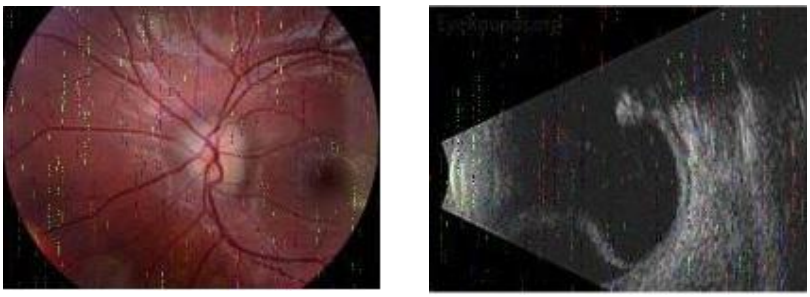

a. PSNR= 35.05dB **b.** PSNR= 35.25dB

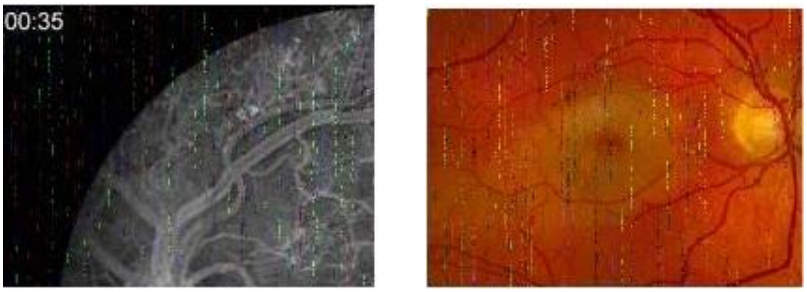

c . PSNR= 35.15dB **d .** PSNR= 35.28dB

Figure 3.9. Received medical images over MC-MC-CDMA system without 2D-Prime interleaving at SNR= 20dB

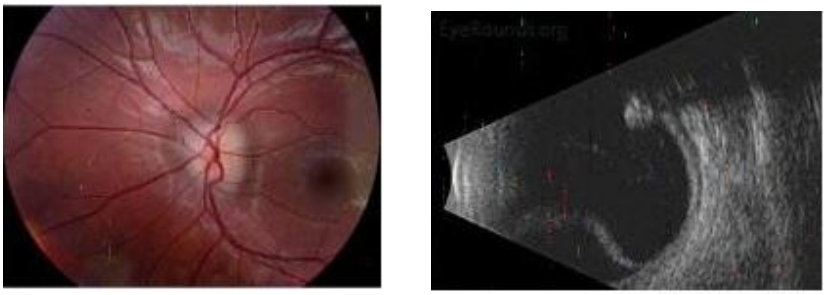

a. PSNR= 37.80dB **b.** PSNR= 36.62dB

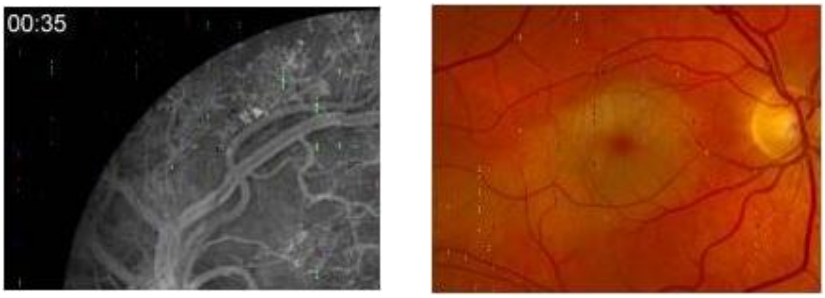

c . PSNR= 37.60dB **d .** PSNR= 37.15dB

Figure 3.10. Received medical images over MC-MC-CDMA system with 2D-Prime interleaving at SNR= 20dB

Received images	**SNR(dB)**						
	0	**5**	**10**	**15**	**20**	**25**	**30**
(a)	19.80	26.90	32.89	33.02	35.05	36.25	40
(b)	18.90	28.61	29.97	34.97	35.25	35.75	39.02
(c)	18.78	27.80	32.15	34.20	35.15	36.85	39.79
(d)	18.52	27.73	32.69	34.42	35.28	35.15	40.06

Table 3.3. PSNR values for the received images in dB without interleaving

Received images	**SNR(dB)**						
	0	**5**	**10**	**15**	**20**	**25**	**30**
(a)	20.16	29	33.12	36.40	37.80	40	44.90
(b)	19.40	27.50	32.15	34.70	36.62	39.40	45.40
(c)	17.55	27.65	32.70	35.30	37.60	40.88	44.40
(d)	18.30	27.95	31.45	35.35	37.15	40.40	44.93

Table 3.4. PSNR values for the received images in dB with 2D-Prime interleaving

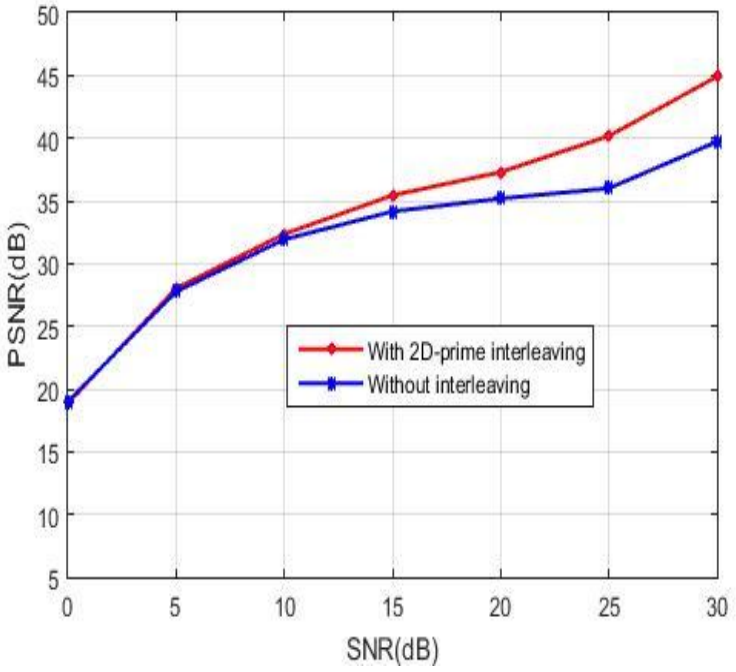

Figure 3.11. Average PSNR versus SNR for the received images over MC-MC-CDMA system.

3.3.2.2 Black and white images

In this section, we transmit images (black and white) shown in Figure 3.12 over MC-MC-CDMA system with and without 2D-prime interleaving. The PSNR performance of received images is presented. A comparison between proposed approach and those presented in [33] is evaluated; the same remarks remain valid for MC-MC-CDMA system performance [12].

The simulation parameters are provided in Table 3.5.

Parameters description	**Value / type**
Code Sequence	Walsh-Hadamard
Spreading Code	Walsh-Hadamard
M-ary symbol (*M*)	8
Number of User(*K*)	4
Number of subcarrier(*L*)	16
Code Sequence length(*N*)	16
Interleaving	Prime – Chaotic
Combining	MRC
Image size	256x256

Table 3.5. Simulation parameters

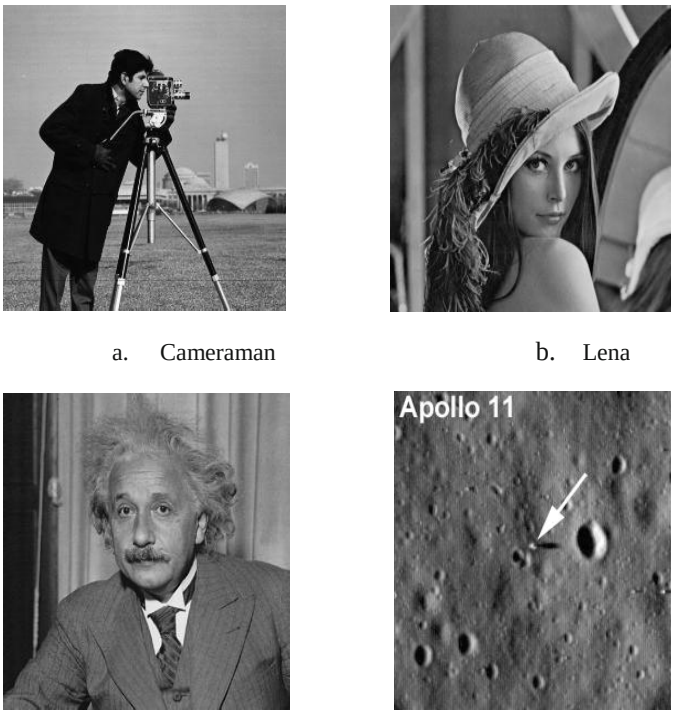

a. Cameraman b. Lena

c. Einstein d. Apollo11

Figure 3.12. The original images.

a. Cameraman is a transmitted image of user 1
b. Lena is a transmitted image of user 2
c. Einstein is a transmitted image of user 3
d. Apollo11 is a transmitted image of user 4

Figure 3.13 and Figure 3.14 show the received images with and without 2D-prime interleaving at SNR=20dB. Figure 3.15 shows the variation of the PSNR summarized in Table 3.6 and Table 3.7, when SNRs are varied from 0 to 30 dB in 5dB steps. From these figures, it is clear that the best results are obtained when we use 2D-prime interleaving.

a. PSNR= 34.90dB b. PSNR= 35.20dB

c . PSNR= 34.95dB d . PSNR= 35.18dB

Figure 3.13. Received images over MC-MC-CDMA system without interleaving at SNR= 20dB.

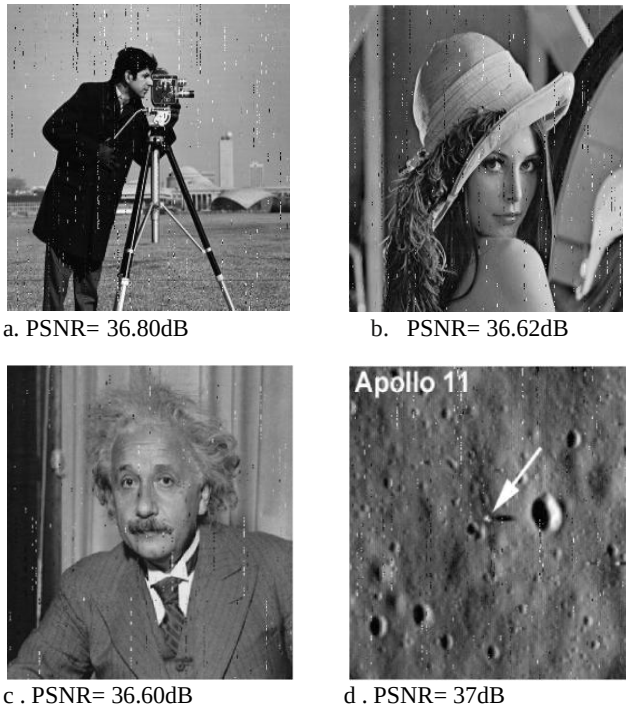

a. PSNR= 36.80dB b. PSNR= 36.62dB

c . PSNR= 36.60dB d . PSNR= 37dB

Figure 3.14. Received images over MC-MC-CDMA system with 2D-Prime interleaving at SNR= 20dB.

Received images	SNR(dB)						
	0	**5**	**10**	**15**	**20**	**25**	**30**
Cameraman	18.80	27.91	31.88	34.01	34.90	36.20	39
Lena	18.40	27.60	30.98	33.98	35.20	35.80	40.01
Einstein	18.77	27.75	31.70	34.40	34.95	35.85	39.80
Apollo11	18.33	27.78	31.79	34.22	35.18	36.15	40

Table 3.6. PSNR values for the received images in dB without interleaving using MRC combiner

Received images	SNR(dB)						
	0	**5**	**10**	**15**	**20**	**25**	**30**
Cameraman	19.10	28	32.02	35.20	36.80	39.50	44.70
Lena	18.41	27.60	32.15	34.90	36.62	39.80	45
Einstein	18.50	27.70	31.90	35.35	36.60	39.88	44.80
Apollo11	18.35	27.80	32.25	35.30	37	40	44.83

Table 3.7. PSNR values for the received images in dB with 2D-Prime interleaving using MRC combiner

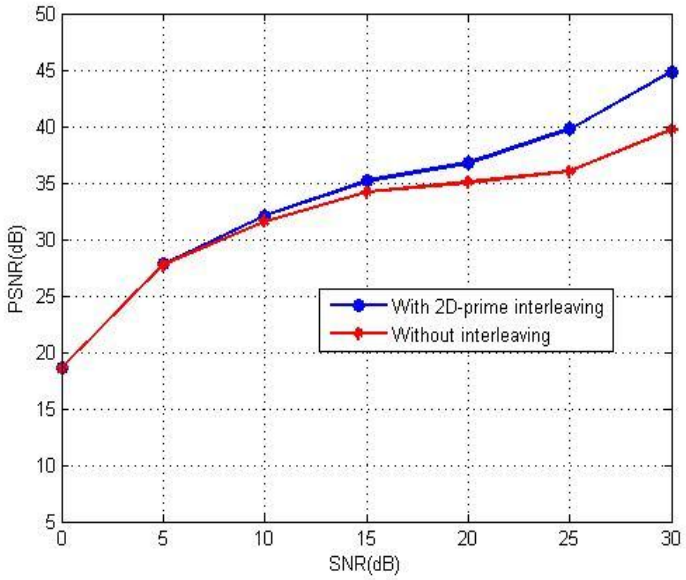

Figure 3.15. Average PSNR versus SNR for the received images over MC-MC-CDMA system.

Figure 3.16 present the PSNR yielded from our proposed system without equalization and its corresponding from previous work [33]. It's seems that our proposed system reach better PSNR over MC-CDMA with chaotic interleaving [33].

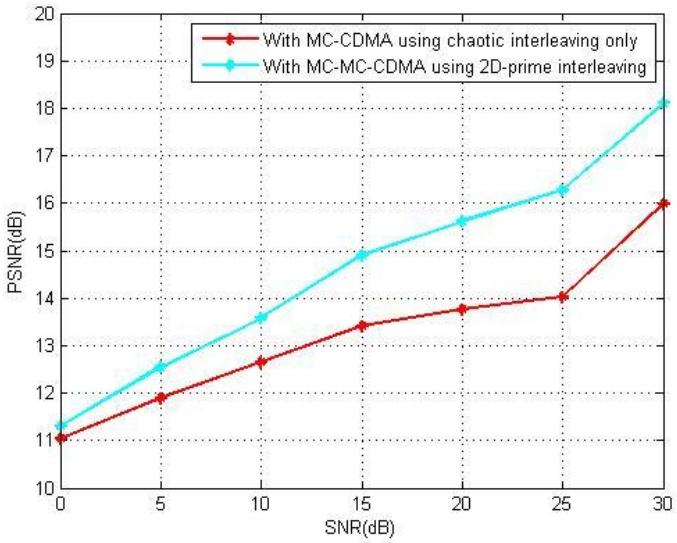

Figure 3.16. PSNR comparison between the received cameraman image over MC-MC-CDMA system with 2D-prime interleaving and MC-CDMA with chaotic interleaving

Conclusions

In this chapter, we have presented a new time-frequency interleaving method based on MC-MC-CDMA systems allowing two-dimensional spreading in both time and frequency domains. The originality of proposed technique lies in fact that we have implemented a two-dimensional interleaving inside the time and frequency diversity. Simulation results showed that the performance is improved with 2D-interleaving and the BER performance of 2D-prime interleaving is found similar to that of 2D-random interleaving. Also, the interleaving gain is larger in a frequency-diversity than time-diversity.

The performance of the images (color, black and white) transmission process has been studied. The obtained results confirm that the important improvement on PSNR in MC-MC-CDMA system with 2D-interleaving.

Conclusions and prospects

Our work has focused on the study of interleaving effect in time-frequency diversity on MC-MC-CDMA system combining the multi-carrier multiple access code division (MC-CDMA) and multi-code multiple access code division (Multi-code CDMA). This ingenious combination was studied carefully for several years and is currently at work in the new wireless communications.

In the first chapter, we introduced the basics to understanding digital transmissions systems. The different effects that influence the signal received after propagation through the radio channel were presented which are: the large-scale fading due to the path loss and shadowing, and the small-scale fading caused by multi-path propagation. This chapter also introduced the general concepts of OFDM and Multiple access technique; we have interested in two-dimensional spreading. We then focused on the different scheme of interleaving.

In the second chapter, the MC-MC-CDMA, Multi-carrier CDMA and Multi-code CDMA were studied; we followed the path of the signal from the transmitter to the receiver via the channel. The study of MC-MC-CDMA systems, allowed us to determine the different signals (transmitter and receiver). Then we presented the results of simulation; to make a comparative study, the BER's of MC-MC-CDMA, Multi-carrier CDMA and Multi-code CDMA systems were determined, which shows that the MC-MC-CDMA system has better performance and could be useful in future transmission systems. Also, the BER performance for MC-MC-CDMA system is evaluated and discussed on the basis of several factors such as: user's number, *M-ary* symbol number, code sequence type and combiner type.

In the last chapter, we have presented a new time-frequency interleaving method based on MC-MC-CDMA systems allowing two-dimensional spreading in both time and frequency domains. The originality of proposed technique lies in fact that we have implemented a two-dimensional interleaving inside the time and frequency diversity. Simulation results showed that the performance is improved with 2D-interleaving and the BER performance of 2D-prime interleaving is found similar to that of 2D-random interleaving. Also, the interleaving gain is larger in a frequency-diversity than time-diversity.

The performance of the images (color, black and white) transmission process has been studied. The obtained results confirm that the important improvement on PSNR in MC-MC-CDMA system with 2D-interleaving.

Prospects

Among the envisaged prospects for our work, we mention the following:

- Designing new interleavers to reduce the effect of correlated channel.
- Performance evaluation of Multiple Input Multiple Output (MIMO) techniques in the context of MC-MC-CDMA systems (MIMO-MC-MC-CDMA).
- Optimization a tradeoff between the data rate and interference so as to obtain a less complex system with better performance.

Appendix A

BPSK M-ary CDMA

System analysis

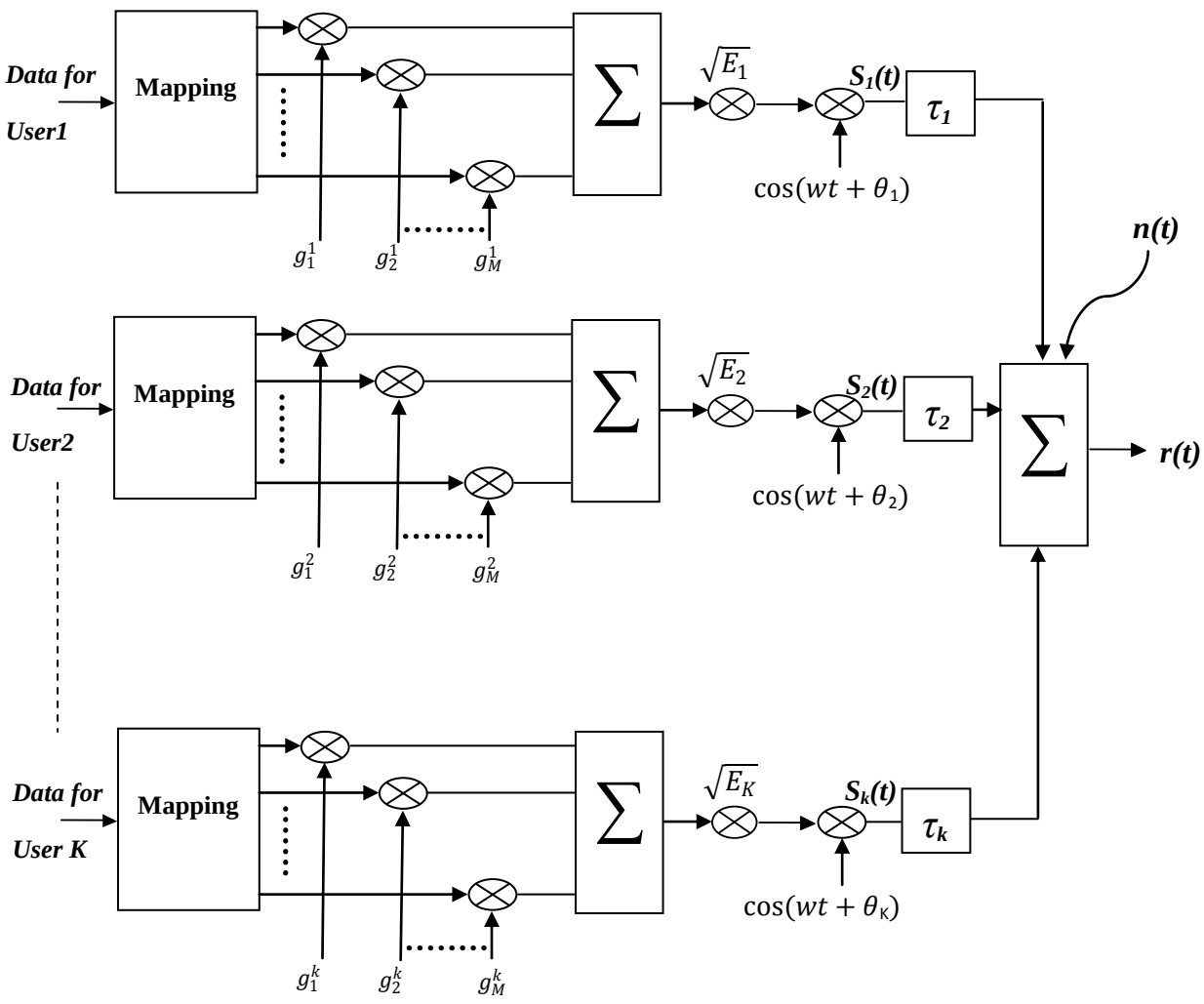

Figure a.1 *K*-user signal formulation process for a BPSK *M-ary* CDMA system [28].

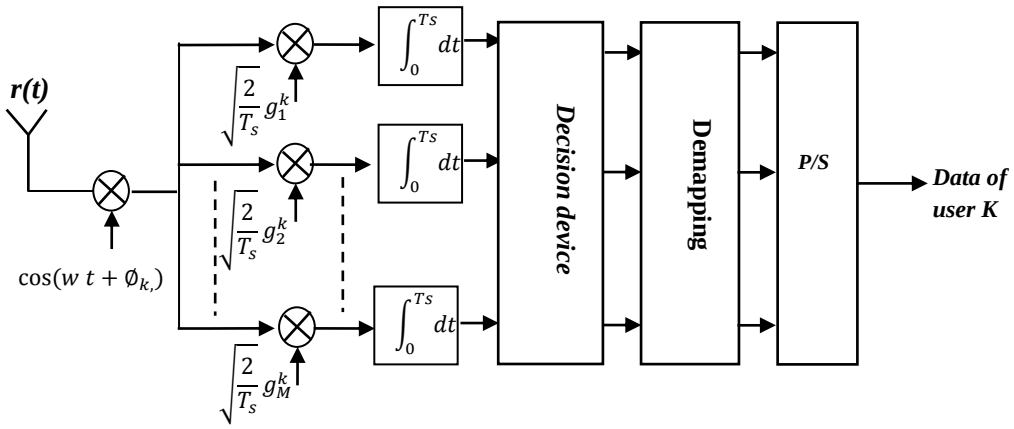

Figure a.2 Receiver of a BPSK *M-ary* CDMA system [28]

The transmitted signal for user 1 is described as [28]:

$$s_1(t) = \sqrt{E_1}\left[\sum_{m=1}^{M} g_m^1(t-\tau_1)d_m^1\right]cos(wt+\theta_1) \qquad (a.1)$$

and all other transmissions become

$$s_K(t) = \sqrt{E_k}\left[\sum_{m=1}^{M} g_m^K(t-\tau_K)\, d_m^K\right]cos(wt+\theta_K) \qquad (a.2)$$

$s_K(t)$ is the signal sent from the k^{th} user, g_m is the m^{th} code available to the transmitter, d_m is the weight coefficient for the m^{th} code after signal mapping, τ_K is the propagation delay for the k^{th} user, and *w* is the angular frequency. θ_k is random phase.

The received signal from user 1 can be written as [28]:

$$r(t) = \sqrt{E_1}\sum_{m=1}^{M} g_m^1(t-\tau_1)\, d_m^1 cos(wt+\theta_1) + r_1(t) + n(t) \qquad (a.3)$$

Where *n(t)* is the AWGN with its power spectral density being $N_0/2$ and $r_1(t)$ is the interference contributed from all other $K-1$ unwanted transmissions can be written as [28]:

$$r_1(t) = \sum_{k=2}^{K}\sqrt{E_k}\left[\sum_{m=1}^{M} g_m^k(t-\tau_k)\, d_m^k\right]\cos(wt+\theta_k) \qquad (a.4)$$

We assume that the receiver has achieved perfect synchronization with the incoming signal from User 1, and thus we let $\tau_1 = 0$ and $\theta_1 = 0$ without losing generality.

The all *K − 1* interference to the detection of the first user signal at the receiver is described as [28]:

$$y_1(t) = \int_0^{T_s} \sqrt{\frac{2}{T_s}} \sum_{k=2}^{K} \sqrt{E_k} \left[\sum_{m=1}^{M} g_m^k(t - \tau_k)\, d_m^k \right] \cos(wt + \theta_k)\, g_m^1(t) \cos(wt)\, dt \qquad (a.5)$$

Appendix B

Pseudo Noise Sequences

Introduction

PN Sequences or Pseudo Noise Sequences are an integral part of existing mobile cellular systems. A PN sequence consists of ones and zeros which are determined by precise mathematical rules [49].

There are three well-known PN Sequence families:

1. m-Sequence.
2. Gold Sequence.
3. Kasami Sequence.

b.1 m-Sequence

The PN generator for spread spectrum is usually implemented as a circuit consisting of XOR gates and a shift register, called a linear feedback shift register (LFSR).
LRSR has all the feedback function (modulo-2 sum) returned to a single of a shift register [50], [51].

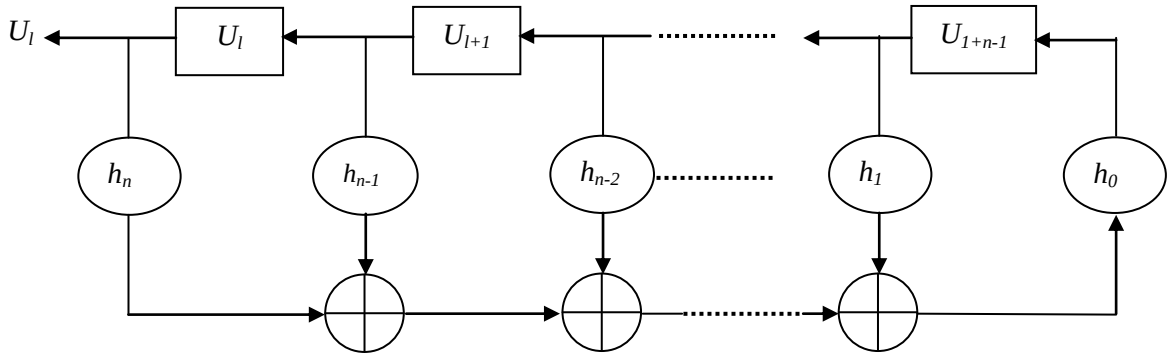

Figure b.1. Binary Linear Feedback Shift Register Sequence Generator [52].

The figure b.1 shows implementation of Linear Feedback Shift Register (LFSR) where:

- '$\oplus$' represents modulo-2 addition (XOR gate), and h_i's take values either 1 or 0. (connection / no connection) [52].
- Hence, the output of the shift register is [52]:
  $u_{l+n} = h_n u_l \oplus h_{n-1}u_{l+1} \oplus \ldots\ldots\ldots\ldots \oplus h_1 u_{l+n-1}$ (b.1)
- '$\square$' represents a single binary storage element, resulting in maximum of 2^n different states for a shift register [52].

LFSRs are described by primitive polynomials or generator polynomials. These polynomials are conveniently and conventionally represented by a binary vector h_l=(h_1, h_2,……. h_n), or the octal notation of the vector. e.g. $G(D) = 1+D^3+D^5$ is a binary vector 101001. Another convention is to represent it as [5,3,0], which is sometimes further abbreviated as [5,3] [52].

When the period (length) of the sequence is exactly $N=2^L-1$ the PN sequence is called a maximum-length sequence or m-sequence. An m-sequence generated from a LFSR has an even number of taps [52].

An example: Let $n = 4$ and $h_0 = h_1 = h_4 = 1$ and $h_2 = h_3 = 0$. Given an initial fill ("state 1") equal to "0001" the other states are depicted in table b.1 [52]:

state1	0	0	0	1
state2	0	0	1	1
state3	0	1	1	1
state4	1	1	1	1
state5	1	1	1	0
state6	1	1	0	1
state7	1	0	1	0
state8	0	1	0	1
state9	1	0	1	1
state10	0	1	1	0
state11	1	1	0	0
state12	1	0	0	1
state13	0	0	1	0
state14	0	1	0	0
state15	1	0	0	0
state16	0	0	0	1

Table b.1. Circuit with Shift Registers for Generating 15 m-Sequence Initial sequence 0001, [52].

The period of the output is 15, and the resulting sequence equals 000111101011001.

If an L-stage LFSR has feedback taps on stages L, K, M and has sequence ....., d_i,d_{i+1}, d_{i+2}
Than the reverse LFSR has feedback taps on L, L-K, L-M and sequence..... $d_{i+2,}$ $d_{i+1,}$ d_i

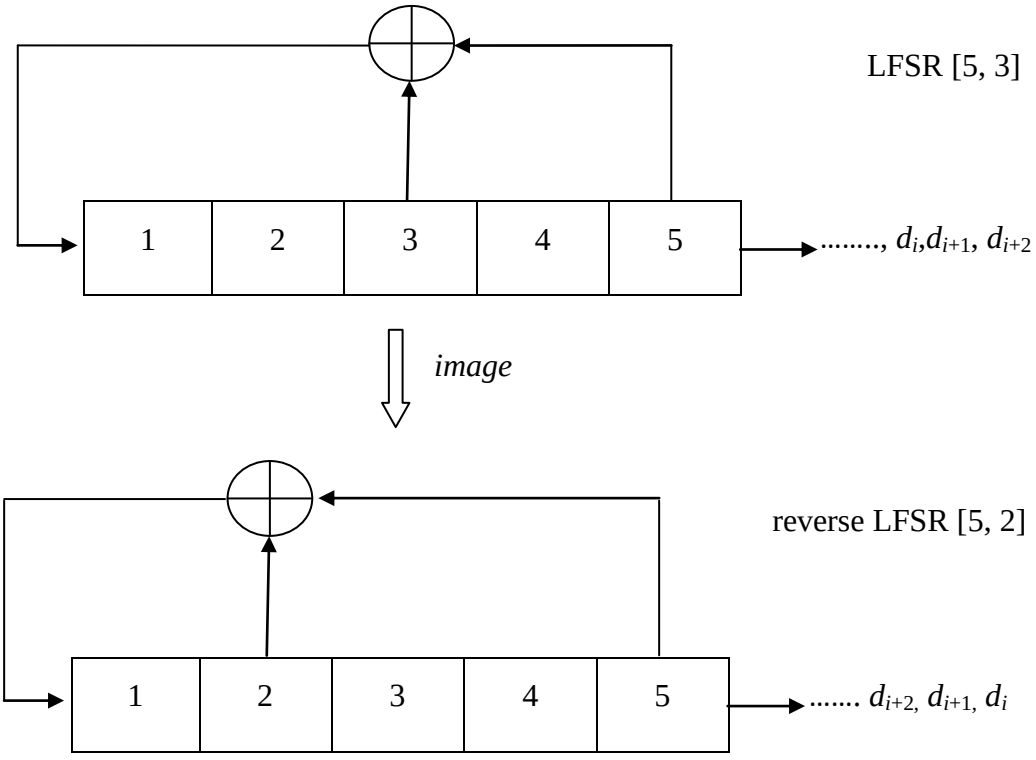

LFSR [5, 3] : -1 -1 -1 -1 1 -1 -1 1 -1 1 1 -1 -1 1 1 1 1 1 -1 -1 -1 1 1 -1 1 1 1 -1 1 -1 1

LFSR [5, 2] : -1 -1 -1 -1 1 -1 1 -1 1 1 1 -1 1 1 -1 -1 -1 1 1 1 1 1 -1 -1 1 1 -1 1 -1 -1 1

Figure b.2. LFSR [5, 3] with image generated, [50].

In the following table b.2 the feedback connections (even number) are tabulated for m-sequence generated with a LFSR (without image set).

Number Of Stages (*L*)	**Code length $N=2^L-1$**	**Feedback taps for m-sequence**
2	3	[2,1]
3	7	[3,1]
4	15	[4,1]
5	31	[5,2][5,4,3,2][5,4,2,1]
6	63	[6,1][6,5,2,1][6,5,3,2]
7	127	[7,1][7,3][7,3,2,1][7,4,3,2] [7,6,4,2][7,6,3,1][7,6,5,2][7,6,5,4,2,1][7,5,4,3,2,1]
8	255	[8,4,3,2][8,6,5,3][8,6,5,2] [8,5,3,1][8,6,5,2][8,7,6,1] [8,7,6,5,2,1][8,6,4,3,2,1]
9	511	[9,4][9,6,4,3][9,8,5,4][9,8,4,1] [9,5,3,2][9,8,6,5][9,8,7,2] [9,6,5,4,2,1][9,7,6,4,3,1] [9,8,7,6,5,3]
10	1023	[10,3][10,8,3,2][10,4,3,1][10,8,5,1] [10,8,5,4][10,9,4,1][10,8,4,3] [10,5,3,2][10,5,2,1][10,9,4,2]
11	2047	[11,1][11,8,5,2][11,7,3,2][11,5,3,5] [11,10,3,2][11,6,5,1][11,5,3,1] [11,9,4,1][11,8,6,2][11,9,8,3]
12	4095	[12,6,4,1][12,9,3,2][]12,11,10,5,2,1 [12,11,6,4,2,1][12,11,9,7,6,5] [12,11,9,5,3,1][12,11,9,8,7,4] [12,11,9,7,6,][12,9,8,3,2,1] [12,10,9,8,6,2]
13	8191	[13,4,3,1][13,10,9,7,5,4] [13,11,8,7,4,1][13,12,8,7,6,5] [13,9,8,7,5,1][13,12,6,5,4,3] [13,12,11,9,5,3][13,12,11,5,2,1] [13,12,9,8,4,2][13,8,7,4,3,2]
14	16383	[14,12,2,1][14,13,4,2][14,13,11,9] [14,10,6,1][14,11,6,1][14,12,11,1] [14,6,4,2][14,11,9,6,5,2] [14,13,6,5,3,1][14,13,12,8,4,1] [14,8,7,6,4,2][14,10,6,5,4,1] [14,13,12,7,6,3][14,13,11,10,8,3]
15	32767	[15,13,10,9][15,13,10,1][15,14,9,2] [15,1][15,9,4,1][15,12,3,1][15,10,5,4] [15,10,5,4,3,2][15,11,7,6,2,1] [15,7,6,3,2,1][15,10,9,8,5,3] [15,12,5,4,3,2][15,10,8,7,5,3] [15,13,12,10][15,13,10,2][15,12,9,1] [15,14,12,2][15,13,9,6][15,7,4,1] [15,4][15,13,7,4]

Table b.2. Feedback connections for linear m-sequences, [53].

b.2 Gold Sequences

For CDMA, we need to construct a family of spreading sequences, one for each user, in which the codes have well-defined cross correlation properties. In general, m-sequences do not satisfy this criterion[51]. One popular set of sequences that does is the Gold sequences. Gold sequences are attractive because only simple circuitry is needed to generate a large number of unique codes [51]. A Gold sequence is constructed by the XOR of two m-sequences with the same clocking. Figure b.3 shows an example; in this example the two shift registers generate the two m-sequences and these are then bitwise XORed [51].

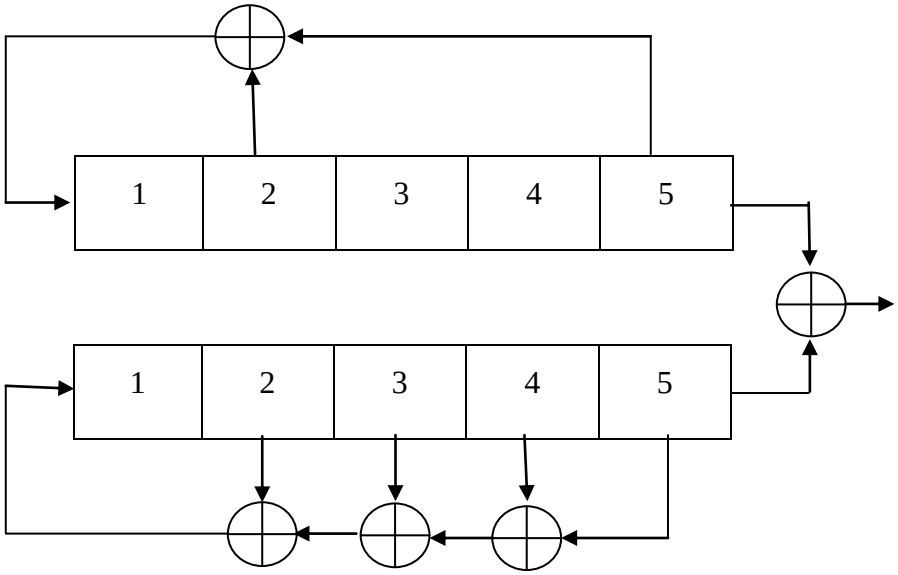

Sequence 1: 11111000110111010100000100101100

Sequence 2: 11111001001100001011010100011110

0shift XOR: 00000001111011011111011101000010

1 shift XOR: 00001010101111000010100001100001

30 shift XOR: 10000100010001010001100011010111

Figure b.3 Example of Generating a Set of Gold Sequences, [51].

Further, the desired Gold sequences can only be generated by **preferred** pairs of m-sequences [51].

Suppose we take an m-sequence represented by a binary vector a of length *N,* and generate a new sequence a' by sampling every q^{th} symbol of a. We use multiple copies of a until we have enough samples to produce a sequence of a' of length *N* [51]. The sequence a' is said to be a **decimation** of the sequence a and is written as a' = *a*[*q*] [51]. The sequence a' does not necessarily have a period *N* and is therefore not necessarily an m-sequence [51]. It can be shown that a' will be an m-sequence, with period *N*, if and only if gcd(*n, q*) = 1, where goo stands for greatest common divisor; in other words, n and *q* have no common factor except 1. For Gold sequences, we need to start with a preferred pair a and a' = a[*q*] that are both m-sequences and that meet the following conditions [51]:

1. $n \bmod 4 \neq 0$ (b.2)
2. q is odd and $q = (2^k + 1)$ or $q = (2^{2k} - 2^k + 1)$ for some k. (b.3)
3. $\gcd(n, k) = \begin{cases} 1 & \text{for } n \text{ odd} \\ 2 & \text{ford } n \bmod 4 = 2 \end{cases}$ (b.4)

The sequence generated is [a, a', a $\oplus$a', a $\oplus$Da', a$\oplus$ D^2a'……a$\oplus$ D^{N-1}a'] where, D=delay element ≈ one bit shift of a' relative to a. Period of Gold sequence is $N = 2^n - 1$

To generate the Gold codes from shift registers, we start with the all-ones vector set in both registers as an initial condition [51]. The resulting sequences are XORed to produce one Gold sequence. This yields the first three sequences in the set [51]. To generate the remaining sequences, the second of the first two sequences is shifted by one bit and the XOR operation performed again. This process continues through all possible shifts, with each additional one-bit shift followed by an XOR producing a new sequence in the set [51], [53].

Gold codes have three-valued autocorrelation and cross-correlation function: {-1, -*t*(*m*), *t*(*m*)-2} where [51]:

$$t(m) = \begin{cases} 2^{(m+2)/2} + 1 & \text{for even } m \\ 2^{(m+1)/2} + 1 & \text{for odd } m \end{cases} \quad \text{(b.5)}$$

b.3. Kasami Sequence

Kasami sequences are also derived from m-sequences and their cross-correlation properties are similar to Gold codes. There are two classes of Kasami sequences: the *small set* and the *large set* [51], [53].

- For generation of small kasami code, n is chosen even. A sequence a is defined with period $N=2^n -1$. This sequence is decimated by $q=2^{n/2} +1$. The resulting sequence a' has period $2^{n/2}-1$. Final sequence is generated by XORing the bits from a and a' [51], [53].

- For generation of large kasami code, one set is defined by starting with an m-sequence, a with a period N. That sequence is decimated by $q=2^{n/2} + 1$ to form a'. That Sequence a' is further decimated by $q= 2^{(n+2)/2} +1$ to form a''. Final set is formed by taking XOR of a, a', a'' [51], [53].

References

[1] R. Prasad and S. Hara, *"An overview of multicarrier CDMA",* in Proc. IEEE Int. Symp. Spread Spectrum techniques and Applications, pp. 107-114, 1996.

[2] Abdel-Majid Mourad *"On the system level performance of MC-CDMA systems in the downlink*", Doctoral thesis, Superior School National Telecommunications of Britain, 2006.

[3] H. Holma, A. Toskala, "*WCDMA for UMTS"*, John Wiley & Sons Ltd, 3rd Edition 2000.

[4] Thomas Sälzer, "*Transmission Strategies Employing Multiple Antennas for the Downlink of Multi-Carrier CDMA Systems"*, Doctoral Thesis, National Institute of Applied Sciences of Rennes, France, 2004.

[5] D.Hsiung et J.Chang, *"Performance of multi-code CDMA in a multipath fading channel "*, IEEE communication, vol.147, pp-365-370, 2000.

[6] Aboura Lamia Touria, "*Performance evaluation of the MC-MC-CDMA system on a channel multipath*", Doctoral Thesis, UDL-SBA, 2014.

[7] C.L. I, R.D Gitlin., "*Multi-Code CDMA Personal Communication Networks,"* IEEE International Conference on Communication, pp.1060-1064, 1995.

[8] H.Rehman, I.Zaka, M.Naeem, S.I.Shah, J.Ahmad, "*Multicode Multicarrier Interleave Division Multiple Access Communication"* in Proc. IEEE, Multitopic Conference, INMIC'06, 2006.

[9] J.Kim, T. Kim, S.Srinivasan, M.Yalamanchi, "*Rate Adaptive Multi-Code Multi-Carrier CDMA Systems in Multipath Fading Channel",* Wireless Communications Term Project Report for Springer, 2003.

[10] Y. Lee, K. Kim, H. Park and D. Kwon, "*effects of subcarrier interleaving on LDPC coded MC-CDMA",* Multi-Carrier Spread-Spectrum: Proceedings from the 5th International Workshop, pp. 425–432, Springer 2006.

[11] T. Kim, J. Kim, J. G. Andrews, and T. S. Rappaport, "*Multi-code Multicarrier CDMA: Performance Analysis*", IEEE International Conference on Communication, vol.2, pp.973-977, 2004.

[12] A.Zouggaret, A.Djebbari, K.Djemal, "*Interleaving in Time-frequency Diversity on Multi-code Multicarrier CDMA System"*, Journal of Electrical and Electronics Engineering, vol. 9, 2016.

[13] Paul F Combes *''Transmission en espace libre et sur des lignes''*, 2nd Edition, Dunod University, 1988.

[14] M.Benyarou, "*Optimization of multi-antenna systems applied to MC-CDMA systems*", Doctoral Thesis, University Abou Bakr Belkaid, Telemcen , 2013.

[15] C. E. Shannon, "*Coding Theorems for a Discrete Source with a Fidelity Criterion,*" IRE International Convention Record, 1959.

[16] Jonathan Letessier. "*Theoretical system performance MIMO pre-equalized and applications with a 3D propagation simulator*." Doctoral thesis. University of Western Brittany. 2005.

[17] Bertrand Devillers. "*MIMO techniques for single carrier modulation and cyclic extension*". Electrical Engineering memory, Catholic University of Louvain, Faculty of Applied Science, Belgium, 2003-2004.

[18] Ikhlef Ismahene, "*Analysis Of Multi-Carrier Acquisition System Direct Sequence (Mc-Ds-Cdma) In Rayleigh Channel",* Doctoral Thesis, Mentouri University, Constantine, 2011.

[19] Nizar Hicheri, *" unified approach to radio transmission techniques on downlink "* Doctoral Thesis, National Conservatory of Arts and Crafts, France, 2004.

[20] Jean-Pierre Bouvet, *" iterative receivers for multi-antenna systems ",* Doctoral thesis, National Institute of Applied Sciences, Rennes, France, 2005.

[21] R. van Nee, R. Prasad, "*OFDM for wireless multimedia communications"*, Artech House Publishers, 2000.

[22] T.S. Rappaport, "*Wireless Communications: Principles & Practice"*, 2nd edition, Prentice Hall, 2002.

[23] S. Nobilet, "*Study and optimization of MC-CDMA technology for future generations of wireless communications systems"* PhD thesis, National Institute of Applied Sciences of Rennes, France, 2003.

[24] B.M. Popovic, "*Spreading Sequences for multicarrier CDMA systems*", IEEE Transactions Communications, vol. 47, pp. 918–926, 1999.

[25] J.G. Proakis, *"Digital Communications"*, McGraw Hill, 1995.

[26] J. Egle, M. Reinhardt, J. Lindner, '*Equalisation and Coding for Extended MC-CDMA over Time and Frequency Selective Channels',* Workshop on Multi-Carrier Spread Spectrum, pp. 127-134, 1997.

[27] A. Persson, T. Ottosson, E. Ström, '*A Per Time-frequency localized CDMA for downlink multicarrier systems*', IEEE Proc. of ISSSTA'02, vol. 1, pp. 118-122, 2002.

[28] Hsiao-Hwa Chen, "*The Next Generation CDMA Technologies",* John Wiley & Sons Ltd, England, 2007.

[29] Rizwan Asghar, "*Flexible Interleaving Sub–systems for FEC in Baseband Processors",* Doctoral thesis, Linköping University, Sweden, 2010.

[30] C. Heegard and S. B. Wicker *" Turbo Coding",* Kluwer Academic Publishers, 1999.

[31] Syed Amjad Ali, "*Performance Analysis Of Turbo Codes Over AWGN And Rayleigh Channels Using Different Interleaver*s", Master thesis, Eastern Mediterranean University, 2001.

[32] Pingzhou Tu, "*Orthogonal frequency division multiplexing for system coexixtence*", PhD thesis, University of Wollongong, Australie, 2008.

[33] E. M. El-Bakary, E. S. Hassan, O. Zahran, S. A. El-Dolil, and F. E. Abd El-Samie *"Efficient Image Transmission with Multi-Carrier CDMA",* Wireless Personal Communications, vol. 69, pp. 979-994, 2013.

[34] Fridrich J. "*Symmetric ciphers based on two-dimensional chaotic maps*", International Journal of Bifurcation and Chaos, vol. 8, pp. 1259–1284,1998.

[35] Han, F., Yu, X., & Han, S. *"Improved baker map for image encryption",* Systems and Control in Aerospace and Astronautics, pp. 1273–1276, 2006.

[36] Hassan, E. S., El-Khamy, S. E., Dessouky, M. I., El-Dolil, S. A., Abd El-Samie, F. E. "*New interleaving scheme for continuous phase modulation based OFDM systems using chaotic maps*". In Proceedings of WOCN-09, Cairo, Egypt, pp. 28–30, 2009.

[37] Hassan, E. S., El-Khamy, S. E., Dessouky, M. I., El-Dolil, S. A., & Abd El-Samie, F. E. "*Chaotic interleaving scheme for continuous phase modulation based single-carrier frequency-domain equalization systems*", Wireless Personal Communications, vol. 62, pp. 183–199, 2012.

[38] P. K. Enge and D. V. Sarwate "*Spread-spectrum multiple-access performance of orthogonal codes: linear receivers*". IEEE Transactions Communications, vol. 35, pp. 1309–1319, 1987.

[39] N. Guo and L. B. Milstein, "*On rate-variable multidimensional DS/SSMA with sequence sharing*". IEEE Journal on Selected Areas in Communications, vol. 17, pp. 902–917, 1999.

[40] H.D. Schotten, H. Elders-Boll, and A. Busboom, *" Adaptive Multi-Code CDMA Systems for Variable Data Rates"*, In Proc. IEEE International Conference on Personal Wireless Communications, Mumbai, 1997.

[41] X. Gui and T. S. Ng, *" Performance of Asyncronous Orthogonal Multicarrier System in a Frequency Selective Fading Channel"*, IEEE International Symposium On Spread Spectrum Techniques & Applications, vol. 2, pp. 494-497, 1998

[42] X. Gui and T. S. Ng, *"Performance of asynchronous orthogonal multicarrier system in a frequency-selective fading channel,"* IEEE Transactions Communications., vol. 47, pp. 1084–1091, 1999.

[43] J. G. Andrews, and T. H. Y. Meng, *"Performance of Multicarrier CDMA with Successive Interference Cancellation in a Multipath Fading Channel"*, IEEE Transactions Communications. vol. 52, 2004.

[44] M. M. Akho-Zahieh, N. Abdellatif, *"Effect of Diversity and Filtering on the Performance of Wavelet Packets Base Multicarrier Multicode CDMA System"*, Journal of Signal and Information Processing, pp. 165-179, 2015.

[45] M. Shukla, *"Performance Analysis of Optimum Interleaver Based on Prime Numbers for Multiuser Iterative IDMA Systems,"* IGI International Journal of Interdisciplinary Telecommunications and Networking, vol. 2, pp. 51-65, 2010.

[46] P. Hanpinitsak, C. Charoenlarpnopparut and P. Suksompong, "*2D Interleaver Design for Image Transmission over Severe Burst-Error Environment"*, ECTI Transactions On Electrical Eng., Electronics, And Communications, vol.12, 2014.

[47] L. Ping, Y. Wu and W. Leung, *"Interleave-Division Multiple-Access"*, IEEE Transactions on Wireless Communication, vol. 5, pp. 938-947, 2006.

[48] EyeRounds.org - Ophthalmology - The University of Iowa, www.webeye.ophth.uiowa.edu/eyeforum/search.htm

[49] Santit Traithavil "*Simulation of PN Code Sequences for Cellular Systems*", Santit-report, The Australian National University, 2006.

[50] Ir. J. Meel "*Spread Spectrum*" Sirius communication, Rotselaar, Belgium, 1999.

[51] W. Stallings, "*Wireless Communications and Networks"*. 2nd Edition, Pearson Education Inc, 2002.

[52] Toni Huovinen, "*TLT-5606 Spread Spectrum Techniques, Chapter 2: Pseudorandom sequences",* Tampere University of Technology, 2011.

[53] Ipsita Bhanja, "*Performance Evaluation Of Phaseoptimized Spreading Codes In Non-Linear Ds-Cdma Receiver"*, Master thesis, National Institute of Technology, Rourkela, India, 2006.

Journal of Electrical and Electronics Engineering

http://electroinf.uoradea.ro/index.php/reviste/jeee.html

Vol. 9, Nr. 1, May 2016 ISSN: 1844-6035

University of Oradea Publisher

JEEE - Journal of Electrical and Electronics Engineering, Vol. 9 , Nr. 1, May 2016

Academy of Romanian Scientists

University of Oradea, Faculty of Electrical Engineering and Information Technology

Journal of Electrical and Electronics Engineering

Vol. 9 , Nr. 1 , May 2016

University of Oradea Publisher

Academy of Romanian Scientists
University of Oradea, Faculty of Electrical Engineering and Information Technology

Volume 9, Number 1, May 2016

Journal of Electrical and Electronics Engineering

University of Oradea Publisher

ISSN 1844 - 6035

This volume includes papers in the following main topics: Electromagnetic field analysis and applications, Microwaves, Electrotechnologies, Energy conversion, Electrical drives and electromechanical systems, Electric and electronic measurement systems, Electronics, Telecommunications, Signal Processing, Multimedia Systems, Cellular Neural Networks, Robotics, Power Systems and Power Electronics, Linear and Non-linear Circuits, Management, Image processing, Medical applications.

Interleaving in Time-frequency Diversity on Multi-code Multicarrier CDMA System

ZOUGGARET Abdelhak[1], DJEBBARI Ali[1], DJEMAL Khalifa[2]

[1] University of Sidi Bel-Abbes, Algeria,
Telecommunications and Digital Signal Processing Laboratory,
P.B.89, 22000 Sidi Bel-Abbes, Algeria, E-Mail: zouggaret@yahoo.fr, adjebari2002@yahoo.fr

[2] University of Evry Val d'Essonne, France,
IBISC Laboratory,
91020 Evry Cedex, France, E-Mail: Khalifa.djemal@ibisc.univ-evry.fr

***Abstract* – This paper presents a new Time-frequency interleaving in a Multi-code Multicarrier CDMA (MC-MC-CDMA) system, which allows two-dimensional spreading in both time and frequency domains. Our contribution consists in implementing a two-dimensional interleaving inside the time and frequency diversity. We demonstrate via simulation results that the proposed method yields better performances in Bit Error Rate (BER). Also, we observe that BER of both the 2D-prime interleaving and the 2D-random interleaving are similar. Furthermore, the interleaving gain is larger in a frequency-diversity than time-diversity. Finally, we reach better Peak Signal to Noise Ratio (PSNR) when we transmit images through the proposed technique.**

***Keywords*: MC-MC-CDMA; Walsh Hadamard; Prime interleaver; MRC.**

I. INTRODUCTION

Future cellular radio networks will offer services that require the transfer data at high rate, while maintaining high mobility users. One approach currently being an important focus of research in this area is multicarrier CDMA technology [1]. Another approach to increase the data rate found in the MC-MC-CDMA association [2].

A multicarrier CDMA system with spreading only in the frequency domain is generally referred to as a MC-CDMA system, while a multicarrier system with spreading only in the time domain is usually called DS-CDMA. The MC-MC-CDMA system offers two-dimensional gains in both the time and frequency domains by using a multi-code signal and multicarrier modulation, respectively [2]. Two-dimensional spreading exploits time-diversity and frequency-diversity. This advantage can allow us implement two-dimensional interleaving both code sequence and subcarriers, thus can minimizes a frequency selective fading and Multiple Access Interference (MAI).

The diversity effects of subcarrier interleaving on MC-CDMA system employing Low Density Parity Check (LDPC) codes with different code rates have been investigated in [3].

The prime interleaving is given in [4], [5] and [6], the idea of extending from 1D prime interleaved into 2D is used in image matrix. Also, the prime interleaving is quite easy to generate and is outperforming of random interleaving in terms of bandwidth consumption problems and computational complexity.

Maximal Ratio Combining (MRC) is an optimum diversity combining technique is evaluated in [7], [8].

In [9], an efficient image transmission approach has been proposed for MC-CDMA system with spreading only in the frequency domain using chaotic interleaving implemented outside the frequency diversity with Linear Minimum Mean Square Error (LMMSE) and Zero-Forcing (ZF) equalizers.

Our work is to use the MC-MC-CDMA system with two-dimensional spreading in both the time and frequency domains this allowed us to implement two-dimensional prime interleaving inside the time and frequency diversity with MRC equalizer. The results of simulations will be presented on the basis of several factors such as subcarrier number and code sequence length. An application of images transmission will be presented with the proposed system.

II. SYSTEM MODEL

We used the same model of MC-MC-CDMA given by [2], with adding 2D block interleaving.

A. *Transmitter model*

As shown in Fig. 1, each user has the same code sequence.

$$G_m(n) = \{g_m(n) / \ 1 \le m \le M\} \qquad (1)$$

where $G_m(n)$ is the total matrix of code sequences.

An *M-ary* symbol $d_{k,i}$ of $log2M$ bits selects one of M Code sequences in $G_m(n)$ for transmission.

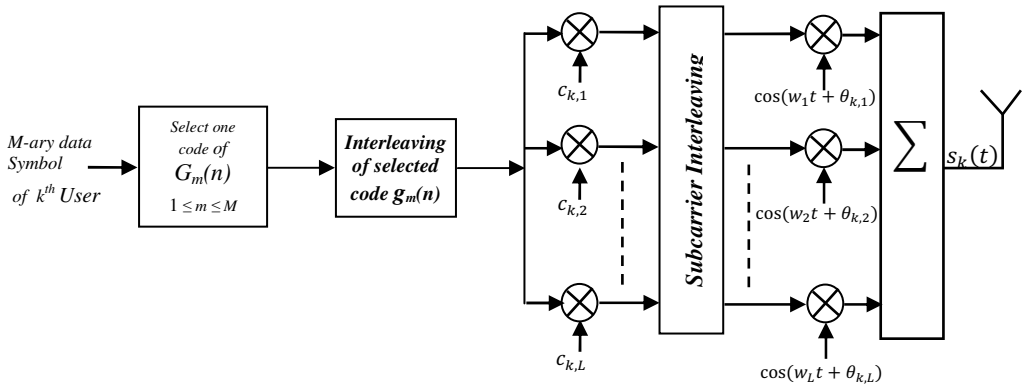

Fig. 1. Transmitter model of MC-MC-CDMA system with 2D-interleaving

The i^{th} code sequence of length N of user K is:

$$S_{k,i}(t) = \sum_{n=0}^{N-1} g_{d_{k,i}}(n) f(t - nT_c - iT_s) \quad (2)$$

where T_s is symbol duration and f is a rectangular pulse of duration T_c.

The selected code sequence $S_{k,i}(t)$ is interleaved and converted into L parallel subcarrier branches, then multiplied with the user specific sequence $c_{k,l}$. After, the output is interleaved in order to modulate one of the L wavelet packets. Finally, we perform the sum of the partial results [2], [3].

The transmitted signal of the K^{th} user can be written as:

$$s_k(t) = \sum_{i=-\infty}^{+\infty} \sum_{l=1}^{L} \sum_{n=0}^{N-1} g_{d_{k,i}}(n) f(t - nT_c - iT_s) c_{k,l}(Ni + n) \cos\left(w_l t + \theta_{k,l}\right) \quad (3)$$

where w_l is l^{th} carrier frequency, $\theta_{k,l}$ is random phase of the l^{th} subcarrier of user K and uniformly distributed over $[0,2\pi]$, and $(Ni + n)$ is the location of l^{th} chip which is multiplied by the n^{th} bit in the i^{th} code sequence of length N.

B. Channel model

Without lose of generality, we consider a frequency-selective Rayleigh fading as a channel model. This choice allows that the MC-MC-CDMA system transmits waveform consisting of a large number of narrowband subcarriers.

Each subcarrier can be writing as a function of a complex flat-fading channel; so, we have [7], [10]:

$$h_{k,l}(t) = h_{k,l}^{I}(t) + j h_{k,l}^{Q}(t) = \beta_{k,l}(t) e^{j\varphi_{k,l}(t)} \quad (4)$$

Which is a complex Gaussian random variable with zero mean and variance σ^2.

The path gains $h_{k,l}(t)$ is assumed uncorrelated and identically distributed for different k and l. $\beta_{k,l}(t)$ is a Rayleigh distributed amplitude attenuation and phase a shift $\varphi_{k,l}(t)$ are considered to be constant over the time interval $[0\ \ T_c]$.

C. Receiver model

At the receiver as shown in Fig. 2, the incoming signal is:

$$r(t) = \sum_{i=-\infty}^{+\infty} \sum_{k=1}^{K} \sum_{l=0}^{L} \sum_{n=0}^{N-1} \beta_{k,l}(t) g_{d_{k,i}}(n) f(t - nT_c - iT_s) c_{k,l}(Ni + n) \cos\left(w_l t + \emptyset_{k,l}\right) + \eta(t) \quad (5)$$

where $\emptyset_{k,l} = \theta_{k,l} + \varphi_{k,l}$ is the received phase and $\eta(t)$ is the additive white Gaussian noise with zero mean and variance σ^2.

The demodulated code sequence of user 1 after subcarrier de-interleaving and dispreading respectively is:

$$y_1(t) = \sum_{j=0}^{N-1} y_{1,j} f(t - jT_c) \quad (6)$$

$$y_{1,j} = \frac{1}{T_c} \int_{jT_c}^{(j+1)T_c} r(t) \sum_{l=1}^{L} c_{1,l}(j) \cos\left(w_l t + \emptyset_{1,l}(j)\right) \alpha_{1,l} dt \quad (7)$$

The de-interleaved demodulated code sequence after the matched filter bank of user 1 is:

$$U_{1,m} = \int_0^{T_s} y_1(t) \sum_{n=0}^{N-1} g_m(n) f(t - nT_c) dt \quad (8)$$

Depending on the choice of $\alpha_{1,l}$ there is a number of combining which can be implemented; in our paper we consider MRC because the best BER performance of such a system is achieved by the use of this combining [7], [8].

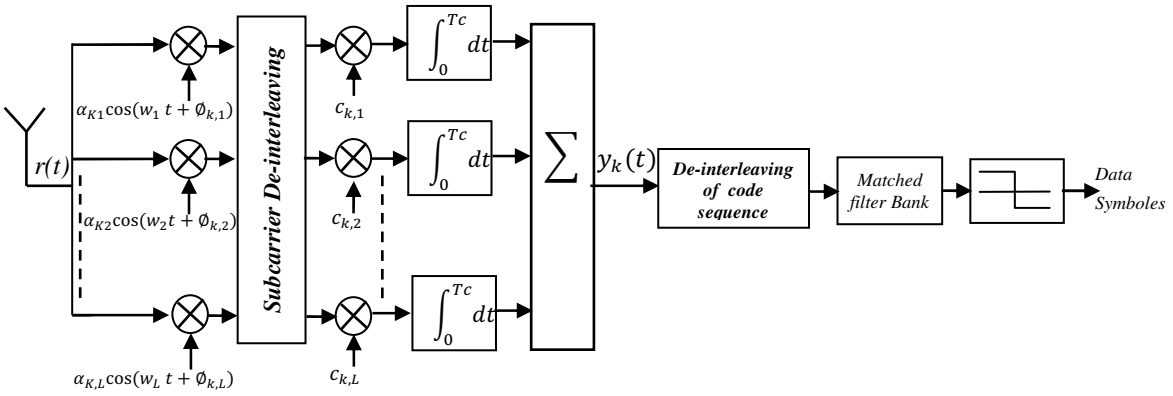

Fig. 2. Receiver model of MC-MC-CDMA system with 2D De-interleaving

III. NEW TIME FREQUENCY INTERLEAVING

There are a lot of varieties of interleaving modules, which can be implemented. So, we present two major 2D-interleaving, such, the 2D-prime and 2D-random interleaving.

A. Two-dimensional Prime interleaving

For understanding the mechanism of 2D-prime interleavers in time-frequency, let us consider a case of 2D-interleaving of matrix size (N x L), where N is a code sequence length and L is a number of subcarriers. Firstly, we distribut the interleaving scheme into code sequence interleaving in row-wise and subcarriers interleaving in column-wise. Secondly, we affect the value of seed as P_{row} (row-wise seed) and P_{col} (column-wise seed) to code sequence and subcarriers interleaving respectively. The new positions of bits after 2D-interleaving will be as follows:

$$n_{new} = (1 + (n-1)P_{row}) mod\ N \quad (9)$$

$$l_{new} = (1 + (l-1)P_{col}) mod\ L \quad (10)$$

where n = 1, 2, 3,……..N and l = 1, 2, 3,……L.

For example if we have a code sequence of length N=8 modulated of L=8 orthogonal subcarriers. we want to apply a 2D-prime interleavers with Prow=5 and Pcol=3. The new bit positions are illustrated in Fig. 3.

B. Two-dimensional random interleaving

Our 2D-random interleaving is the same of 2D-prime interleaving. It is also distributed into 1D row-wise and 1D column-wise interleaving. But, it uses random permutation for interleaving instead of using an exchange follows the value of seed.

Time(code sequence) →

Frequency (subcarrier)	$g_{m(1)}$	$g_{m(2)}$	$g_{m(3)}$	$g_{m(4)}$	$g_{m(5)}$	$g_{m(6)}$	$g_{m(7)}$	$g_{m(8)}$
$C_{k,1}$	1	2	3	4	5	6	7	8
$C_{k,2}$	9	10	11	12	13	14	15	16
$C_{k,3}$	17	18	19	20	21	22	23	24
$C_{k,4}$	25	26	27	28	29	30	31	32
$C_{k,5}$	33	34	35	36	37	38	39	40
$C_{k,6}$	41	42	43	44	45	46	47	48
$C_{k,7}$	49	50	51	52	53	54	55	56
$C_{k,8}$	57	58	59	60	61	62	63	64

a. Befor 2D-prime interleaving

Time(code sequence) →

Frequency (subcarrier)	$g_{m(1)}$	$g_{m(4)}$	$g_{m(7)}$	$g_{m(2)}$	$g_{m(5)}$	$g_{m(8)}$	$g_{m(3)}$	$g_{m(6)}$
$C_{k,1}$	1	4	7	2	5	8	3	6
$C_{k,6}$	41	44	47	42	45	48	43	46
$C_{k,3}$	17	20	23	18	21	24	19	22
$C_{k,8}$	57	60	63	58	61	64	59	62
$C_{k,5}$	33	36	39	34	37	40	35	38
$C_{k,2}$	9	12	15	10	13	16	11	14
$C_{k,7}$	49	52	55	50	53	56	51	54
$C_{k,4}$	25	28	31	26	29	32	27	30

b. After 2D-prime interleaving

Fig. 3. 2D-prime interleaving of 8 subcarriers and code sequence length N = 8

IV. RESULTS AND DISCUSSIONS

In section IV.A, the BER performance of MC-MC-CDMA system with/without using 2D-interleaving is analyzed.

In section IV.B, the PSNR performance of received images over MC-MC-CDMA with and without 2D-iterleaving is presented. A comparison between proposed approach and those presented in [9] is evaluated. The parameters listed in Table 1 are used for the simulation in this section.

TABLE 1. Simulation parameters

Parameters description	Value / type
Code Sequence	Walsh-Hadamard
Spreading Code	Walsh-Hadamard
M-ary symbol (*M*)	8
Number of User(*K*)	4
Number of subcarrier(*L*)	16
Code Sequence length(*N*)	16
Interleaving	Random – Prime – Chaotic
Combining	MRC
Image size	256x256

A. Performance evaluation of MC-MC-CDMA with 2D-interleaving

Fig. 4 shows the BER performance of MC-MC-CDMA scheme with both 2D-random interleaving and 2D-prime interleaving with MRC detection. From this figure we can see that the performance with 2D-interleaving is far better than that without interleaving. Also the BER performance of 2D-prime interleaving comes out similar to that of BER performance of 2D-random interleaving with MRC detection.

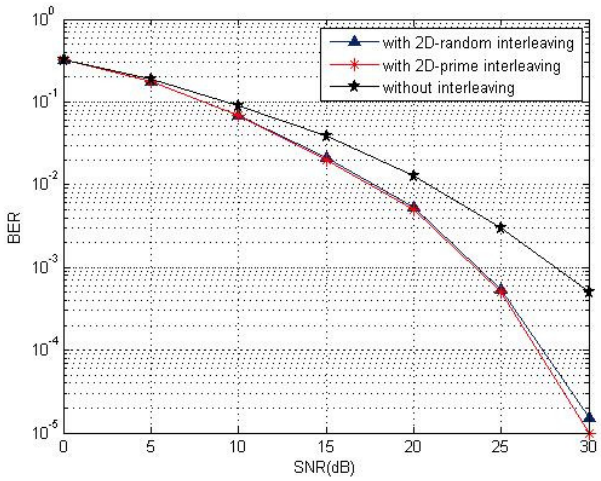

Fig. 4. BER comparison of MC-MC-CDMA system with/without 2D-interleaving. *L*=16.

Fig. 5 shows a comparison between interleaved code sequence and interleaved subcarrier. It is seen that the interleaving gain is larger in a frequency-diversity than time-diversity.

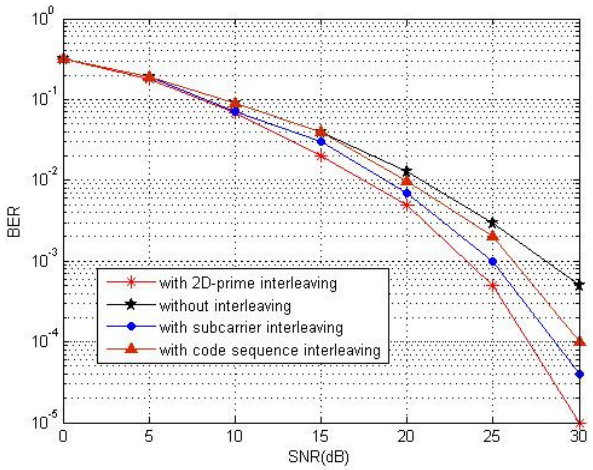

Fig. 5. Comparison between code sequence and subcarrier Interleaving for MC-MC-CDMA.

B. Images transmission over MC-MC-CDMA with 2D-interleaving

To confirm the results found previously of BER performance, we transmit images shown in Fig. 6 over MC-MC-CDMA system with and without 2D-prime interleaving. The simulation parameters are provided in Table 1.

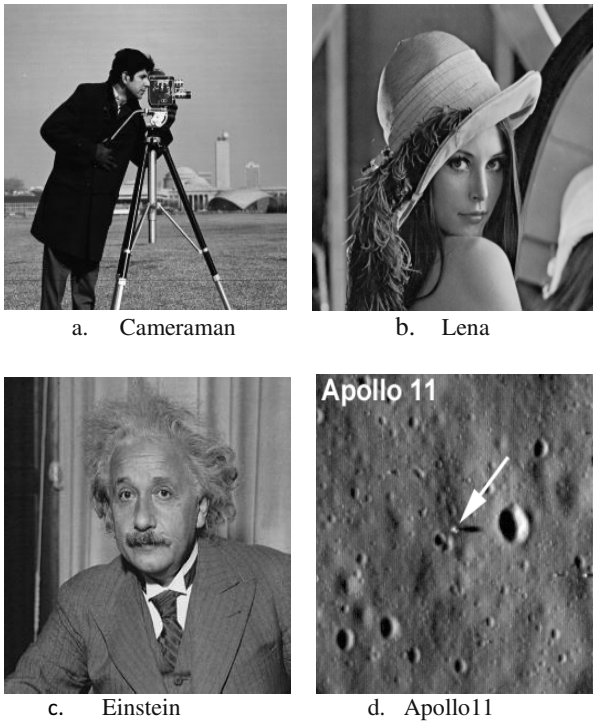

a. Cameraman b. Lena

c. Einstein d. Apollo11

Fig. 6. The original images.

a. Cameraman is a transmitted image of user 1
b. Lena is a transmitted image of user 2
c. Einstein is a transmitted image of user 3
d. Apollo11 is a transmitted image of user 4

The PSNR metric, is used to measure the quality of the reconstructed images at the receiver, which is defined as [9]:

$$PSNR = 10.Log_{10}\left(\frac{MAX^2}{MSE}\right) \quad (11)$$

where *MAX is* the maximum possible pixel value of the image. The Mean Squared Error *MSE* is defined as:

$$MSE = \frac{1}{e.f}\sum_{i=0}^{e-1}\sum_{j=0}^{f-1}[A(i,j) - B(i,j)]^2 \quad (12)$$

where *(e . f)* is the image size. *A* and *B* are the original and the recovered images, respectively.

a. PSNR= 34.90dB b. PSNR= 35.20dB

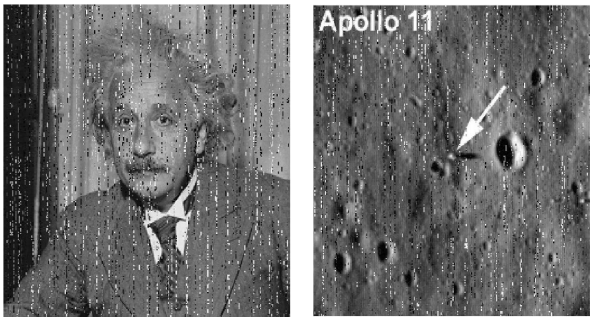

c . PSNR= 34.95dB d . PSNR= 35.18dB

Fig. 7. Received images over MC-MC-CDMA system without interleaving at SNR= 20dB.

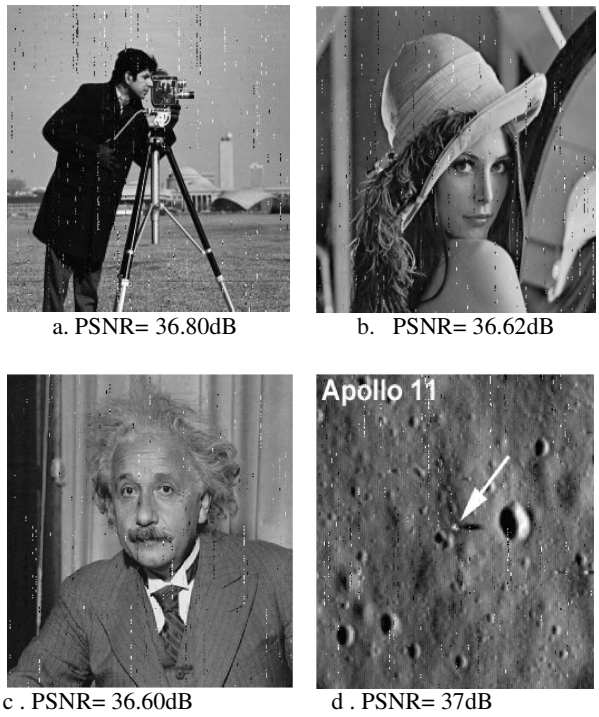

a. PSNR= 36.80dB b. PSNR= 36.62dB

c . PSNR= 36.60dB d . PSNR= 37dB

Fig. 8. Received images over MC-MC-CDMA system with 2D-Prime interleaving at SNR= 20dB.

Fig. 7 and Fig. 8 show the received images with and without 2D-prime interleaving at SNR=20dB. Fig. 9 shows the variation of the PSNR summarized in Table 2 and Table 3, when SNRs are varied from 0 to 30 dB in 5dB steps. From these figures, it is clear that the best results are obtained when we use 2D-prime interleaving.

Fig.10 present the PSNR yielded from our proposed system without equalization and its corresponding from previous work [9]. It's seems that our proposed system reach better PSNR over MC-CDMA with chaotic interleaving [9].

TABLE 2. PSNR values for the received images in dB without interleaving using MRC combiner

Received images	SNR(dB)						
	0	5	10	15	20	25	30
Cameraman	18.80	27.91	31.88	34.01	34.90	36.20	39
Lena	18.40	27.60	30.98	33.98	35.20	35.80	40.01
Einstein	18.77	27.75	31.70	34.40	34.95	35.85	39.80
Apollo11	18.33	27.78	31.79	34.22	35.18	36.15	40

TABLE 3. PSNR values for the received images in dB with 2D-Prime interleaving using MRC combiner

Received images	SNR(dB)						
	0	5	10	15	20	25	30
Cameraman	19.10	28	32.02	35.20	36.80	39.50	44.70
Lena	18.41	27.60	32.15	34.90	36.62	39.80	45
Einstein	18.50	27.70	31.90	35.35	36.60	39.88	44.80
Apollo11	18.35	27.80	32.25	35.30	37	40	44.83

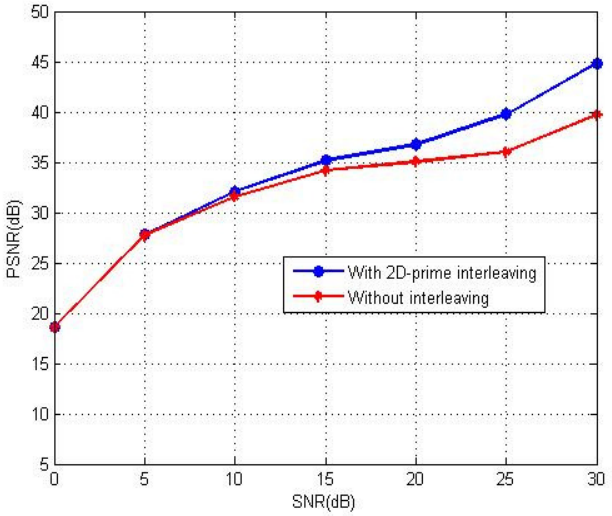

Fig. 9. Average PSNR versus SNR for the received images over MC-MC-CDMA system.

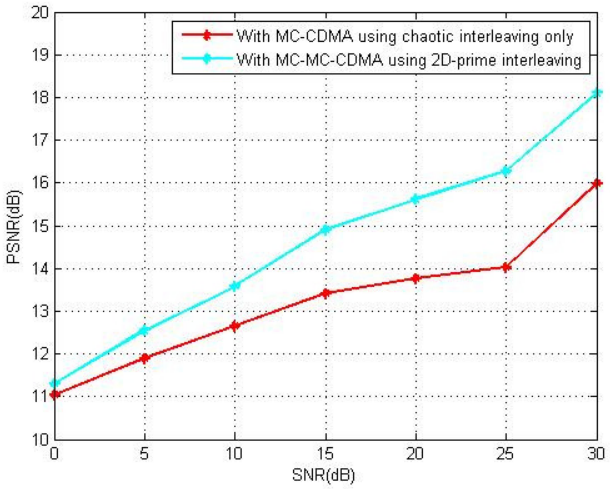

Fig. 10. PSNR comparison between the received cameraman image over MC-MC-CDMA system with 2D-prime interleaving and MC-CDMA with chaotic interleaving

V. CONCLUSIONS

In this paper, we have presented a new time-frequency interleaving method based on MC-MC-CDMA systems allowing two-dimensional spreading in both time and frequency domains. The originality of proposed technique lies in fact that we have implemented a two-dimensional interleaving inside the time and frequency diversity. Simulation results showed that the performance is improved with 2D-interleaving and the BER performance of 2D-prime interleaving is found similar to that of 2D-random interleaving. Also, the interleaving gain is larger in a frequency-diversity than time-diversity.

The performance of the images transmission process has been studied. The obtained results confirm that the important improvement on PSNR in MC-MC-CDMA system with 2D-interleaving compared to MC-CDMA system with chaotic interleaving.

REFERENCES

[1] R. Prasad and S. Hara, *"An overview of multicarrier CDMA"*, in Proc. IEEE Int. Symp. Spread Spectrum techniques and Applications, pp. 107-114.J. C, Sept. 1996.

[2] T. Kim, J. Kim, J. G. Andrews, and T. S. Rappaport, *"Multi-code Multicarrier CDMA: Performance Analysis"*, in Proc.IEEE Int. Conf. Comm,. vol.2, pp.973-977, June 2004.

[3] Y. Lee, K. Kim, H. Park and D. Kwon, *"effects of subcarrier interleaving on LDPC coded MC-CDMA"*, Multi-Carrier Spread-Spectrum: Proceedings from the 5th International Workshop, pp. 425–432, 2006 Springer.

[4] M. Shukla, *"Performance Analysis of Optimum Interleaver Based on Prime Numbers for Multiuser Iterative IDMA Systems,"* IGI International Journal of Interdisciplinary Telecommunications and Networking, vol. 2, no. 3, pp. 51-65, 2010.

[5] P. Hanpinitsak, C. Charoenlarpnopparut and P. Suksompong, *"2D Interleaver Design for Image Transmission over Severe Burst-Error Environment"*, ECTI Transactions On Electrical Eng., Electronics, And Communications, vol.12, no.2, August 2014.

[6] L. Ping, Y. Wu and W. Leung, *"Interleave-Division Multiple-Access"*, Trans. on Wireless Communication, 5 (4), IEEE. 938-947. 2006.

[7] X. Gui and T. S. Ng, *"Performance of asynchronous orthogonal multicarrier system in a frequency-selective fading channel,"* IEEE Trans. Commun., vol. 47, pp. 1084–1091, July 1999.

[8] M. M. Akho-Zahieh, N. Abdellatif, *"Effect of Diversity and Filtering on the Performance of Wavelet Packets Base Multicarrier Multicode CDMA System"*, Journal of Signal and Information Processing, pp. 165-179, May 2015.

[9] E. M. El-Bakary, E. S. Hassan, O. Zahran, S. A. El-Dolil, and F. E. Abd El-Samie *"Efficient Image Transmission with Multi-Carrier CDMA"*, Wireless Personal Commu., DOI 10.1007/s11277-012-0622-6. 2013.

[10] J. G. Andrews, and T. H. Y. Meng, *"Performance of Multicarrier CDMA with Successive Interference Cancellation in a Multipath Fading Channel"*, IEEE Trans. Commun. voL. 52, no. 5, May 2004.